DEVELOPMENT OF SOL-GEL-BASED BIOACTIVE PAPER
SENSING PLATFORMS TOWARD NEUROTOXIN DETECTION

DEVELOPMENT OF SOL-GEL-BASED BIOACTIVE PAPER
SENSING PLATFORMS TOWARD NEUROTOXIN DETECTION

By

Roger Elliot Luckham, B.Sc.

A Thesis Submitted to the School of
Graduate Studies in Partial Fulfillment of
the Requirements for the Degree of

Master of Science

McMaster University

MASTER OF SCIENCE (2009)   **McMASTER UNIVERSITY**

                                         HAMILTON, ONTARIO

TITLE: DEVELOPMENT OF SOL-GEL BASED BIOACTIVE PAPER SENSING PLATFORMS TOWARD NEUROTOXIN DETECTION

Author: Roger Elliot Luckham, B.Sc. (University of Guyana)

Supervisor: Professor John D. Brennan

Number of Pages: x, 147

Abstract

We report on a new solid-phase colorimetric bioassay format based on enzyme-catalyzed enlargement of gold nanoparticles (AuNP) that are co-entrapped with the enzyme in a sol-gel based silica material. Biocatalysed hydrolysis of the enzyme substrate, acetylthiocholine (ATCh) leads to formation of thiocholine, which in turn reduces Au(III) onto the entrapped nanoparticles, producing particle growth and a concomitant increase in color intensity that can be correlated to the amount of substrate or inhibitor present in test solutions. The entrapped AuNP cannot leach from the silica material, leading to a solid-phase assay that has the potential to be integrated into a portable biosensing platform that can utilize visual detection of a color change as a simple readout. Toward this end, we cast an AChE-doped silica material onto a 40%MTMS/TMOS functionalized paper substrate to form the portable biosensor. Treatment with 40%MTMS/TMOS affords a more uniform paper surface allowing for more reproducible enzyme loading and better control over liquid penetration. Our results show that the assay is sufficiently sensitive to allow for detection of Paroxon to 1 μM. For automated sensor fabrication, we investigated piezoelectric inkjet printing of enzyme doped silica sols. A unique sandwich type fabrication technique was devised whereby sol-gel materials (at stable pH) and the bio-materials were

printed separately and in layers so that AChE was sandwiched between layers of silica to form the sensor. For these biosensors, a standard Ellman assay was used to monitor AChE activity with the cationic polymer, PVAm (polyvinylamine, 1.5 MDa), employed to trap and preserve the colored anionic product molecules (5-thio-2-nitrobenzoate) over a finite region. With this novel approach, a series of Paraoxon and Aflatoxin B_1 levels were assessed and it was determined that these compounds can be detected to 100 nM and 1 nM respectively, in ca. 5 min. The paper-based, colorimetric sensing platforms presented in this thesis are simple, cost-effective, portable, user-friendly, and need neither sophisticated instruments nor additional handling steps. Detection can be made by eye or by digital camera and image analysis software.

Acknowledgements

TABLE OF CONTENTS

Chapter 3: Colorimetric Detection of Enzyme Inhibitors using Sol-Gel/Enzyme/AuNP Composites. Part 1: Optimizing Enzyme-Catalyzed Enlargement of Sol-Gel Entrapped Gold Nanoparticles

Chapter 4: Colorimetric Detection of Enzyme Inhibitors using Sol-Gel/Enzyme/AuNP Composites. Part 2: Development of Bioactive Paper Sensors for Acetylcholinesterase Inhibitors

Chapter 5: Development of a Bioactive Paper Sensor for Detection of Neurotoxins Using Piezoelectric Inkjet Printing of Sol-Gel Derived Bioinks

Chapter 6: Conclusions

LIST OF TABLES

LIST OF FIGURES

Chapter 1: Introduction

1.1 Thesis Goals

Over the past four decades, biosensors have become an important area of study in analytical chemistry, given their versatility, sensitivity, portability, cost effectiveness, reliability and ease of use.[1–5] Biosensors are defined as analytical devices which measure (whether quantitatively or semi-quantitatively) a given target analyte by utilizing a biological response that is converted (*via* a transducer) into a measurable signal.[6] These devices are categorized according to the bio-recognition elements employed and the type of transducers used.[2] There are four basic categories of transducers and these are: optical, electrochemical, thermal or mass sensitive devices,[7] while common bio-recognition elements or bio-receptors include:[2] antibodies, enzymes, nucleic acids, DNA aptamers, and whole cells[8,9] (for *e.g.*, yeast cells and bacteria).

There are several advantages associated with biosensors. As a result of the specific interactions between bio-recognition element and target molecules, biosensors are normally highly selective and sensitive and (in most cases), resistant to matrix effects. Some of these devices are also capable of on site, rapid screening,[10] owing to their relative portability. Moreover, in the developing world where expensive instrumentation is usually not available, biosensors are particularly useful as they are normally cheaper than traditional analytical devices and give, in some cases, comparable accuracy.[11] Furthermore, biosensors are also

versatile in the sense that they can be used for detecting (at clinically relevant and sub-lethal levels) a wide range of target molecules, some of which are: biomedical analytes,[9] gases,[12] metal ions,[13] explosives,[14] narcotics,[15] bacteria[16] and viruses.[9,17]

Notwithstanding these advantages, there are a few issues that need to be overcome with current biosensors. For instance, most biosensors can only sense single analytes and require power, whether to facilitate a detector response or to propagate mechanical functions. This is particularly evident in the case of some optical[18] and electrochemical sensors,[19,20] immunoassay,[34,21] semiconductor and quantum dot[22] based biosensors as well as traditional microfluidic devices, where power is needed to pump[23,24] reagents along micro-channels. Also, such devices are not amenable to rapid detection of pathogens where incubation for assays[25,26,27] and plate cultures can take days. Furthermore, in most of the aforementioned biosensing platforms, skilled personnel are required to operate expensive and sophisticated instrumentation, and to interpret data. This can be a deterrent, especially in the developing world where such equipment and personnel are not readily available.

Diagnostic devices for the developing world must be inexpensive, rugged, lightweight, and independent of supporting infrastructure.[28-34] Among the most successful of current systems are those that rely on lateral movement of fluids across nitrocellulose strips to distribute reagents (*e.g.,* dipsticks and lateral flow systems).[29,33] These systems are useful, but, as noted below, are limited in their

capabilities.[29,34] There is therefore significant interest in the development of portable and reliable bioassays for rapid and facile detection of small molecules, proteins and pathogens in the environment or food industries without the need of expensive and sophisticated instrumentation.

To address this need, several research groups have been investigating the potential of biologically modified paper as a platform for rapid detection of analytes. These include research networks such as the Sentinel Bioactive Paper Network in Canada[35] and VTT Technical Research Centre in Finland[36] as well as a growing number of research laboratories in the United States,[2] Australia[37] and Japan.[38] The key goal has been to utilize the unique properties of paper, such as its inherent potential for chromatography and movement of fluids by capillary action, compatibility with biological agents, sterility, abundance, cost effectiveness for large scale production and amenability to various formats such as dipsticks, lateral flow devices or filters, for applications is areas ranging from medicine[2] to environmental monitoring.[5,6]

Paper based sensors dates back to the mid twentieth century, with the first report, in 1956, and could monitor glucose levels in urine in the range of 0 – 2 wt% using physisorbed glucose oxidase, horseradish peroxidase and o-tolidine.[39] Since then, a number of simple test-strip based sensors have been reported, the most successful of which are based on lateral flow devices,[40,41] (e.g., the home pregnancy test strip) but such devices have not been developed for either multi-analyte detection or cellular targets, which are not easily adapted to lateral flow

and/or sandwich assays.[9,10] However, as reported by No et al.,[42] there are some commercially available lateral flow devices for pesticide and mycotoxins monitoring, such as the: Aflatoxin Test kit (Quicking Biotech Co., Ltd), Eclox™-Pesticide Strips, Neuro-IQ Tox Test Kit™, OP-Stick Sensor and Organophosphate/Carbamate Screen Kit. These devices are capable of detecting extremely toxic compounds, including: sarin, VX and Aflatoxin B_1 at levels approaching 20 ppb. However, the reproducibility and reliability of most of these test kits are not satisfactory. This was demonstrated in a recently conducted study by the U.S. Environmental Protection Agency which showed that 80% of the assays showed poor precision while 55% of tests carried out gave false positive results.[43] Therefore, there remains a need for more reliable, user friendly and multi-analyte lateral flow/dip-stick sensors.

In addressing this need, Martinez et al. (2007), proposed a rapid, colorimetric, paper-based biosensing platform where multiple bioassays are run simultaneously, in separate compartments, through hydrophobic channels on an absorbent paper surface that allows for analyte solutions to be directed into well-defined sensing areas. While this work is novel and exciting, the fabrication of the device itself required several time consuming and expensive steps, which preclude large-scale production. Consequently, the same group reported on a low cost printing technique for creating the hydrophobic patterns.[44] Parallel to this, other groups have proposed alternative methods to create such patterns. Abe et al. and Li et al. utilized ink-jet deposition of polystyrene and plasma treatment of

hydrophobic paper, respectively, for creating defined channels. Of these techniques, only ink-jet printing is scalable, cost effective and time efficient.[45-47] The others can be tedious and time consuming, and is not ideal for large scale manufacturing. Furthermore, in the aforementioned paper-based sensing platforms, the bio-recognition elements are physically adsorbed onto the paper surface, which can be of limited use in terms of retaining long term bio-activity of fragile enzymes and antibodies.[48,20] This leads to the major objectives of this thesis project, which includes the development of a simple, efficient, potable and cost effective biosensing platform that utilizes biocompatible sol-gel derived silica to not only entrap biomaterials, in fabricating portable sensors, but also to preserve enzyme bioactivity over prolonged periods and allow the extension of bioactive paper sensors to small molecule screening. Furthermore, toward automated sensor fabrication, we also investigated dip-casting and piezoelectric ink-jet printing as possible methods for the deposition of bio-doped sol-gel derived silica onto paper substrates. As part of this project, methods for the generation of enzyme-mediated color changes on paper were also investigated.

1.2 Project Description

The encapsulation of bio-molecules in sol-gel derived materials (mostly silica based) has provided a simple and viable platform for the development of portable, "solid-phase" and easily recycled bioanalytical devices for the detection of various target molecules – ranging from clinical[49] to environmental analytes.[50]

Furthermore, sol-gel encapsulation has been shown to enhance the activity of various bio-molecules over prolonged periods.[51, 20] Additionally, in this work, we demonstrate that sol-gel silica can be successfully integrated with paper substrates and is also compatible with piezoelectric ink-jet deposition. Taking advantage of these features, we have examined the potential of biocompatible sol-gel derive materials as a medium to co-entrap both an enzyme[23-56] and small gold nanoparticles (colorimetric reagent), which is printed onto a paper support, to allow for rapid solid-phase assaying of enzyme substrates and inhibitors; whether in the lab or onsite.

In recent times, gold nanoparticles (AuNP), owing to their bio-compatibility and high extinction coefficient, have been used in a number of areas ranging from biological labels, markers, and stains for various microscopies.[57] More recently, the use of AuNP have ventured into the realm of analytical chemistry and has been used fruitfully as molecular-recognition elements and signal amplifiers in sensors and biosensors, in addition to serving as components in various optical devices.[58] There have been a series of novel optical and electrochemical assays have been described based on the aggregation/deaggregation[59] or catalytic enlargement[60] of gold or other metal nanoparticles (NPs). In the first case, the biomolecule (usually DNA) is tagged with gold nanoparticles (AuNP), and addition of analyte leads to assembly or disassembly of NP labelled DNA, leading to a change in the distance of NPs and a color change. Nucleic acid functionalized semiconductor NPs have also been used as labels for the

electrochemical,[61] optical,[62] or photoelectrochemical[63] detection of DNA and as a sensing platform for aptamer and DNAzyme based sensors.[64] It is also possible to integrate this assay into a lateral flow device to perform solid-phase aptamer or antibody based assays.[65]

Moreover, the biocatalytic growth of AuNPs has also been employed as a sensing mechanism. Willner *et al.* have reported on several enzyme-mediated AuNP assays, including: the optical detection of NAD^+-dependent biocatalytic transformations based on the catalytic enlargement of AuNPs by the reduction of Au(III)[66] or Cu(II)[67] with NAD(P)H cofactors; analysis of tyrosinase-generated neurotransmitters,[68] the detection of glucose either directly[69] or using an Os(III) mediator;[70] and the detection of AChE inhibitors using the thiocholine product to reduce Au(III) onto AuNPs that were immobilized onto glass slides.[71] In all these examples, a unique feature of AuNP are utilized where particle growth results in an increase of the localized plasmon absorbance band associated with NP of such dimensions and a concomitant increase in color intensity that can be correlated to the amount of analyte present. Specifically in our work, the use of AuNP as a sensing mechanism has an added advantage in that, unlike organic chromophores, grown AuNP cannot leach from the silica material, allowing for retention of signal and lower limits of detection. This leads to a solid-phase assay that has the potential to be integrated into a portable biosensing platform that can utilize visual detection or simple color intensity analysis of optical images – negating the need for sophisticated and expensive instrumentation.

As the bio-recognition element, we chose the enzyme acetylcholinesterase (AChE) as a model system, owing to its relatively high stability, established colorimetric assays and its importance as a bio-recognition element in areas ranging from environmental monitoring[72-76] to food handling.[77,78] Furthermore, this enzyme has previously been shown to remain functional in sol-gel derived materials,[79] and can be used to catalyze the hydrolysis of acetylthiocholine (ATCh) to thiocholine (Th), which had earlier been shown to reduce Au(III) onto AuNPs in solution.[71] This forms the basis of our proposed paper-based, colorimetric, small-molecule, solid-phase biosensing platform.

1.3 Thesis Outline

The goals of this thesis include: (1) the integration of the AuNP based solution assay[71] into a solid-phase platform and to assess whether or not AuNP can be quantitatively grown within the confines of a sol-gel matrix; (2) assessing the compatibility of sol-gel derived silica with paper-based materials; (3) the investigation of deposition techniques for bio-doped sol-gel materials onto paper substrates and; (4) assessment of the applicability of the assay platform in detecting inhibitors of AChE.

Chapter 2 provides a literature review that describes the background details of biosensors and bioactive paper, immobilization methods, sol-gel processing, deposition techniques for sensor fabrication, as well as a brief description of our

model system and its components, the significance of AChE along with AuNP plasmon theory and applications.

In Chapter 3 the development of the solid phase AChE assay based on enlargement of sol-gel entrapped gold nanoparticles is described. Using a 96-well plate format, we first investigated whether or not it was possible to quantitatively grow AuNPs within the confines of a sol-gel derived silica matrix. Once this was established, issues such as optimization of silica materials, effect of AuNP capping agent as well as the influence of reagent levels on signal and background intensities, and the time dependence of particle enlargement within the pores of silica materials were examined. Using optimum conditions, the effect of inhibitor concentration on AChE activity, AuNP growth and signal levels were also assessed.

Chapter 4 describes a simple dip-casting method to deposit AChE/AuNP doped sol-gel derived silica onto paper strips in order to show that this solid-phase assay platform can remain functional on such surfaces. In this section we also examined the effects of paper type, surface coating/modification and silica material composition on coating stability, signal levels and long term stability of AChE and demonstrated the potential of the AuNP assay method for development of paper based dipstick sensors.

In Chapter 5 the use of piezoelectric ink-jet printing as a method for automated deposition of sol-gel derived materials containing AChE is described, focusing mainly on strategies for printing these materials onto paper and retaining

bio-activity. For assaying, the standard Ellman method[80] was used to reduce assay times. Issues with the Ellman assay when coupled to our sol-gel based platform, such as leaching and bleaching of the color forming agent were also addressed with the employment of a novel capture agent which also enhanced signal levels. Results from inhibition studies are also provided.

Finally, Chapter 6 provides a summary of this thesis project, overall conclusions and discusses the future outlook as well as the significant contributions of this work to the development of bioactive paper.

1.4 Reference

1. Manihar Situmorang, M.; Gooding J.J.; Hibbert, D.B. *Analytica Chimica Acta* **1999,** *394(2-3),* 211-223

2. Martinez, A.W.; Phillips, S.T.; Butte, M.J.; Whitesides, G.M. *Agnew. Chem. Int. Ed.* **2007,** *46,* 1318-1320.

3. Rhemrev-Boom, M. M.; Korf, J.; Venemaa, K.; Urban, G.; Vadgama, P. *Biosensors and Bioelectronics,* **2001,** *16(9-12),* 839-847.

4. Bucur, B.; , Danet, A.F.; Marty, J-L. *Biosensors and Bioelectronics.* **2004,** *20(2),* 217-225.

5. Hossain, S.M.Z.; Luckham, R.E.; Smith, A.M.; Lebert, J.M.; Davies, L.M.; Pelton, R.H.; Filipe, C.D.M.; Brennan, J.D. *Anal. Chem.*, 2009, in press.

6. Hall, E.A.H.; *Biosensors,* Prentice Hall, **1991,** 6-7.

7. Vo-Dinh, T.; Cullum, B. *Fresensius J. Anal. Chem.* **2000,** *366,* 540-551.

8. Wittman, C., Riedel, K., Schmid, R.D., 1997. Microbial and enzyme sensors for environmental monitoring. In: Kress-Rogers, E. (Ed.), Handbook of Biosensors and Electronic Noses. CRC, Boca Raton, FL, pp. 299-332.

9. Gonchar, M.; Maidan, M.; Korpan, Y.; , Sibirny, V.; Kotylak, Z.; Sibirny, A. *FEMS Yeast Research, 2(3),* **2006,** 307-314.

10. Martinez, A.W.; Phillips, S.T.; Carrilho. E.; Thomas, S.W. (III); Sindi, H.; Whitesides, G.M. *Anal. Chem. 80,* **2008,** 3699-3707.

11. Lazcka, O.; Del Campo, F.J.; Munoz , F.X. *Biosensors and Bioelectronics,* **2007,** *22* 1205–1217.

12. Kaisheva, A.; Iliev, I.; Christov S.; Kazareva R. *Sensors and Actuators B: Chemical* **1997**, *44 (3),* 571-577.

13. Liu, J.; Yi Lu, Y. *J. Am. Chem. Soc.*, **2003,** *125 (22),* 6642–6643.

14. Bart, C.J.; Judd, L.L.; Hoffman, K.E.; Wilkins, A.M.;. Kusterbeck, A.W. *Environ. Sci. Technol.*, **1997,** *31(5),* 1505–1511.

15. Nath, N.; Eldefrawi, M.; Wright, J.; Darwin, D.; Huestis, M. *J Anal Toxicol.* **1999,** 23*(6),* 460-467.

16. Rowe, C.A.; Tender, M.L.; Feldstein, M.J.; Golden, J.P.;. Scruggs, S.B.; MacCraith, B.D.; Cras, J.J.; Ligler. F.S. *Anal. Chem.* **1999,** *71,* 3846-3852.

17. Brennan, J.D.; *J. Fluorescence, 9(4),* **1999,** 295-302.

18. Lin, T.-J.; Huang, K.-T.; Liu, C.-Y. *Biosens. Bioelectron.* **2006**, *22*, 513-518.

19. Sotiropoulo, S.; Chaniotakis, N.A.; *Anal. Bioanal. Chem.* **2003,** *375,* 103.

20. Hrapovic, S.; Liu, Y.; Male, K.; Luong, J.H. *Anal. Chem.* **2004,** *76,* 1083.

21. Micheli, L.; Greco, R.; Badea, M.; Moscone, D.; Palleschi, G. *Biosens. Bioelectron.* **2005**, *21*, 588-596.

22. Gill, R.; Bahsahi, L.; Freeman, R.; Willner, I. *Angew. Chem.* **2008**, *120,* 1700-1703.

23. Chou, H.-P.; Spence, C.; Schere, A.; Quake, S. *Proc. Natl. Acad. Sci. U.S.A.* **1999**, *96*, 11-13.

24. Anderson, J. R.; McDonald, J. C.; Stone, H. A.; Whitesides, G. M. *Anal. Chem*. appeared

25. Masuda, G.; Tomoika, S.; Hasegawa, M. *The Journal of Antibiotics*. **1976,** *29(6),* 662-664

26. Aitman, T.J. *Br. Med. J.* **2001,** *323,* 611-615.

27. Chang, A.-C.; Gillespie, J.B.; Tabacco, M.B. *Anal. Chem.* **2001**, *73, 467.470.*

28. Martinez, A.W.; Phillips, S.T.; Carrilho, E; Thomas (III), S.W.; Sindi, H.; Whitesides, G.M. *Anal. Chem.* **2008**, *80 (10),* 3699–3707.

29. Chin, C.D.; Linder, V.; Sia, S.K. *Lab Chip.* **2007,** *7,* 41–57.

30. Daar, A.S.; Thorsteinsdóttir, H.; Martin, D.K.; Smith, A.C.; Nast, S.; Singer, P.A. *Nat Genet.* **2002,** *32,* 229–232.

31. Sia, S.K.; Linder, V.; Parviz, B.A.; Siegel, A.; Whitesides, G.M. *Angew Chem Int Ed Engl.* **2004**,*. 43,* 498–502.

32. David Mabey, D.; Peeling, R.W.; Ustianowski, A.; Perkins, M.D. *Nat Rev Microbiol.* **2004,** *2,* 231–240.

33. von Lode, P. *Clin Biochem.* **2005,** *38,* 591–606.

34. Willis, R.C. *Anal Chem.* **2006,** *78,* 5261–5265.

35. SENTINEL - The Bioactive Paper Network; www.bioactivepaper.com.

36. VTT Technical Research Centre – Finland; www.vtt.fi

37. Li, X.; Tian, J.; Nguyen, T.; Shen, W. *Anal. Chem.* **2008,** *80,* 9131-9134.

38. Abe, K.; Suzuki, K.; Citterio, D. *Anal. Chem.* **2008,** *80,* 6928-6934.

39. Comer, J.P. *Anal. Chem.* **1956,** *28,* 1748-1750.

40. von Lode, P. *Clin. Biochem.,* **2005,** *38,* 591-599.

41. Mabey, D.; Peeling, R.W.; Ustianowski, A.; Perkins, D.M. *Nat. Rev.,* **2004,** *2,* 231-240.

42. No, H-Y.; Kima, Y.A.; Lee Y.T.; Lee, H-S. *Analytica   Chimica Acta.* **2007,** *594,* 37–43.

43. Detecting Chemical Agents and Pesticides in Water, Using Enzymatic Test Kits – www.epa.gov/nhsrc/news/news070708a.html

44. Bruzewicz, D.A.; Reches, M.; Whitesides, G.M. *Anal. Chem.* **2008,** 80 (9), 3387–3392.

45. deGans, B.J.; Hoeppener, S.; Schubert, U.S.; *Adv. Mater.* **2006,** *18,* 910-913.

46. deGans, B.J.; Hoeppener, S.; Schubert, U.S.; *J. Mater.Chem.* **2007,** *17,* 3045-3050.

47. Schubert, U.S. *Macromol. Rapid Cpmmun.* **2005,** *26,* 237.

48. Pandey, P.C.; Upadhyay, S.; Pathak, H.C.; Pandey, C.M.D.; Tiwari, I. *Sensors and Actuators B,* **2000,** 62, 109–116.

49. Sampath, S.; Lev, O. *J. Electroanalysis.* **1996,** *8,* 1112.

50. Du, D.; Chen, S.; Cai, J.; Zhang, A. *Talanta* **2008,** *74,* 766-772.

51. Jin, W; Brennan, J.D. *Anal. Chim. Acta,* **2002,** *461,* 1-36.

52. Gill, I. *Chem. Mater.* **2001**, *13*, 3404-3421.

53. Avnir, D.; Coradin, T.; Lev. O.; Livage, J. *J. Mater. Chem.* **2006**, *16*, 1013–1030.

54. Pierre, A.C. *Biocat. Biotrans.* **2004**, *22*, 145-170.

55. Coradin. T.; Boissiere, M.; Livage, J. *Curr. Med. Chem.* **2006**, *13*, 99-108.

56. Besanger, T.R.; Brennan, J.D. *J. Sol-Gel Sci. Technol.* **2006**, *40*, 209-225.

57. Matsumoto, M.; Yoshimura, H.; Kulkarni, V.S.; Nagayama, K. *Colloid Polym. Sci.* **1990**, *268*, 1174.

58. Daniel, M.C.; Astruc, D. *Chem. Rev.* **2004**, *104*, 293.

59. Elghanian, R.; Storhoff, J.J.; Mucic, R.C.; Letsinger, R.L; Mirkin, C.A. *Science* **1997**, *277*, 1078-1080.

60. Willner, I; Baron, R; Willner, B. *Adv. Mater.* **2006**, *18*, 1109-1120.

61. (a) Wang, J.; Liu, G.; Polsky, R.; Merkoci, A. *Electrochem. Commun.* **2002**, *4*, 722-726. (b) Wang, J.; Liu, G.; Merkoci, A. *J. Am. Chem. Soc.* **2003**, *125*, 3214-3215. (c) Wang, J.; Xu, D. K.; Kawde, A. N.; Polsky, R. *Anal. Chem.* **2001**, *73*, 5576-5581.

62. (a) Bruchez, M.; Moronne, M.; Gin, P.; Weiss, S.; Alivisatos, A. P. *Science* **1998**, *281*, 2013-2016. (b) Chan, W.C.W.; Nie, S. *Science* **1998**, *281*, 2016-2018.

63. Willner, I.; Patolsky, F.; Wasserman, J. *Angew. Chem. Int. Ed.* **2001**, *40*, 1861-1864.

64. Pavlov, V.; Xiao, Y.; Shlyahovsky, B.; Willner, I. *J. Am. Chem. Soc.* **2004**, *126*, 11768 –11769.

65. Liu, J.; Mazumdar, D.; Lu, Y. *Angew. Chem. Int. Ed.* **2006**, *45*, 7955-7959.

66. Xiao, Y.; Pavlov, V.; Levine, S.; Niazov, T.; Markovitch, G.; Willner, I. *Angew. Chem.* **2004**, *116*, 4619–4622; *Angew. Chem. Int. Ed.* **2004**, *43*, 4519–4522.

67. Shlyahovsky, B.; Katz, E.; Xiao, Y.; Pavlov, V.; Willner, I. *Small* **2005**, *1*, 213-216.

68. Baron, R.; Zayats, M.; Willner, I. *Anal. Chem.* **2005**, *77*, 1566-1571.

69. Zayats, M; Baron, R; Popov, I; Willner, I. *Nano Lett.* **2005**, *5*, 21-25.

70. Xiao, Y.; Pavlov, V.; Shlyahovsky, B.; Willner, I. *Chem. Eur. J.* **2005**, *11*, 2698-2704.

71. Pavlov, V.; Xiao, Y.; Willner, I. *Nano Lett.* **2005**, *5*, 649-653.

72. Trojanowicz, M.; Hitchman, M.L. *Trends in Analytical Chemistry.* **1996**, *15(1)*, 38-45.

73. Nunes, G.S.; Montesinos, T.; Marques, P.B.O.; Fournier, D.; Marty, J.L. *Analytica Chimica Acta.* **2001**, *434(1)*, 1-8.

74. No, H.; Kim, Y.A.; Lee, Y.T.; Lee, H. *Analytica Chimica Acta.* **2007**, *594*, 37–43.

75. Sotiropoulou, S.;. Chaniotakis, N.A . *Anal. Chim. Acta* **2005**, *530*, 199–204.

76. Amine, A.; Mohammadi, H.; Bourais, L.; Palleschi, G. *Biosens. Bioelectron.* **2006**, *21*, 1405–1423.

77. Arduini, F.; Errico, I.; Amine, A.; Micheli, L.; Palleschi, G.; Moscone, D. *Anal. chem.* **2007**, *79*, 3409-3415.

78. Kolosova, A.Y.; De Saeger, S.; Sibanda, L.; Verheijen, R.; Van Peteghem, C. *Anal Bioanal Chem.* **2007**, *389*, 2103–2107.

79. a) Anitha, K,.; Mohan, S.V.; Reddy, S.J. *Biosens. Bioelectron.* **2004**, *20*, 848-856; b) Doong, R.-A.; Tsai, H.-C. *Anal. Chim. Acta* **2001**, *434*, 239-246; c) Du, D.; Chen, S.; Cai, J.; Zhang, A. *Biosens. Bioelectron.* **2007**, in press.

80. Ellman, G. L.; Courtney, K. D.; Andres, V.; Featherstone, R. M. *Biochem. Pharmacol.* **1961,** 7, 88-95.

Chapter 2: Literature Review

2.1 Biosensors

Over the past four decades, biosensors have become an important area of study in analytical chemistry; given their versatility, sensitivity, portability, cost effectiveness, reliability and ease to use. [1–5] Biosensors are defined as analytical devices which measure (whether quantitatively or semi-quantitatively) a given target analyte by utilizing a biological response that is converted (*via* a transducer) into a measurable signal.[6] These devices are categorized according to the bio-recognition elements employed and the type of transducers used.[2] There are four basic categories of transducers and these are: optical, electrochemical, thermal or mass sensitive devices[7] while common bio-recognition elements or bio-receptors include[2]: antibodies, enzymes, nucleic acids, and whole cells[8,9] (for *e.g.*, yeast cells and bacteria). These allow for high sensitivity and selectivity.

There are several advantages associated with biosensors. Apart from their high sensitivity and selectivity and (in most cases), resistance to matrix effects, these devices can be made portable.[10] As a result, some biosensors can be taken into the field to do on site, rapid screening.[5] Furthermore, in the developing world where expensive instrumentation is usually not available, biosensors are particularly useful as they are normally cheaper than traditional analytical devices and give (in some cases) comparable accuracy.[11] Furthermore, biosensors are also versatile in the sense that they can be used for detecting (at clinically relevant and

sub-lethal levels) a wide range of target molecules, some of which are: biomedical analytes,[9] gases,[12] metal ions,[13] narcotics,[14] bacteria[15] and viruses.[9,16]

Notwithstanding these advantages, there are a few issues that need to be overcome with current biosensors, and as noted earlier, lead to the work of Martinez *et al.* (2007) which describes simple paper biosensors that requires no power or sophisticated instruments. In this work, papers' inherent features, such as its ability to support capillary action are utilized to rapidly screen for multiple analytes. Furthermore, with current biosensors, only a limited number of analytes can be detected. Moreover, such devices are not amenable to rapid detection of pathogens where incubation times for assays[17,18,19] and plate cultures can take days. Also, taking into consideration that *E.coli* are responsible for an estimated 73,000 cases of infection and 61 deaths per year in the United States alone (Center for Disease Control and Prevention) the sensitivity of bacteria sensors are of critical importance. Typical sensors report limits of detection on the order of 2.5×10^4 cells/mL[20] of live *E. coli* O157: H7 and with the presence of a single strain being potentially fatal,[21] leaves much scope for further improvement.

With recent bioterror attacks[22] and the unleashing of biowarfare,[23] much attention has been placed on developing biosensors to detect a wide range of neurotoxins; ranging from organophosphate and carbamate pesticides to nerve gasses and mycotoxins. Biosensors for the determination of these compounds include: optical and electrochemical biosensors,[24-27] surface plasmon resonance,[28] semiconductor quantum dots,[29] ion-selective field-effect transistors (ISFET),[30]

carbon nanotube,[31] and nanoparticle based sensors,[32,33] as well as several immunoassays.[34,34] Though these systems have high selectivity and adequate sensitivity, almost all of them either required sophisticated instrumentation, skilled operators, significant sample pretreatment, and/or long analysis times. Moreover, most of these detection systems are not amenable to rapid screening in emergency situations, in remote settings or in developing countries, where simple and portable bioassays are essential for monitoring toxic compounds in the environment or foodstuffs. Consequently, as reported by No et al.,[35] a number of commercial test kits were developed to screen for these compounds, which include: Envirologix EP-014 (Portland, USA.), Organophosphate/Carbamate Screen kit (Abraxis, Warminster, USA), Neuro-IQ Tox Test Kit (Aqua Survey Inc., Flemington, USA), GT Pesticide Test Kit (gttestkit@gttestkit.com), OP Stick Sensor (Protein-Biosensor, Toulouse cedex, France), EcloxTM – Pesticide Strips (Seven Trent Services, Colmar, USA), AgraQuant® kits, Aflatoxin Test kit (Quicking Biotech Co., Ltd), Eclox™-Pesticide Strips, Neuro-IQ Tox Test Kit™, and Graintec (Pty Ltd). However, the reproducibility and reliability of most of these test kits are not satisfactory. This was demonstrated in a recently conducted study by the U.S. Environmental Protection Agency which showed that 80% of the assays showed poor precision; while 55% of tests carried out gave false positive results.[36] Therefore, there remains a need for more reliable, user friendly and multi-analyte lateral flow/dip-stick sensors.

2.2 Bioactive Paper

In recent times there has been widespread interest in the development of cost effective assay platforms with regard to rapid screening of specific target analytes whether in the health sector, food industry or in the environment. Paper, being relatively cheap, sterile and abundant has been the focus of much attention with regards to the development of paper based analytical devices. Consequently, research networks such as the Sentinel Bioactive Paper Network in Canada[37] and VTT Technical Research Centre in Finland as well as a few research laboratories in the United States,[6] Japan[38] and Australia;[39] have been working to develop "bioactive paper" which is essentially a platform for simple, portable and economically feasible biosensors. These products not only target the global market, but specifically the developing world.

The vision of Sentinel (The Canadian Network for the Development and use of Bioactive Paper) is to exploit the unique properties of paper such as its sterility and defined porosity to create bioactive paper that will not only capture but deactivate pathogens in air, water and food.[12] Also, it is envisioned that such paper devices be used as passive barriers and filters in food packaging and for (quick and easy) water purification in remote areas.[12] The latter being of particular importance in underdeveloped countries where the availability of safe drinking water[40] is at present, non-existent.

A brief review of literature for bioactive paper devices is provided in chapter 1.
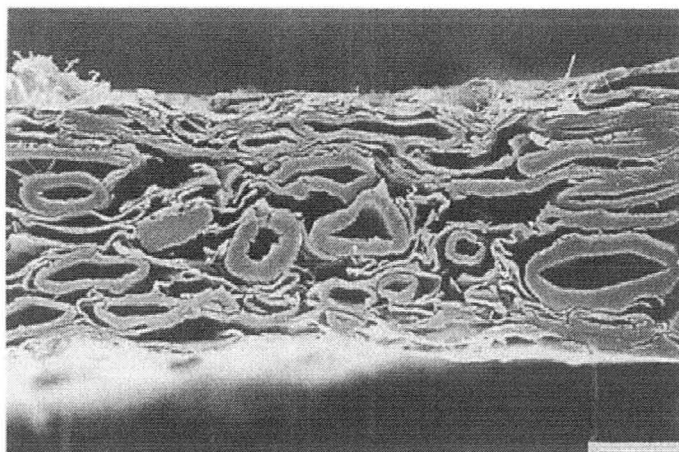
Figure 2.1. *SEM image depicting a cross section of newsprint paper substrate. Image shows paper thichness of ~ 8 fibres. Side bar = 25μm. Image extracted from J.C. Roberts.*[41]

2.3 Overview of Paper Chemistry

Paper substrates are derived from fibrous cellulose based plant material and have been a part of human civilization for at least 2 millennia. J.C. Roberts[42] defines paper as a sheet material made up of a network of natural cellulosic fibres which has been deposited from an aqueous suspension. The resulting product consists of a network of interlocking fibres, layered to a thickness of about 3 – 300 μm. The thickness of individual fibres fall in the range of between 10 – 50 μm, hence, as illustrated in Figure 2.1, a sheet of paper on the order of 100 μm thick would comprise of about 5 – 10 layered cellulosic fibres.
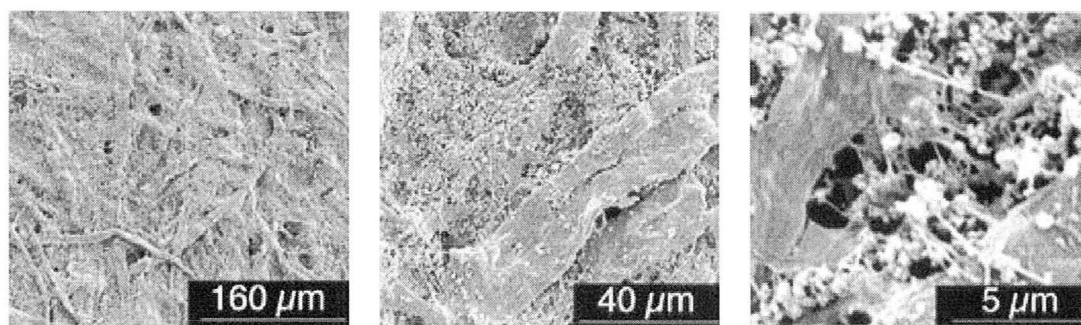
Figure 2.2. *SEM images showing the non-uniform nature of a paper substrate at different magnification.*
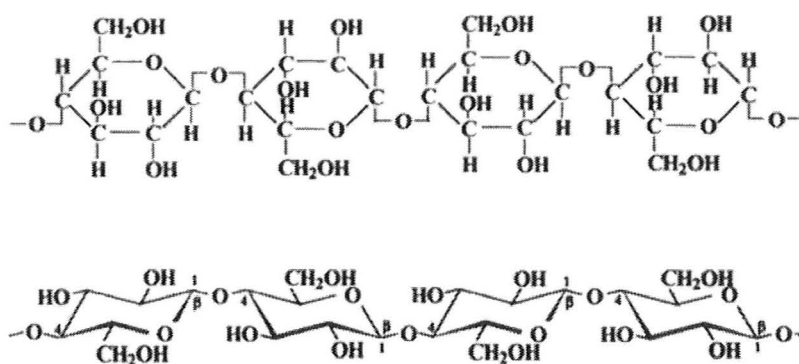
Figure 2.3. *Molecular structure of cellulose. Image extracted from J.C. Roberts*[43]

The non-uniform nature of paper is also evident in the above figure but more so in Figure 2.2. On the microscopic level, most paper types do not possess a homogeneous topography and so quantitative loading of any material on its surface[39] such as bio-material loading for biosensor fabrication, is not easy. However, paper materials are very versatile in the sense that they can be tuned,

both physically and chemically, with a wide range of fillers and additives to suit specific applications.

Cellulose, being the major component of paper, has significant bearing on the physical and chemical properties of this material. For instance, the surface charge of uncoated paper is inherently negative, in most part due to ionized hydroxyl groups associated with this polymer (Figure 2.3). Other ionisable groups include carboxylic groups, sulphonic acid groups, catecholic groups and phenolic groups. Even though not naturally associated with cellulose, these functional groups are present on cellulosic paper fibres due to the presence of other wood components such as uronic acid residues and through chemical processes, such as sulphite bleaching during paper making.[44] The surface charge imparts high hydrophilicity to the material and given its relative high porosity, aqueous solutions are readily absorbed and can spreads through the material in unpredictable ways.[39]

To offset this, various fillers and additives are used to change the physio-chemical properties of the paper material; to suit defined purposes. For instance fillers such as: kaolin, titanium dioxide, calcium carbonate, hydrated alumina, silica and talc are used to give paper added bulk as well as to improve its opacity and printing properties,[45] by increasing the control with which liquids can penetrate. The various coated paper types used in this work, which ranged from coated packing material to high gloss calendar paper, all utilize fillers of some sort, however, the exact composition was not disclosed by manufacturers, though
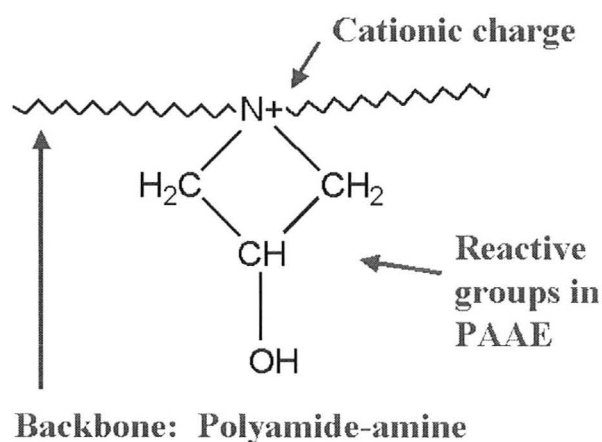
Figure 2.4. *Simplified structure of polyamidoamine-epichlorohydrin resin (PAAE) depicting reactive groups and cationic binding sites. Image taken from Mini-Encyclopedia of Papermaking.*[46]

such fillers are likely to be either clay (kaolin) or chalk (calcium carbonate) as these are relatively cheap and abundant.

Other features of paper that can be tailored are the wet and dry-strengths, which refer to the tensile strength of the paper matrix and its ability to withstand moisture, respectively.[47] Chemical additives, both dry-strength and wet-strength additives, are used to enhance the quality of the paper, by increasing its tensile, burst, internal bonds, and wet strengths. Paper strength is dependent of the strength of individual fibres, the strength of inter-fibre bonds and the distribution of such bonds.[48] In relatively untreated paper types, such as tissue paper and, in the case of this work, Timbec softwood pulp, hydrogen bonding and van der Waals interact are responsible for the integrity of the cellulose network. These relatively weak bonds are water sensitive and so in the presence of moisture, significant swelling and network disruption can occur. This is not particularly

useful for making paper-based biosensors and dip-sticks. Therefore, as a result of the need for paper products that can retain some strength when exposed to high humidity or when soaked in water, chemical wet-strength resins have been developed. Wet-strength additives such as: polyamidoamine-epichlorohydrin, urea-formaldelyde resins, melamine-formaldehyde resins, epoxidised polyamide resins and gyloxalated polyacrylamide resins, being cationic (at pH > 8), bond to the negatively charged cellulose fibres and given the presence of functional groups such as amino, carboxyl, and hydroxyls groups (Figure 2.4), result in homo and co-crosslinking which gives rise to a paper matrix that is more resistant to moisture.[49] Consequently, some cardboard type paper materials, such as the mead brand, have significantly greater wet strength relative to paper materials such as Timbec softwood pulp and so can tolerate immersion into aqueous solutions, for longer periods, without bending or curling. These paper types are preferred, especially in this work, where immersion into aqueous solution is required.

In a similar way to wet-strength additives, dry-strength additives enhance paper strength by enhancing inter-fibre bond strengths as well as increasing the number of binding events that may occur. Common dry-strength additives are cationic starch, vegetable gum and polyacrlamide resins.[50] All of these additives work in the same way – with the ultimate aim being to decrease the average distance between fibres, within the network, in promoting H-bonding. Cationic starch binds to cellulose fibres and given its bulk, fills in spaces within the matrix

allowing for H-bonding interaction between adjacent fibres and adsorbed starch molecules. This creates a more rigid network that is able to withstand greater shear. Similarly, vegetable gum, a hydrophilic, viscous polysaccharide also provides bulk while supplying more H-bonding sites between adjacent fibres to enhance rigidity. On the other hand, polyacrlamide resins provided additional bonding for fibres that are too far apart for H-bonding to occur.[51]

With the use of fillers and additives, cellulose fibres can be molded into paper that meet specific needs, such like tissue papers' ability to disintegrate in water, chromatography papers' capacity to absorb liquids without disintegration, and the ability of cardboard type materials to withstand liquid immersion for prolonged periods.

2.4 Protein Immobilization and Sol-gel Entrapment

There are many immobilization techniques available where biosensor components are fixed in place.[52,53] The most commonly used methods for immobilizing biomolecules onto solid supports are based on physical adsorption,[54] covalent binding to the surface,[55] entrapment in semi-permeable membranes,[56] and encapsulation against hydrogels and polymeric microspheres[57,58] (Figure 2.5). There are many advantages and disadvantages associated with these immobilization methods, some of which are discussed below with emphasis on its potential toward bioactive paper sensor assembly.
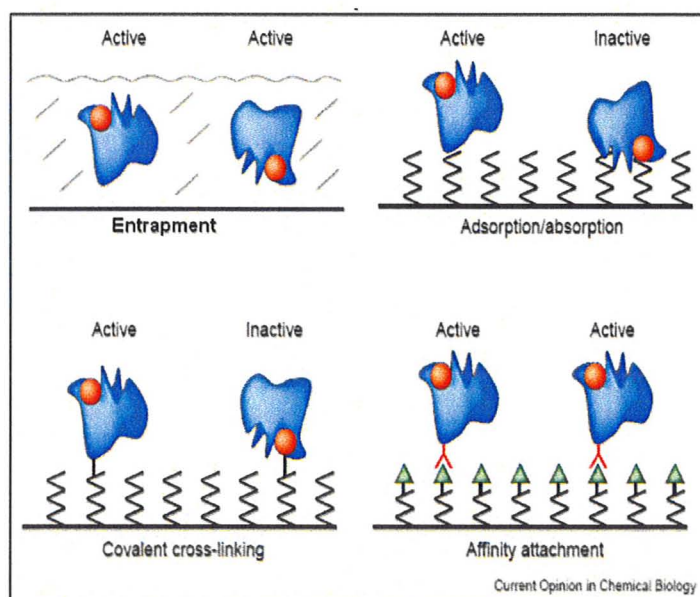
Figure 2.5. *Methods for immobilizing protein on solid supports for sensing. Figure modified from: Zhu and Snyder, 2003.*

Physisorption is the most simple and the most commonly used immobilization technique in bioactive paper sensor fabrication. Here biological species are immobilized by simple addition to the surface of choice, and based on electrostatic interactions, H-bonding, Van der Waals interactions, etc, are fixed in place. There are many disadvantages associated with this method as simple washing steps can remove the immobilized species from the surface. Furthermore, there is no control over the orientation[59] of the bio-recognition element and in the case of enzymes and other such species, the active sites can be blocked and so render it inactive.

Covalent immobilization of bio-recognition elements utilizes a covalent interaction between recognition molecules and the support surface. For example,

Vienello, *et al.* covalently attached laccase onto a hydrophilic matrix by carbodiimide chemistry in fabricating an amperometric flow biosensor to monitor phenolics in olive oil mill waste water.[60] This sensor detected phenolics on the order of 30 nM; however, the immobilization of the enzyme required multiple steps with no control over active site orientation (Figure 2.5). Another disadvantage of this immobilization technique is that the biomolecules may require chemical modification in order to be bound to the surface, which may lead to denaturation.[24] Multiple steps and surface pre-treatment may not be suited to bioactive paper sensor manufacture where certain delicate paper types (*e.g.* chromatography paper) may not be able to withstand such processing. Furthermore, multiple steps and surface pre-treatment could increase production costs which preclude low cost paper biosensors.

Perhaps the best means of protein attachment, in terms of control over orientation, is by highly specific affinity, covalent interactions.[61,62] Here, proteins are fixed to surfaces by high-affinity tags at their amino or carboxylic terminus, hence, all proteins should orient themselves, in similar manner, away from the surface. A typical example is illustrated by Johnsson *et al.*,[63] who investigated affinity interaction strategies such as: primary amine group attachment, thiol/disulfide exchange, aldehyde and biotin-avidin coupling; for immolilizating antibodies onto a carboxymethyl dextran-based surface. Their results showed reduced activities of immobilized antibodies; which they attributed to deterioration of the antibodys' active site that was induced by variation of the

coupling conditions. Furthermore, such methods require expensive reagents[64] and with an objective of large scale production of cheap paper sensors, it is not ideal.

The forth of the immobilization techniques is entrapment, where the bio-recognition molecules are entrapped within a three-dimensional matrix. Typical matrices include organic polymers such as nylon or poly(acrylamide),[65] and inorganic materials such as sol-gel derived silica.[66] In this case, the species entrapped are not bound to the support surface, but are orientated within the three-dimensional network of the entrapment media in such a way that the active regions are accessible from all directions. The porosity of the matrix is such that it allows for the entrapment of the relatively large biomolecules while allowing for the flow of small analyte molecules and substrates into the region containing the biosensing agents. Potential disadvantages of encapsulation within organic polymers are the chemical processing conditions, which may lead to degradation of the biological species. Furthermore, some polymer materials may also be prone to swelling[67] when in contact with aqueous solutions and so leaching of the biomaterials could result.

The revelation that various biomaterial can be entrapped within sol-gel derived silica and retain significant bioactivity, has paved the way for a variety of sensing applications. Sol-gel is a process whereby porous ceramic and glass materials are made from a precursor colloidal solution, at room temperature[68]. As a result, this makes biomaterial encapsulation possible with relative ease, which is perhaps the most intriguing aspect of sol-gel immobilization. Molecular

incorporation is achieved by simply adding the desired dopant to the gelation buffer followed by mixing of buffer and silica precursor.

The sol-gel process comprises multiple steps that utilize metal or semimetal alkoxide precursors such as: tetraethylorthosilicate[69] (TEOS) tetramethylorthosilicate[20] (TMOS) or more biocompatible precursors such as sodium silicate[70] (SS) or diglyceryl silane[71] (DGS). The alkoxysilane is hydrolysed (with the exception of the pre-hydrolysed precursor; SS and DGS, which do not require an acid catalyst) in the presence of an acid catalyst, forming hydroxylated silicone species and an alcohol by-product (*e.g.* ethanol in the case of TEOS and methanol in the case of TMOS).[20,33]

The hydroxysilane species then interact with each other in multiple condensation reactions, releasing water and forming siloxane bonds. Figure 2.6 shows the process for protein entrapment in a SS matrix. Further condensation and poly-condensation steps continues with time, resulting in interconnected siloxane bonds in a specific region, consequently forming colloidal particles on the order of 50-100 nm throughout the sol. The rate of the poly-condensation reaction is dependent in the pH and ionic strength of the solution; as a result gelation times can vary from a few minutes to a few days.
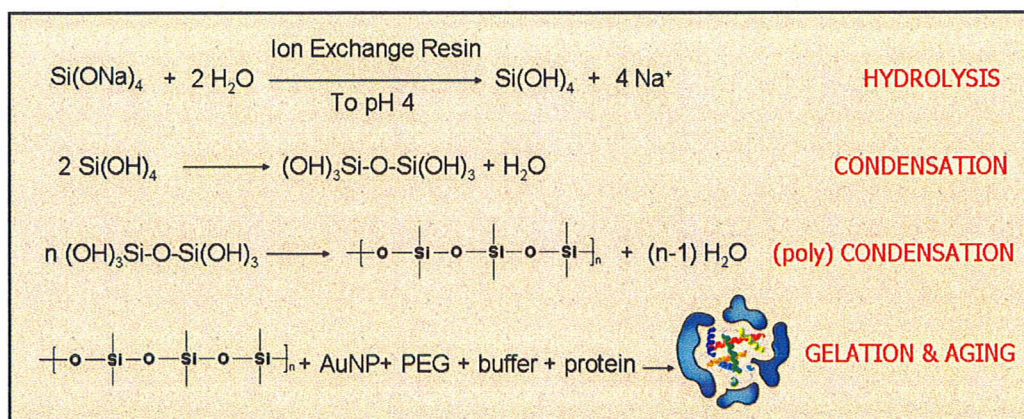
Figure 2.6: *The sol-gel encapsulation process using sodium silicate.*

Given sufficient time, the colloidal particles and condensed silica species link together to form a rigid three-dimensional network in which biologicals and other reagents can be entrapped.

The use of silica-based precursors for the encapsulation of biomaterials has many advantages, and has been extensively reviewed by major contributors such as Avnir, [72,73] Brennan[74,75] and Lev.[76] In the first case, the glass matrix formed is optically clear and non-fluorescent; allowing for spectroscopic studies. Secondly, the sol-gel derived matrices have tunable porosity, allowing small molecules to diffuse though the matrix while entrapping larger biomolecules and higher molecular weight polymers (Figure 2.7). In addition, organically modified silanes and polymers can be added to further alter the porosity of the matrix to suit specific purposes. Thirdly, there is a significant amount of interstitial water molecules within the glass matrix, which help to hydrate the immobilized biomaterials – which is necessary for bioactivity retention after immobilization.[77]
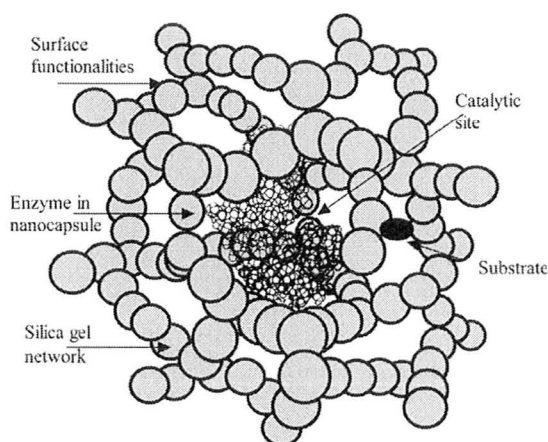
Figure 2.7. *Method of entrapping bio-materials within sol-gel derived silica materials. Figure extracted from: Pierre, 2004.*

Fourthly, sol-gel derived glass materials are chemically inert, photochemically and thermally stable and resistant to biodegradation – making these materials highly suited for biosensor fabrication. Fifthly, the gels using the aforementioned silica materials are formed at ambient temperatures and so biomaterial degradation due to elevated temperatures is not an issue. The polarity of the matrix can also be altered with the addition of various polymers and organically modified silanes making these material highly versatile.

Given the many advantages of biomaterial encapsulation by sol-gel derived materials, we chose this as the method of biomaterial immobilization for our solid phase paper-based biosensing platform. However, an important area of focus is the choice of deposition technique; which is essential in large scale manufacturing of such devices.

2.5 Methods for Sol-Gel Material Deposition in Biosensor Fabrication

There are a number of techniques available from which biomaterial and other reagents are deposited onto solid supports for the fabrication of portable devices and biosensors. For biosensor fabrication (in general), and more so, in the case of this work, deposition of encapsulated biomolecules on a solid surface is a critical step. Several conventional deposition techniques such as dip-coating,[78] spin coating,[79] aerosol spraying,[80] screen printing,[81] and electrophoretic deposition[82] have been used to deposit sol-gel materials. Among these, aerosol spraying, dip and spin coating are not favorable for large-scale production, as they are often time consuming and become unattractive and wasteful when dealing with expensive bioreagents.[80] Screen printing, and electrophoretic deposition are used usually for electrochemical electrode fabrication and can be used for efficient sol-gel sol deposition, however, these procedures can be expensive and tedious to operate.

In recent times, ink-jet printing of biomaterials has attracted much attention. This reflects the fact that this technique is scalable, and able to perform selective non-contact deposition[83-88] which is more suited to the deposition of bio-doped sol-gel derived materials than the aforementioned techniques. Moreover, given the non-contact capabilities of this technique, a variety of biomaterials can be deposited on a solid support in single and multiple layers at ambient temperature with activity retained for an extended period.[78] Using this technology, cells/ tissue,[89,90,91] DNA,[92] antibody,[70] and protein/ enzyme[79,93] have been dispensed,

deposited or patterned in either 2D or 3D arrangements,[38] with bio-activity retained.

The most critical part of ink-jet printing is the formulation of bio-ink and its physical properties, in particular the viscosity and surface tension.[75,76] The specific challenge associated with the formulation of enzyme containing bio-inks for reliable piezoelectric ink-jet printing has been reported.[81] Besides, printing of biocompatible sol-gel inks can be a tricky matter. Short gelation times become a major issue, with respect to ink-jet nozzle clogging, especially when specific proteins (in buffer) are added to the sol-gel material. At physiological pH where most enzymes thrive, gelation of most biocompatible sol-gel precursors occur within a minute to an hour, depending on buffer strength and type of buffer and additives being used. Therefore, there is a need to devise strategies for dispensing bio-doped sol-gel silica materials while using this technique.

2.6 Significance of Acetylcholinesterase

In the development of our portable, paper-based assay platform, acetylcholine esterase (EC 3.1.1.7, AChE) was employed as a model bio-recognition element. Major advantages of this model system lies in the fact that there are several rapid colorimetric assays available. Furthermore, this bio-recognition element allows for the detection of several interesting small molecule analytes; some of which include: organophosphate esters (OPs),[94] aflatoxins[24] and metal ions.[95]

Bioanalytical assays for the determination of AChE inhibitors date back to 1949 when Hestrin[96] reported a hydroxamic acid method, this method was modified in 1956 by Bonting and Featherstone[97] to detect cholinesterase levels in small quantities of cells cultured *in vitro*. However, it was not until 1961 when Ellman *et al.* developed a colorimetric assay, where enzyme activity is monitored by following the increase in yellow colour (TNB) produced from the reaction of enzymatic hydrolysis product thiocholine (Th) and dithiobisnitrobenzoate ion (DTNB), that a simple and reliable assay for AChE activity was found. To this day this assay remains the bench-mark for AChE activity monitoring in solution.

There is one major setback when incorporating the Ellman assay into our sol-gel based platform and this is leaching of the small molecule chromophore. While the pores of the silica matrix are small enough to entrap AChE, it is too large to trap small molecules – which readily leach. Consequently, lower signal intensities are achieved resulting in less sensitive assays.

An alternative sensing mechanism involves the enzyme-mediated deposition of metals onto NPs to cause particle growth to occur, which can be used for detection of enzymes, substrates or enzyme inhibitors.[98] Willner *et al.* have reported on several enzyme-mediated AuNP assays, including: the optical detection of NAD^+-dependent biocatalytic transformations based on the catalytic enlargement of AuNPs by the reduction of Au(III)[99] or Cu(II)[100] with NAD(P)H cofactors; analysis of tyrosinase-generated neurotransmitters,[101] the detection of glucose either directly[102] or using an Os(III) mediator;[103] and the detection of

AChE inhibitors using the thiocholine product to reduce Au(III) onto AuNPs that were immobilized onto glass slides.[104] This new technique has the potential to solve leaching issues and loss of signal associated with sol-gel based colorimetric assays which utilize small molecule chromophores – as grown metal particles cannot leach from the silica matrix.

2.7 Gold Nanoparticle Theory

Noble metal nanoparticles (such as gold, silver and platinum) possess a unique feature in that depending on its shape, size, size distribution and surrounding environments,[105,106,107] absorbs light of specific wavelengths, normally in the visible region and so appearing colored. On the other hand, this feature is not evident in bulk materials or individual atoms.[108] For instance; the color of a gold nanoparticle solution (5-10 nm diameter) is intense red, owing to a manifestation of the localized surface plasmon resonance that is associated with gold particles of this size. Localized surface plasmons (LSPs) are charged density oscillations confined to metallic nanoparticles and metallic nanoclusters[109] (Figure 2.8). Excitation of LSPs by an electric field (light) at an incident wavelength that resonance occurs (Figure 2.8), results in strong light scattering and gives rise to the presence of intense surface plasmon (SP) absorbance bands, and an enhancement of the local electronic fields.[110]

There are a number of mathematical representations proposed describing the effect of nanoparticle size on its optical properties.[111,112,113]
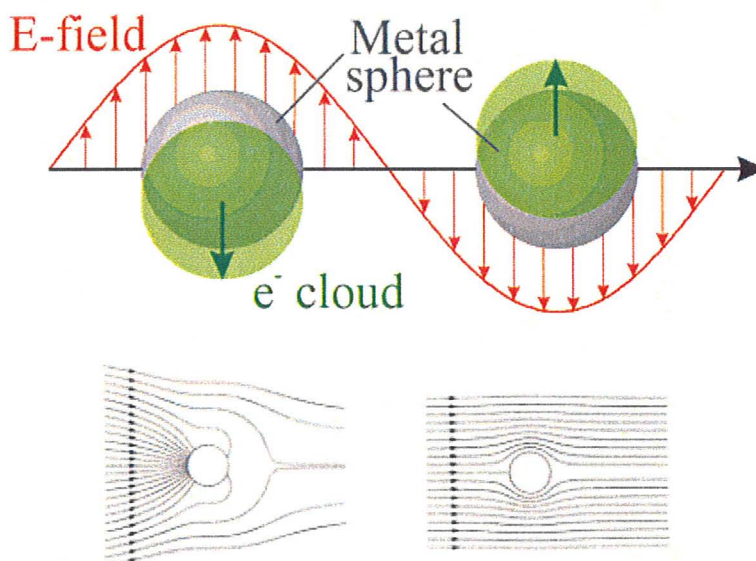
Figure 2.8. *Schematic of plasmon oscillations for a sphere, showing the displacement of the conduction electron charge cloud relative to the nuclei. Bottom: Field lines of the Poynting vector (excluding that scattered) around a small aluminium sphere illuminated by light of energy 8.8 eV where resonance occurs (left hand side) and 5 eV where there is not resonance (right hand side). Figure extracted from: Hutter and Fendler.*

Ground breaking work from Mie in 1908,[61] gave rise to the Mie theory, which describes in detail, plane electromagnetic wave interactions with spherical nanoparticles. From the solution of Maxwell equation, Mie was able to derive a formula for the extinction cross section, σ_{ext}:[114,115]

$$\sigma_{ext} = \frac{2}{x^2}\sum_{n=1}^{\infty}(2n + 1)[\text{Re}(a_n + b_n)]$$

[1]

in which the size parameter , x, is given by:

$$x = \frac{2\pi R n_{m}}{\omega}$$

[2]

where R is the radius of the particle, n_{m} ; the refractive index of the medium, ω; the wavelength of the incident light *in vacuo,* and a_{n} and b_{n} are the scattering coefficients expressed in terms of the well known Ricatti-Bessel expressions.[116] From these expressions it is clear that the size of the particle, among other factor, directly affect the extinction cross section. In agreement with this, these expressions works well for particles on the order of 1000 nm or less whose extension coefficients are affected by particle size, however, particles in the limit $2R \ll \lambda$ (where R is the radius of the particle and λ is the wavelength of the light in the media) does not satisfy equations [1-2] as with particles of such dimensions, only the electric dipole term contributes significantly to the extinction cross section.[117,118,119] Therefore, for these particles, the Mie theory takes the following form:[120]

$$\sigma_{ext} = 9\frac{\omega}{c}\epsilon_{m}^{3/2}V\frac{\epsilon_{2}(\omega)}{[\epsilon_{1}(\omega) + 2\epsilon_{m}]^{2} + [\epsilon_{2}(\omega)]^{2}}$$

[3]
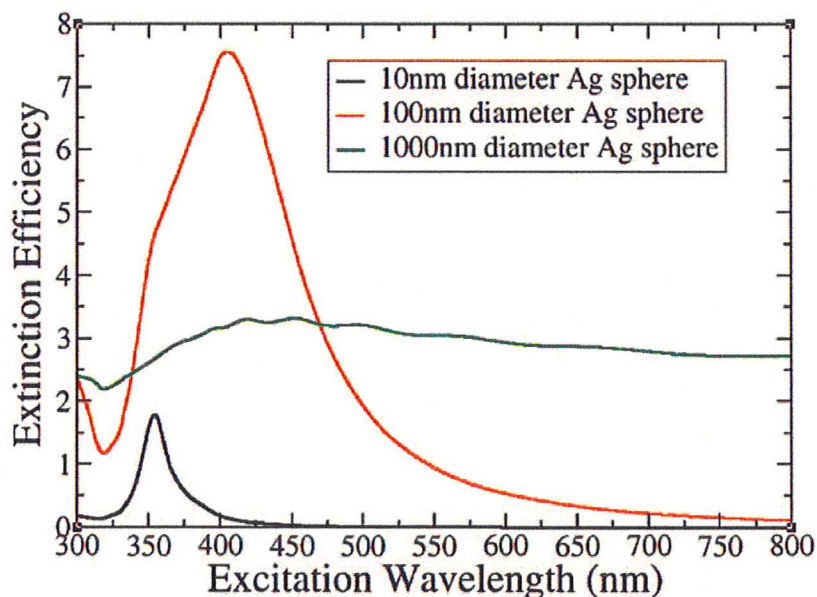
Figure 2.9. *Extinction efficiency spectra for Ag spheres with diameters of 10 (black), 100 (red) and 1000 (green). Figure extracted from Zhao el al. 2008[76].*

where $V = (4\pi/3)R^3$ is the volume of the spherical particle, ω is the angular frequency of the exciting light, c is the velocity of light, and ϵ_m and $\epsilon(\omega) = \epsilon_1(\omega) + i\epsilon_2(\omega)$ are the dielectric functions of the surrounding medium and the material itself, respectively. This gives an explanation as to why solutions containing a similar number of large (>20 nm) and small (1 nm) nanoparticles have contrasting absorption spectra. This is further illustrated in Figure 2.9, where the intensity of the plasmon absorption band broadens, red shifts and intensifies significantly for 100 nm particles relative to 10nm ones, with 1000 nm particles showing no significant peak. For larger NPs (100 < NP < 1000 nm), incident light can no long polarize nanoparticles homogeneously[75] therefore particles such as these show higher mulipole resonances to the blue of the dipole resonance.[121] As a result,

retardation effects of the electromagnetic field across the particle can result in significant increases and shifts in the plasmon absorbance resonance band.[75] This does not hold for particles > 1000 nm as the finite size of the particle relative to the incident wavelength negates plasmon resonance effects[76] leading to extinction spectra that is seen in Figure 2.9.

2.8 Gold Nanoparticles for Sensing

In recent times, AuNP, owing to their bio-compatibility and high extinction coefficients, have been used in a number of areas ranging from biological labels, markers, and stains for various microscopies.[122,123] More recently, the use of AuNP have ventured into the realm of analytical chemistry and has been used fruitfully as molecular-recognition elements and signal amplifiers in sensors and biosensors, in addition to serving as components in nano-scale optical devises.[124]

There have been a series of novel optical and electrochemical assays that have been described based on the aggregation/deaggregation[125] or catalytic enlargement[126] of gold or other metal nanoparticles (NPs). In the first case, the biomolecule (usually DNA) is tagged with gold nanoparticles (AuNP), and addition of analyte leads to assembly or disassembly of NP labelled DNA, leading to a change in the distance of NPs and a color change. Nucleic acid functionalized semiconductor NPs have also been used as labels for the electrochemical,[127] optical,[128] or photoelectrochemical[129] detection of DNA and as a sensing platform for aptamer and DNAzyme based sensors.[130] It is also possible

to integrate this assay into a lateral flow device to perform solid-phase aptamer or antibody based assays.[131]

Moreover, the biocatalytic growth of AuNPs has been employed as a sensing mechanism. The catalytic deposition of metals onto NPs has been utilized extensively for "amplified" biosensing of antigen–antibody complexes,[132] DNA hybridization processes[133] and aptamer–protein binding.[134] The catalytic enlargement of AuNP-labeled DNA complexes between electrodes has also been used for conductivity-based biosensing of DNA.[135] Furthermore, as mentioned earlier, Willner *et al.* have reported on several enzyme-mediated AuNP assays that utilize enzymatically grown nanoparticles.[96-101] These assays are able to directly detect analytes which ranged from protein to small molecules. This technique is also robust in the sense as it can incorporate mediators ions such as Os(III) which aids in the indirect detection of glucose.[103] Furthermore, the aforementioned sensing platform can also be used in solid-phase assaying and also has the potential to be coupled with sol-gel based materials   to   form biosensors which produce high signals resulting from minimum leaching of grown nanoparticles.

2.9 Reference

1. Manihar Situmorang, M.; Gooding J.J.; Hibbert, D.B. *Analytica Chimica Acta* **1999,** *394(2-3),* 211-223

2. Martinez, A.W.; Phillips, S.T.; Butte, M.J.; Whitesides, G.M. *Agnew. Chem. Int. Ed.* **2007,** *46,* 1318-1320.

3. Rhemrev-Boom, M. M.; Korf, J.; Venemaa, K.; Urban, G.; Vadgama, P. *Biosensors and Bioelectronics,* **2001,** *16(9-12),* 839-847.

4. Bucur, B.; , Danet, A.F.; Marty, J-L. *Biosensors and Bioelectronics.* **2004,** *20(2),* 217-225.

5. Hossain, S.M.Z.; Luckham, R.E.; Smith, A.M.; Lebert, J.M.; Davies, L.M.; Pelton, R.H.; Filipe, C.D.M.; Brennan, J.D. *Anal. Chem.,* 2009, Article ASAP.

6. Hall, E.A.H.; *Biosensors,* Prentice Hall, **1991,** 6-7.

7. Vo-Dinh, T.; Cullum, B. *Fresensius J. Anal. Chem.* **2000,** *366,* 540-551.

8. Wittman, C., Riedel, K., Schmid, R.D., 1997. Microbial and enzyme sensors for environmental monitoring. In: Kress-Rogers, E. (Ed.), Handbook of Biosensors and Electronic Noses. CRC, Boca Raton, FL, pp. 299-332.

9. Gonchar, M.; Maidan, M.; Korpan, Y.; , Sibirny, V.; Kotylak, Z.; Sibirny, A. *FEMS Yeast Research, 2(3),* **2006,** 307-314.

10. Martinez, A.W.; Phillips, S.T.; Carrilho. E.; Thomas, S.W. (III); Sindi, H.; Whitesides, G.M. *Anal. Chem. 80,* **2008,** 3699-3707.

11. Lazcka, O.; Del Campo, F.J.; Munoz , F.X. *Biosensors and Bioelectronics,* **2007,** *22* 1205–1217.

12. Kaisheva, A.; Iliev, I.; Christov S.; Kazareva R. *Sensors and Actuators B: Chemical* **1997***, 44 (3),* 571-577.

13. Liu, J.; Yi Lu, Y. *J. Am. Chem. Soc.,* **2003,** *125 (22),* 6642–6643.

14. Nath, N.; Eldefrawi, M.; Wright, J.; Darwin, D.; Huestis, M. *J Anal Toxicol.* **1999,** 23*(6),* 460-467.

15. Rowe, C.A.; Tender, M.L.; Feldstein, M.J.; Golden, J.P.;. Scruggs, S.B.; MacCraith, B.D.; Cras, J.J.; Ligler. F.S. *Anal. Chem.* **1999,** *71,* 3846-3852.

16. Brennan, J.D.; *J. Fluorescence, 9(4),* **1999,** 295-302.

17. Masuda, G.; Tomoika, S.; Hasegawa, M. *The Journal of Antibiotics.* **1976,** *29(6),* 662-664

18. Aitman, T.J. *Br. Med. J.* **2001,** *323,* 611-615.

19. Chang, A.-C.; Gillespie, J.B.; Tabacco, M.B. *Anal. Chem.* **2001**, *73,* 467.470.

20. Gehring, A.G.; Patterson , D.L.; Tu, S.-I, *Analytical Biochemistry.* **1998,** *258(2),* 293-298.

21. Griffin, P.M.; Tauxe, R.V. *Epidemiol Rev.***1991,** *13(1),* 60-98.

22. Kristof, N.D. *The New York Times.* 20 March, **1995** –
www.nytimes.com/1995/03/20/world/poison-gas-fills-tokyo-subway-six-die-and-hundreds-are-hurt.html?scp=6&sq=japan+sarin&st=nyt

23. Nannayakara,U. *Tamil eelam,* 09 April, **2009** –
www.tamileelamnews.com/news/publish/tns_11291.shtml

24. Arduini, F.; Errico, I.; Amine, A.; Micheli, L.; Palleschi, G.; Moscone, D. *Anal. chem.* **2007**, *79,* 3409-3415.

25. Harmon, H.J. *Biosens. Bioelectron.* **2001**, *16,* 1035-1041.

26. Arduini, F.; Amine, A.; Moscone, D.; Ricci, F.; Palleschi, G. *Anal. Bioanal. Chem.* **2007**, *388,* 1049-1057.

27. Goryacheva, Y.; De Saeger, S.; Eremin, S.A.; Petehhem, C.V. *Food Add. Cont.* **2007**, *24(10),* 1169-1183.

28. Lin, T.-J.; Huang, K.-T.; Liu, C.-Y. *Biosens. Bioelectron.* **2006**, *22,* 513-518.

29. Gill, R.; Bahsahi, L.; Freeman, R.; Willner, I. *Angew. Chem.* **2008**, *120,* 1700-1703.

30. Hai, A.; Ben-Haim, D.; Korbakov, N.; Cohen, A.; Shappir, J.; Oren, R.; Spira, M.E.; Yitzchaik, S. *Biosens. Bioelcetron.* **2006**, *22,* 605-612.

31. Liu, N.; Cai, X.; Lei, Y.; Zhang, Q.; Chan-Park, M.B.; Li, C.; Chen, W.; Mulchandani, A. *Electroanalysis* **2007**, *19 (5)*, 616-619.

32. Pardo-Yissar, V.; Katz, E.; Wasserman, J.; Willner, I. *J. Am. Chem. Soc.* **2003**, *125*, 622-623.

33. Pavlov, V.; Xiao, Y.; Willner, I. *Nano Lett.* **2005**, *5(4)*, 649-653.

34. Micheli, L.; Greco, R.; Badea, M.; Moscone, D.; Palleschi, G. *Biosens. Bioelectron.* **2005**, *21*, 588-596.

35. No, H-Y.; Kima, Y.A.; Lee Y.T.; Lee, H-S. *Analytica Chimica Acta.* **2007**, *594*, 37–43.

36. Detecting Chemical Agents and Pesticides in Water, Using Enzymatic Test Kits – www.epa.gov/nhsrc/news/news070708a.html

37. SENTINEL - The Bioactive Paper Network; www.bioactivepaper.com.

38. Abe, K.; Suzuki, K.; Citterio, D. *Anal. Chem.* **2008,** *80,* 6928-6934.

39. Li, X.; Tian, J.; Nguyen, T.; Shen, W. *Anal. Chem.* **2008,** *80,* 9131-9134.

40. Gundry, S.; Wright, J.; Conroy, R. *Journal of Water and Health,* **2004,** *2(1),* 1-13.

41. Roberts, C.J. *The Chemistry of Paper Chemistry,* Royal Society of Chemistry, London, **1996.** p. 2.

42. Roberts, C.J. *The Chemistry of Paper Chemistry,* Royal Society of Chemistry, London, **1996.** p. 1-2.

43. Roberts, C.J. *The Chemistry of Paper Chemistry,* Royal Society of Chemistry, London, **1996.** p. 20.

44. Roberts, C.J. *Paper Chemistry,* Chapman and Hall, New York, **1991.** p. 162.

45 . Roberts, C.J. *Paper Chemistry,* Chapman and Hall, New York, **1991.** p. 170.

46. Mini-Encyclopedia of Papermaking – www4.ncsu.edu/~hubbe/Defnitns/WetStren.htm

47. Roberts, C.J. *Paper Chemistry,* Chapman and Hall, New York, **1991.** p.63,77.

48. Roberts, C.J. *Paper Chemistry,* Chapman and Hall, New York, **1991.** p.76.

49. Roberts, C.J. *Paper Chemistry,* Chapman and Hall, New York, **1991.** p.76-92.

50. Roberts, C.J. *Paper Chemistry,* Chapman and Hall, New York, **1991.** p.65.

51. Roberts, C.J. *Paper Chemistry,* Chapman and Hall, New York, **1991.** p.65-74.

52. Collings, A.F.; Caruso, F.; *Rep. Prog. Phys.,* **1997**, 1397-1445.

53. Zhu, H., Snyder, M.. *Current Opinion in Chemical Biology.* **2003**, *7*, 55-63.

54. Vandenberg, E. T.; Brown, R. S.; Krull, U. J. Immobilization of Proteins for Biosensor Development. In *Immobilized Biosystems in Theory and Practical Applications*; Veliky, I. A., Mclean, R. J. C., Eds.; Blackie: Glasgow, U.K., 1994; pp 129–231.

55. Weetall, H. H. *Appl. Biochem. Biotechnol.* **1993**, *41*, 157–188.

56. Doretti, L.; Ferrara, D.; Lora, S. *Biosens.Bioelectron.* **1993**, *8*, 443–450.

57. Scouten, W. H. *Methods Enzymol.* **1987**, *135*, 30–65.

58. O'Driscoll, K. F. *Methods Enzymol.* **1976**, *44*, 169–183.

59. Livshits, A.; Mivzabekov, A.D. *Biophysics,* **1996,** *71,* 2795-2801.

60. Vianello, F.; Ragusa, S.; Cambria, M.T.; Rigo, A. *Biosensors and Bioelectronics.* **2006,** *21(11),* 2155-2160.

61. Templin, M.F.; Stoll, D.; Schrenk, M.; Traub, P.C.; Vohringer C.F.; Joos, T.O. *Trends Biotechnol.,* **2002,** *20,* 160–166.

62. Zhu, H.; Klemic, J.F.; Chang, S.; Bertone, P.; Casamayor, A.; Klemic, K.G.; Smith, D.; Gerstein, M.; Reed, M.A.; Snyder, M. *Nat. Genet.* **2000,** *26,* 283–289.

63. Johnsson, B.; Löfås, S.; Lindquist, G.; Edström, A.; Hillgren, R.-M.M.; Hansson, A. *Journal of Molecular Recognition.* **2004,** *8 (1-2),* 125 – 131.

64. Zhu, H.; Bilgin, M.; Bangham, R.; Hall, D.; Casamayor, A.; Bertone, P.; Lan, N.; Jansen, R.; Bidlingmaier, S.; Houfek T. *Science,* **2001,** *293,* 2101–2105.

65. O'Discoll, K.F.; *Methods Enzymol.,* **1976,** *41,* 157-188.

66. Pierre, A.C., *Biocatalysis and Biotransformation,* **2004,** *22 (3),* 145-170.

67. Maleki, A.; Kjøniksen A.L.; Knudsen, K.D.; Nyström, B. *Polymer International,* **2006,** *55, 365.*

68. Brinker, C.J.; Scherer, G.W. *Sol-Gel Science,* AcademicPress, New York, **1990.**

69. Gupta, R.; Chaudhury, N.K. *Biosensors and Bioelectronics,* **2007,** *22(11),* 2387-2399

70. Bhatia, R.B.; Brinker, C.J. *Chem. Mater.* **2000,** *12,* 2434-2441

71. Cruz-Aguado, J.A.; Chen, Y.; Zhang, Z.; Brook, M.A.; Brennan, J.D. *Anal. Chem.,* *2004, 76(14),* 4182–4188.

72. Avnir, D.; Coradin, T.; Lev, O.; Livage, J. *J. Mater. Chem.* **2006,** *16,* 1013–1030.

73. Avnir, D.; Braun, S.; Lev, O.; Ottolenghi. M. *Chem. Mater.,* **1994,** *6 (10),* 1605–1614

74. Brennan, J.D. *Acc. Chem. Res.* **2007,** *40,* 827–835

75. Jin, W.; Brennan, J. D. *Anal. Chim. Acta.* **2002,** *461,* 1–36.

76. Lev, O.; *Analysis,* **1992,** 20, 543-553.

77. Rappoport, Z., Apeloig, Y., *The Chemistry of Organic Silicon Compounds, Vol. 2,* John Wiley and Sons, Ltd., **1998,** pp. 2317-2361.

78. Brinker, C.J.; Scherer, G.W. *Sol-Gel Science,* AcademicPress, New York, **1990.** p. 788-795.

79. Brinker, C.J. and Scherer, G.W. *Sol-Gel Science,* AcademicPress, New York, **1990.** p. 795-797.

80. Jordan, J.D.; Dunbar, R.A.; Bright. F.V. *Analytica Chimica Acta.* **1996,** *332,* 83-91.

81. Wang, J.; Pamidi, P.V.A.; Park, D.S. *Anal. Chem.* **1996,** *68,* 2705-2708.

82. Katagiri, K.; Hasegawa, K.; Matsuda, A.; Tatsumisago, M.; Minami, T. *J. Am. Ceram. Soc.* **1998,** *81(9),* 2501–2503.

83. Le, H.P. Progress and trends in ink-jet printing technology. *J. Imag. Sci. Technology* **1998,** *42(1),* 49-62.

84. Percin, G.; Khuri-Yakub, B.T. *Rev. Sci. instrum.* **2003,** *74(2),* 1120-1127.

85. Tsai, M.H.; Hwang, W.S.; Chou, H.H.; Hsieh, P.H. *Nanotechnol.* **2008,** *19,* 335304-335313.

86. Harrell, T.M.; Hosticka, B.; Power, M.E.; Cemke, L.; Hull, R.; Norris, P.M. *J. sol-gel sci. technol.* **2004,** 31, 349-352.

87. Calvert, P. Injet printing for materials and devices. Chem. Mater. **2001,** *13(10),* 3299-3305.

88. De Gans, B.-J.; Duineveld, P.C.; Schubert, U.S. *Adv. Mater.* **2004,** *16(3),* 203-213.

89. Xu, T.; Jin, J.; Gregory, C.; Hickman, J.J. *Biomaterials* **2005,** *26,* 93-99.

90. Wilson, J.W.C.; Boland, T. *Anat. Rec. Part A* **2003,** 272A, 491-500.

91. Ilkhanizadeh, S.; Teixeira, A.I.; Hermanson, O. *Biomaterials,* **2007,** 28, 3936-3943.

92. Bietsch, A.; Hegner, M.; Lang, H.P.; Gerber, C. *Langmuir* **2004,** 20, 5119-5122.

93. Di Risio, S.; Yan, N. *Macromolecular Rapid Communication* **2007,** 28 (18-19), 1934-1940.

94. Marrs, T.C., *Pharmacol. Ther.,* **1993,** *58(1),* 51-66.

95. Stoytcheva, M.; Sharkova, V.; Panayotova, M. *Analytica Chimica Acta,* **1998,** *364,* 195-201.

96. Hesterin, S.; The Journal of Biological Chemistry, **1949,** 249-261.

97. Bonting S.; Featherstone R.M. *Arch. Biochem. Biophys.* **1956,** *61*, 89.

98. Willner, I; Baron, R; Willner, B. *Adv. Mater.* **2006**, *18*, 1109-1120.

99. Xiao, Y.; Pavlov, V.; Levine, S.; Niazov, T.; Markovitch, G.; Willner, I. *Angew. Chem.* **2004**, *116*, 4619–4622; *Angew. Chem. Int. Ed.* **2004**, *43*, 4519–4522.

100. Shlyahovsky, B.; Katz, E.; Xiao, Y.; Pavlov, V.; Willner, I. *Small* **2005**, *1*, 213-216.

101. Baron, R.; Zayats, M.; Willner, I. *Anal. Chem.* **2005**, *77*, 1566-1571.

102. Zayats, M; Baron, R; Popov, I; Willner, I. *Nano Lett.* **2005**, *5*, 21-25.

103. Xiao, Y.; Pavlov, V.; Shlyahovsky, B.; Willner, I. *Chem. Eur. J.* **2005**, *11*, 2698-2704.

104. Pavlov, V.; Xiao, Y.; Willner, I. *Nano Lett.* **2005**, *5*, 649-653.

105. Mie, G. *Ann. Phys.* **1908**, *25*, 377.

106. Underwood, S. Mulvaney, P. *Langmuir,* **1994**, *10*, 3427.

107. Mulvaney, P. *Langmuir* 1996, **12**, 788.

108. Stephan Link, S.; El-Sayed, M.A. *J. Phys. Chem. B* **1999**, *103,* 4212-4217.

109. Kreibig, U.; Vollmer, M. *Optical Properties of Metal Clusters*, Springer-Verlag, Berlin, Germany **1995**.

110. Hutter, E.; Fendler, J. H. *Adv. Mater.* **2004**, *16(19),* 1685-1706.

111. Henglein, A. *J. Phys. Chem.* **1993**, *97*, 8457.

112. Chumanov, G.; Sokolov, K.; Gregory, B. W.; Cotton, T. M. *J. Phys.Chem.* **1995**, *99*, 9946.

113. Fletcher, P.; Howe, A.; Robinson, B. *J. Chem. Soc., Faraday Trans.I* **1987**, *83*, 985.

114. Genzel, L.; Martin, T. P.; Kreibig, U. *Z. Phys. B* **1975**, *21*, 339.

115. Novotny, L.; Hecht, B. *Principles of Nano-Optics*; Cambridge, U.K., 2006.

116. Kreibig, U.; Vollmer, M. *Optical Properties of Metal Clusters*; Springer: Berlin, 1995.

117. Papavassiliou, G. C. *Prog. Solid State Chem.* **1980**, *12*, 185.

118. Mulvaney, P. *Langmuir* **1996**, *12*, 788.

119. Kreibig, U.; Genzel, U. *Surf. Sci.* **1985**, *156*, 678.

120. Ghosh, S.K.; Pal, T.Chem. Rev. **2007,** 107, 4797-4862.

121. Zhao, J.; Pinchuk, A.O.; McMahon, S.L.; Ausman, L.K.; Atkinson, A.L.; Schatz, G.C. *Accounts of Chemical Research.* **2008,** *41(12),* 1710-1720.

122. D. G. Richards, D. L. McMillin, E. A. Mein, C. D. Nelson, *Int. J. Neurosci.* **2002**, *112*, 31.

123. M. Matsumoto, H. Yoshimura, V. S. Kulkarni, K. Nagayama, *Colloid Polym. Sci.* **1990**, *268*, 1174.

124. Daniel, M.C.; Astruc, D. *Chem. Rev.* **2004**, *104*, 293.

125. Elghanian, R.; Storhoff, J.J.; Mucic, R.C.; Letsinger, R.L; Mirkin, C.A. *Science* **1997**, *277*, 1078-1080.

126. Willner, I; Baron, R; Willner, B. *Adv. Mater.* **2006**, *18*, 1109-1120.

127. (a) Wang, J.; Liu, G.; Polsky, R.; Merkoci, A. *Electrochem. Commun.* **2002**, *4*, 722-726. (b) Wang, J.; Liu, G.; Merkoci, A. *J. Am. Chem. Soc.* **2003**, *125*, 3214-3215. (c) Wang, J.; Xu, D. K.; Kawde, A. N.; Polsky, R. *Anal. Chem.* **2001**, *73*, 5576-5581.

128. (a) Bruchez, M.; Moronne, M.; Gin, P.; Weiss, S.; Alivisatos, A. P. *Science* **1998**, *281*, 2013-2016. (b) Chan, W.C.W.; Nie, S. *Science* **1998**, *281*, 2016-2018.

129. Willner, I.; Patolsky, F.; Wasserman, J. *Angew. Chem. Int. Ed.* **2001**, *40*, 1861-1864.

130. Pavlov, V.; Xiao, Y.; Shlyahovsky, B.; Willner, I. *J. Am. Chem. Soc.* **2004**, *126*, 11768 –11769.

131.Liu, J.; Mazumdar, D.; Lu, Y. *Angew. Chem. Int. Ed.* **2006**, *45*, 7955-7959.

132. a) Velev, O.O.; Kaler, E.W. *Langmuir* **1999**, *15*, 3693 –3698; b) Cao, Y. C.; Jin, R.; Nam, J.-M.; Thaxton, C.S.; Mirkin. C.A. *J. Am. Chem.* Soc. **2003**, *125*, 14676-14677; c) Faulds, K.; Smith, W.E.; Graham, D. *Anal. Chem.* **2004**, *76*, 412 –417.

133. a) Wang, J.; Rincon, O.; Polsky, R.; Dominguez, E. *Electrochem. Commun.* **2003**, *5*, 83–86; b) Nam, J.M.; Thaxton, C.S.; Mirkin, C.A. *Science* **2003**, *301*, 1884–1886.

134. Pavlov, V.; Xiao, Y.; Shlyahovsky, B.; Willner, I. *J. Am. Chem. Soc.* **2004**, *126*, 11768 –11769.

135. Park, S.J.; Taton, T.A.; Mirkin, C.A. *Science* **2002**, *295*, 1503–1506.

Chapter 3: Colorimetric Detection of Enzyme Inhibitors using Sol-Gel/Enzyme/AuNP Composites. Part 1: Optimizing Enzyme-Catalyzed Enlargement of Sol-Gel Entrapped Gold Nanoparticles

The following chapter was submitted to the scientific journal *Analyst,* for review, under the Title: **Colorimetric Detection of Enzyme Inhibitors using Sol-Gel/Enzyme/AuNP Composites. Part 1: Optimizing Enzyme-Catalyzed Enlargement of Sol-Gel Entrapped Gold Nanoparticles** Roger E. Luckham and John D. Brennan.* Submitted on 7th May 2009 under the Manuscript ID: B909073H

I was responsible for all data collection and analysis. I wrote the first draft of the manuscript and Dr. Brennan provided editorial input to generate the final draft.

Abstract

We report on a new solid-phase colorimetric bioassay format based on enzyme catalyzed enlargement of gold nanoparticles (AuNP) that are co-entrapped with the enzyme in a sol-gel based silica material. Data are presented using acetylcholinesterase (AChE) as a model system. Test solutions containing acetylthiocholine (ATCh) and a Au(III) salt are added externally to silica materials containing AChE and small (3 nm diameter) AuNP, which are present within the wells of 96 well plates. Biocatalysed hydrolysis of ATCh *via* AChE leads to formation of thiocholine, which in turn reduces the Au(III) onto the entrapped nanoparticles, producing particle growth and a concomitant increase in color intensity that can be correlated to the amount of substrate or inhibitor present in test solutions. The entapped AuNP cannot leach from the silica material, leading to a solid-phase assay that has the potential to be integrated into a portable biosensing platform that can utilize visual detection of a color change as a simple readout. This is the first demonstration that gold nanoparticles can be grown via a biocatalytic method when entrapped in sol-gel-derived silica materials. Our results show that the assay is sufficiently sensitive to allow for detection of Paroxon and Aflatoxon B_1 with detection limits of 3 μM and 15 nM, respectively, when using a platereader for detection of color changes. Similar detection limits are possible using a digital camera and image processing software, suggesting that the method should be amenable to studies in the field.

3.1 Introduction

In recent years a series of novel optical and electrochemical assays have been described based on the aggregation/deaggregation[1] or catalytic enlargement[2] of gold or other metal nanoparticles (NPs). In the first case, the biomolecule (usually DNA) is tagged with gold nanoparticles (AuNP), and addition of analyte leads to assembly or disassembly of NP labelled DNA, leading to a change in the distance of NPs and a color change. Nucleic acid functionalized semiconductor NPs have also been used as labels for the electrochemical,[3] optical,[4] or photoelectrochemical[5] detection of DNA and as a sensing platform for aptamer and DNAzyme based sensors.[6] It is also possible to integrate this assay into a lateral flow device to perform solid-phase aptamer or antibody based assays.[7]

More recently, the biocatalytic growth of AuNPs has been employed as a sensing mechanism. The catalytic reduction of metal ions onto NPs has been utilized extensively for "amplified" biosensing of antigen–antibody complexes,[8] DNA hybridization processes[9] and aptamer–protein binding.[6] The catalytic enlargement of AuNP-labeled DNA complexes between electrodes has also been used for conductivity-based biosensing of DNA.[10] An alternative sensing mechanism involves the enzyme-mediated reduction of metal ions onto NPs to cause particle growth to occur, which can be used for detection of enzymes, substrates or enzyme inhibitors.[2] There have been several reports of enzyme-mediated AuNP assays, including: the optical

detection of NAD^+-dependent biocatalytic transformations based on the catalytic enlargement of AuNPs by the reduction of Au(III)[11] or Cu(II)[12] with NAD(P)H cofactors; analysis of tyrosinase-generated neurotransmitters,[13] the detection of glucose either directly[14] or using an Os(III) mediator;[15] and the detection of AChE inhibitors using the thiocholine product to reduce Au(III) onto AuNPs that were immobilized onto glass slides.[16] Other metal salts, such as Ag(I), have also been utilized to allow detection of enzymatic reactions such as the hydrolysis of *p*-aminophenol phosphate by alkaline phosphatase to yield *p*-aminophenol, which catalyzes the reduction of Ag^+ onto Au NPs.[17]

While this method has been demonstrated for a variety of enzyme-mediated platforms,[2] to date the assay has only been applied to enzymes in solution, and has not been demonstrated in a solid-phase assay format. The extension of this technology to solid-phase assays has significant potential for the development of a new class of colorimetric biosensors. The development of low-cost, portable and technically straightforward assay technologies is of critical importance in a number of areas, including rapid testing of food or water quality, point-of-care diagnostics (i.e. field or home setting), and the rapid detection of bioterror agents. Development of such bioassays could also be useful for performing routine analysis in underdeveloped countries, or as an alternative to more expensive technologies for rapid testing in emergency situations, since it is possible to

detect a signal visually without the need for complex instrumentation.[18]

The development of portable, solid-phase colorimetric assays requires a method for immobilization of the biorecognition element (protein, DNA, etc) onto a suitable substrate[19,20] as well as an appropriate method to generate a detectable color change. Toward this end, we have investigated the use of biocompatible sol-gel derived materials as a medium to co-entrap both an enzyme[21-26] and a small gold nanoparticle (colorimetric reagent) to allow for solid-phase assaying of enzyme substrates and inhibitors. Key issues in the assay development centered on finding conditions that would allow enzyme stimulated enlargement of gold nanoparticles within the pores of sol-gel materials, finding suitable conditions that would prevent the reduction of Au(III) by other assay components, and on optimizing this platform for solid-phase colorimetric assays.

As a starting point, we have utilized acetylcholinesterase (AChE) as the model enzyme. The enzyme has previously been shown to remain functional in sol-gel derived materials,[27] and can be used to catalyze the hydrolysis of acetylthiocholine to thiocholine, which has previously been shown to reduce Au(III) onto AuNPs.[16] This enzyme is also important as a biorecognition element for detection of organophosphates, which can be used as pesticides or biowarfare agents,[28] and for detection of aflatoxins,[29] which is a biomarker of food spoilage.[30] Herein we describe the optimization of assay conditions to achieve the best assay performance, and show the quantitative

detection of both substrates and inhibitors of AChE using the colorimetric sol-gel derived solid-phase assay platform.

3.2 Experimental Section

Materials: Sodium silicate solution (~ 14% NaOH, ~ 27% SiO_2), Dowex 50WX8-100 ion-exchange resin, acetylcholinesterase (AChE, from *Electrophorus electricus*, EC 3.1.1.7), acetylthiocholine iodide (ATCh), gold(III)chloride trihydrate, adenosine 5′-triphosphate disodium salt (ATP), diethyl 4-nitrophenyl phosphate (Paraoxon) and Aflatoxin B_1 (AFB$_1$) were obtained from Sigma-Aldrich. Costar® 96 well half area plates were obtained from Fisher Scientific. Distilled deionized water was obtained from a Milli-Q Synthesis A10 water purification system. All reagents were used as received.

Safety Conditions: The stock solutions of paraoxon and Aflatoxon B_1 (highly toxic compounds) were handled with precaution at all times. To avoid skin contact, a designated fume-hood was used throughout with the appropriate personal safety equipment, such as: gloves, masks and safety glasses. These were employed at all times when handling this substances.

Procedures

Preparation of ATP-Capped Gold Nanoparticles: ATP-AuNPs were prepared as described by Zhao *et al.*[31] Briefly, 60 μL of 10 mM gold chloride solution

was added to 60 µL of 10 mM ATP solution. To this, 2.75 mL of deionized water was added followed by shaking and incubation for 30 minutes at room temperature. 100 µL of freshly prepared 0.01 M $NaBH_4$ solution was then added and the resulting solution was shaken for 10 seconds followed by incubation at room temperature for 3 hrs. The resulting solution of nanoparticles has a mean diameter of 2-3 nm, and can withstand up to 1 M NaCl without aggregation.

Preparation of Sol-Gel Materials: Sodium silicate sols were prepared by mixing 10 mL of ddH_2O with 2.9 g of sodium silicate solution (pH ~13) followed by addition of 5 g of Dowex cation exchange resin to replace Na^+ with H^+. The mixture was stirred for 30 seconds to reach a final pH of ~4, and then vacuum filtered through a Büchner funnel. The filtrate was then further filtered through a 0.45 µM membrane syringe filter to remove any particulates in the solution.

ATP-AuNPs (volume of 0 – 4 µL per 50 µL) were added to the SS precursor sol, which was then mixed in a 1:1 volume ratio with a buffered solution (100 mM Tris-HCl buffer, pH 8.0) containing AChE at room temperature (20 ± 1 °C) to provide a final volume of 100 µL of material in the well of 96-well plate, with a final enzyme concentration of 0 – 50 Units.mL^{-1} (1 Unit = 1 µmole of acetylcholine hydrolyzed per min at 37 °C). In all assays, 30 µL of the AChE/ATP-AuNP doped SG sol was allowed to gel and cure for 72 hrs at 4 °C prior to performing assays. Note: The concentrations of ATP-AuNP were

calculated given the molar extinction coefficient: 6.5×10^5 cm^{-1} for particle on the order of 2-3 nm, as reported by Pavlov *et al.*

Optimization Studies: A series of different *sol-gel* materials containing varying levels of AChE and ATP-AuNP were prepared as described above. The 30 µL gels were then allowed to cure for 72 hours at 4 °C. In all cases, 30 µL of a solution containing varying levels of ATCh and gold chloride was added to the wells and left for 1 h. at room temperature while shaking. Controls included materials with no AChE or no AuNPs and the use of solutions with no ATCh or no gold chloride to ensure that any color changes were due to enzyme catalyzed enlargement of AuNPs within the gels. After 1 hr the absorbance spectra of the materials was measured from 400 nm to 900 nm using a TECAN Safire microwell plate reader. The absorbance at 550 nm were plotted against the concentrations of the various reagents (AChE, ATCh, Au(III) or AuNP) to determine the effect of reagent concentration on signal levels.

Inhibition Assays: To the 30 µL AChE/ATP-AuNP doped SS in the microwell, 10 µL of inhibitor solution was over spotted and incubated at room temperature while stirring for 1 hr. 20 µL of a solution containing appropriate concentrations of Au(III) and ATCh along with an identical concentration of inhibitor (to avoid dilution of inhibitor) was then added and shaken for 1 hr. Absorbance of the wells was then measured using a TECAN Safire microwell plate reader. The

absorbance at 550 nm was plotted against inhibitor concentration to derive IC_{50} plots.

Long Term Stability Studies: Microwell plates containing *sol-gel* based assay system (AChE and AuNPs) were sealed with Parafilm® and stored at 4 °C for up to 6 weeks. 30 µL of a test solution containing the optimized amounts of ATCh and Au(III) were then added at various time points, the plate was shaken for 1 hr and absorbance measurements obtained using a TECAN Safire microwell plate reader. Activity was referenced to that obtained from a sample that had been aged for 3 days.

Transmission Electron Microscopy: ATP-AuNP doped sol-gel materials were imaged by TEM before and after assays to determine the extent of particle growth during assays. Sample gels of approximately 0.5 g were immersed in 500 µL methanol and sonicated for 30 min at room temperature. This sample was dried and immediately placed on a TEM grid for imaging. Images were acquired using a JEOL Ltd. (Tokyo, Japan) JEM-1200EX instrument operating at 80 kV.

3.3 Results and Discussion

Proof of Concept: The choice of gold nanoparticles is of particular importance in this work for two reasons: the primary nanoparticles must (1) be able to

withstand relatively high buffer salt concentrations (~50 mM) as is commonly used when entrapping proteins within sol-gel derived silica materials and (2) be biocompatible in the sense that it will not degrade the biological component(s) in any way. A solution-based AuNP assay for the detection of AChE inhibitors was previously described by Pavlov and coworkers[6] where citrate capped AuNPs were employed as the platform for particle growth. As a starting point, a similar protocol[31] was used in this work, however it was discovered that the citrate capped AuNPs were very sensitive to increasing salt concentration, with significant aggregation occurring above 5 mM (data not shown), which made it difficult to develop reproducible assays. The primary AuNPs provide the physical platform upon which elemental gold is deposited – resulting in particle growth. Hence, it is important that the primary particles remain in a non-aggregated form within the matrix. As a result of the relative instability of the citrate capped AuNPs to salt, a more stable primary AuNP was required. To achieve this goal, we utilized highly stable, biocompatible AuNPs in which ATP was used as the capping agent.[32] These nanoparticles showed good stability, with no aggregation occurring even at buffer salt concentrations of 200 mM, and were therefore used for all solution and solid-phase assays.

The general reaction scheme for the AChE catalyzed growth of ATP-capped AuNPs in the solid-phase assay is shown in Figure 3.1.
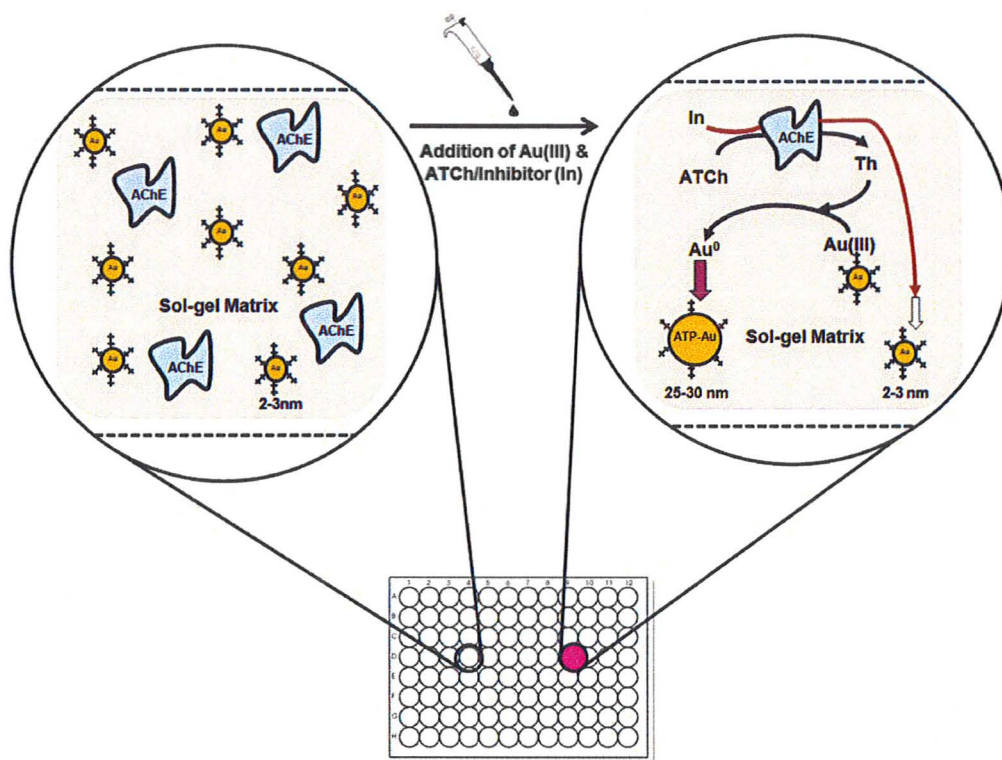
Figure 3.1.   *Schematic of the solid-phase assay involving enzymatically catalyzed enlargement of entrapped ATP-capped gold nanoparticles as a means of detecting inhibitors of AChE.*

In this assay, 2-3 nm primary AuNPs and AChE are co-entrapped in a silica matrix which is present in a microwell of a 96-well plate.   Solutions containing inhibitor ATCh/Au(III) are introduced and these reagents are able to diffuse into the silica matrix.   AChE catalyzed hydrolysis of the ATCh substrate results in the production of thiocholine, which is able to reduce Au(III) onto the entrapped AuNPs.   This causes enlargement of the AuNPs to a diameter of 25-30 nm or greater and a concomitant increase in absorance and color intensity.   It is important to note that materials that do not contain

primary AuNPs do not produce a color change; the co-entrapped AuNPs are necessary in order to produce nucleation sites for rapid particle growth (see below).

As a starting point for assay development, we set out to demonstrate that it was possible to perform enzymatically catalyzed enlargement of primary AuNPs within the pores of a sol-gel derived silica matrix. For this purpose, AChE and ATP-AuNPs were entrapped in a biocompatible silica matrix derived from sodium silicate and the Au(III) and ATCh solutions were added externally. Sodium silicate was chosen as it is an easily prepared, optically transparent, biocompatible silica precursor that is known to maintain the activity of enzymes,[33] and does not produce byproducts (i.e. alcohols, glycerol, etc) that might interfere with the growth of AuNPs.

Figure 3.2 shows an image of a microwell plate in which a series of solid-phase assays and control experiments were performed. The original image was processed using ImageJ to enhance the contrast and brightness and increase the color saturation. No other processing was performed. The top row (A1-A7) shows the ATP-AuNP and AChE doped silica before addition of substrate and gold chloride. In this case, the samples are completely colorless and transparent, showing that the low concentration of small ATP-AuNPs does not produce a significant background absorbance. Absorbance measurements of the wells performed using a TECAN Safire platereader
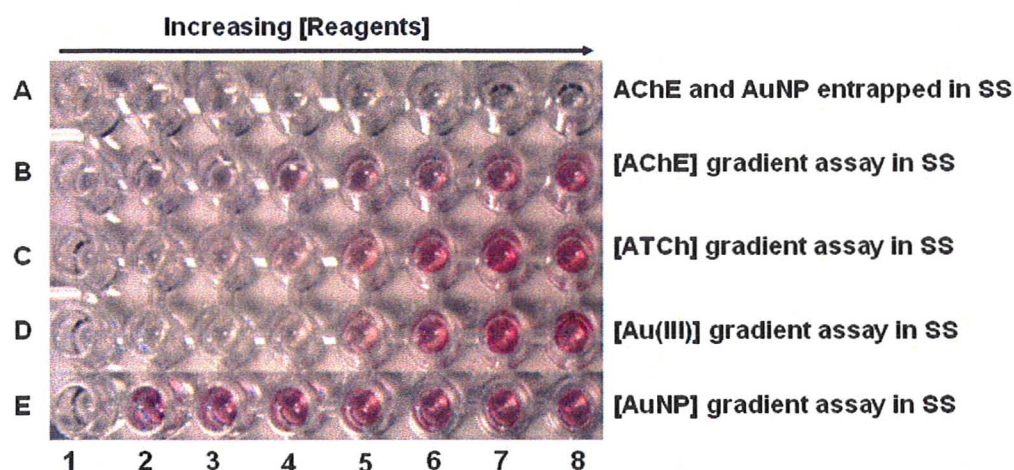
Figure 3.2. *Proof of concept and control experiments for the solid-phase bioassay (showing that all reagents are necessary for nanoparticle growth). Wells were filled with sol-gel derived materials containing the reagents indicated. A: Appearance of well before over spotting of ATCh and Au(III); B: Assay of varying [AChE] (0 to 40 unit/mL) at constant [ATCh], [Au(III)] and [ATP-AuNP]. C: Assay of varying [ATCh] (0 to 0.45 mM) at constant [AChE], [Au(III)] and [ATP-AuNP]. D: Assay of varying [Au(III)] (0 to 0.83 mM) at constant [AChE], [ATCh] and [ATP-AuNP]. E: Assay of varying [ATP-AuNP] (0 to 1x 4 conc. units) at constant [AChE], [ATCh] and [Au(III)].*

confirmed this as the characteristic plasmon absorbance band for AuNP, between 510 and 550 nm, was not detectable (data not shown). Wells B1-E1 show control experiments in which silica materials were formed or assays were run with one of the assay components missing; AChE (B1), ATCh (C1), Au(III) (D1) or entrapped primary AuNPs (E1). All other reagents were present at the highest concentrations used in the assay, which are present in the last column (B7-E7). In all cases, there was no change in the color of the material, indicating that the silica material and assay reagents (i.e., buffer salts, substrates, etc) did not cause significant reduction of

Au(III) or conversion of ATCh to a product that could promote reduction of Au(III) and subsequent enlargement of primary AuNPs.

Row B shows the effect of increasing AChE concentration on the reaction. Here it is seen that as the concentration of AChE is increased from 0 to 40 unit/mL (B1-B7), a color gradient is formed as the concentration of AChE is increased. For this assay the concentration of ATP-AuNP, Au(III) and ATCh were kept constant. This assay establishes that the presence of the highest level of AChE produced the largest change in color, indicative of the greatest extent of enlargement of the entrapped AuNPs. These experiments also conclusively demonstrate that ATP-capped AuNPs can be bio-catalytically grown within the confines of a sol-gel matrix and also show that the growth of AuNPs is due to the activity of the entrapped enzyme and not due to background interferences related to the sol-gel material or other components of the reaction mixture.

Row C of Figure 3.2 shows assays involving increasing amounts of ATCh incubated over the silica material; as in the case with the AChE gradient assay, there was also a progression of colour that was formed, from low to high, as the concentration of ATCh was increased. A similar trend was observed for rows D and E, where the concentration of Au(III) and ATP-AuNP was varied. This demonstrates that the presence of all reagents is necessary for signal generation, and that color intensity increases with the concentration of each assay reagent, as expected.[16]   Hence, this system

provides a suitable platform for a colorimetric solid-phase assay.

TEM Imaging: To confirm that the color changes were the result of entrapped nanoparticle growth, AChE/AuNP doped silica monoliths were imaged by TEM before and after performing a solid-phase AChE assay. Microtoming is a common sample preparation technique used when taking TEM images of materials such as these. However, microtoming requires that the sample be completely devoid of moisture, meaning that the sol-gel material would have to be desiccated. Dehydration of bulk gels resulted in significant shrinkage, which lead to aggregation of entrapped AuNPs, producing images that were not representative of the particle size within hydrated silica materials. To make samples amenable to TEM, they were first immersed in methanol with sonication to remove water and soluble organic components, and then placed on TEM grids and dried. Figure 3.3 shows the TEM images obtained before (Fig. 3.3A) and after (Fig. 3.3B) performing the enzymatic assay. As shown in Figure 3.3A, there are essentially no AuNPs with an average size greater than 2-3 nm (resolution limit of the instrument) prior to performing the assay. However, after performing the assay there are large numbers of metal nanoparticles that have sizes ranging from 25 – 30 nm, clearly indicating growth of the nanoparticles within the silica matrix. The entrapped particles show relatively regular spherical shapes after enlargement, indicating that the
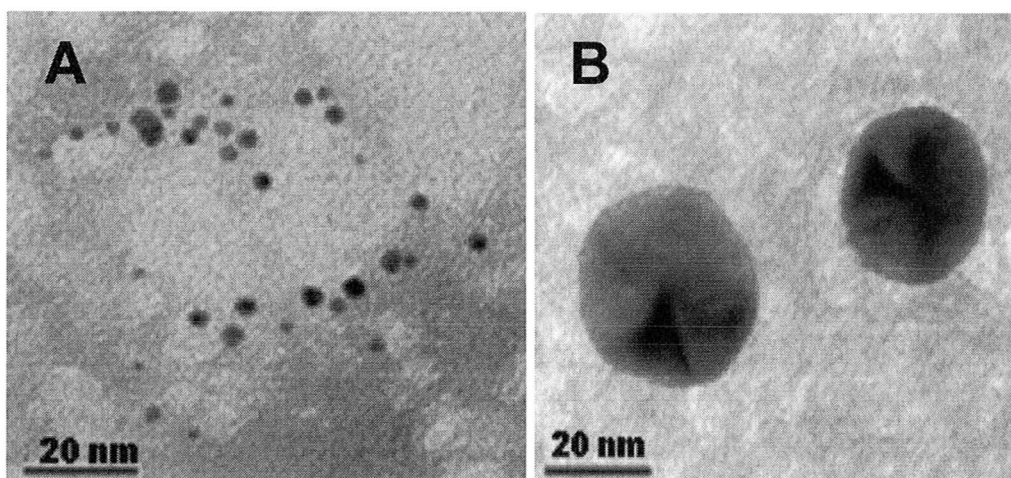
Figure 3.3. *TEM Images of ATP-AuNPs within sol-gel derived silica before (Panel A) and after (Panel B) performing the solid-phase enzyme assay.*

matrix does not preclude formation of large particles that can produce significant color changes. Thus, the enlarged particles can be used for visual detection of the enzymatic reaction using this solid-phase assay platform.

Optimization of Solid-Phase Assay: To optimize the reagents for the assay, AChE/ATP-AuNP doped silica materials were prepared with varying concentrations of AChE and ATP-AuNPs, and were assayed using varying concentrations of ATCh and Au(III). Figure 3.4A-D shows the results obtained when each of the four components was varied systematically with the other three reagent concentrations held constant. All assays were run for a period of 1 h, after which an absorbance spectrum was obtained. Figure 3.4A shows the effect of varying the concentration of entrapped AChE from 0 – 50 Unit/mL
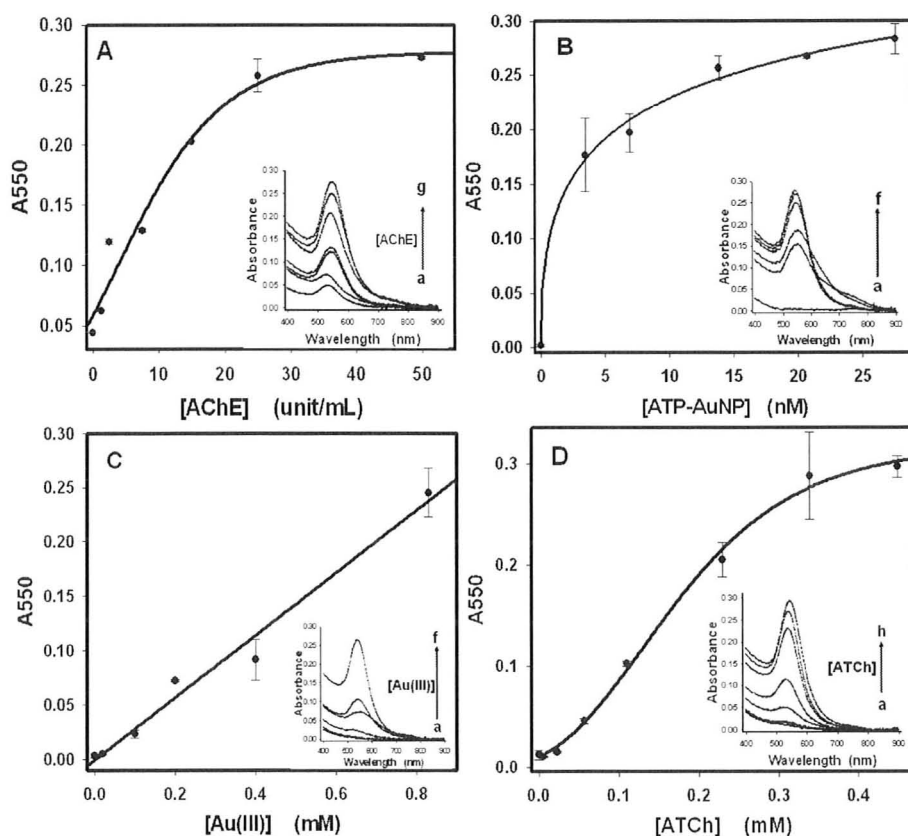
Figure 3.4. Reagent optimization assays. *(A) Inset: Normalized absorption spectra showing the effect of [AChE] on the growth of ATP-AuNPs in a SS derived SG matrix. [AChE]: (a) 0 unit/mL; (b) 1.25 unit/mL; (c) 2.50 unit/mL; (d) 7.5 unit/mL; (e) 15.0 unit/mL; (f) 25.0 unit/mL; (g) 50.0 unit/mL. In all assays the system includes: [ATCh] = 0.45 mM; [Au(III)] = 0.83 mM; [ATP-AuNP] = 28 nM. (B) Inset: Normalized absorbance spectra showing the effect of [ATP-AuNP] on the signal achieved at constant [AChE], [Au(III)] and [ATCh]: 50.0 unit/mL, 0.83 mM and 0.45 mM respectively. [ATP-AuNP]: (a) 0 nM; (b) 3.5 nM (c) 6.9 nM (d) 14 nM; (e)   21 nM (f) 28 nM. (C) Inset: Normalized absorption spectra showing the effect of [Au(III)] on the growth of ATP-AuNPs in a SS derived SG matrix. [Au(III)]: (a) 0 mM; (b) 0.02 mM; (c) 0.10 mM; (d) 0.20 mM; (e) 0.40 mM; (f) 0.83 mM. In all assays the system includes: [ATCh] = 0.45 mM; [AChE] = 50.0 unit/mL; [ATP-AuNP] = 28 nM (D) Inset: Normalized absorbance spectra showing the effect of [ATCh] on the growth of ATP-AuNPs at constant [AChE], [Au(III)] and [ATP-AuNP]: 50.0 unit/mL, 0.83 mM and 28 nM respectively. [ATCh]: (a) 0 mM; (b) 0.0056 mM; (c) 0.023 mM; (d) 0.057mM; (e) 0.11 mM; (f) 0.23 mM; (g) 0.34 mM; (h) 0.45 mM .*

when using constant concentrations of AuNP (28 nM), ATCh (0.45 mM) and Au(III) (0.83 mM). The data show that the absorbance increases linearly as the concentration of AChE is increased up to 25 Unit/mL, and then levels off, suggesting that higher levels of AChE may lead to aggregation of the enzyme and loss of activity. The inset of Figure 3.4A shows the absorbance spectra obtained for the reaction run at different AChE concentrations. This plot clearly shows an increase in the characteristic plasmon absorbance band, which provides strong evidence for growth of the entrapped AuNPs. An important point is that the signal level is not zero when AChE is absent; this likely reflects slow autohydrolysis of the ATCh with a concomitant reduction of Au(III) to produce an increase in absorbance.

Figure 3.4B shows the effect of the concentration of entrapped AuNPs at a constant concentration of AChE (50 Units/mL), ATCh (0.45 mM) and Au(III) (0.83 mM). Once again, the signal increases asymptotically with the concentration of added reagent, and in this case clearly shows that systems that do not contain entrapped AuNPs do not produce any discernable signal while systems with high levels of AuNPs (on the order of 28 nM) provide large color changes. The data demonstrate that primary AuNP particles are necessary to support growth of larger particles; systems that do not contain primary particles cannot support particle growth upon reduction of Au(III) and hence provide no color change. Interestingly, the shape of the absorbance spectra change with the concentration of entrapped AuNPs. Assays in which higher concentrations of

primiary AuNPs are present show sharper plasmon absorbance bands, likely reflecting more homogenous particle growth.

Figure 3.4C shows the effect of Au(III) concentration on signal levels, with constant levels of AChE (50 unit/mL), ATCh (0.45 mM) and AuNP (28 nM). In this case the signal changes linearly with the concentration of Au(III), and does not approach a saturation level. The experiment was terminated at 0.83 mM as there was a significant background gold color present above this level which made it difficult to detect the color change by eye.

Once the other reagents were optimized, the effect of substrate concentration on absorbance was evaluated by varying the concentration of ATCh at constant levels of AChE (50 unit/mL), AuNP (28 nM) and Au(III) (0.83 mM). The response was in general agreement with the expected Michaelis-Menten response (though it must be noted that we plot an endpoint value after 1 h rather than a rate), with the signal showing saturation at 0.45 mM. The experimental apparent K_M value for ATCh is ~150 µM, which is in good agreement with the literature value of 140 µM obtained from AuNP based solution assays.[16] The lag in response at very low ATCh concentrations may reflect mass transfer limitations and/or issues with partitioning of the cationic substrate into the sol-gel material, which have been previously observed for enzymes entrapped in sol-gel materials.[34]
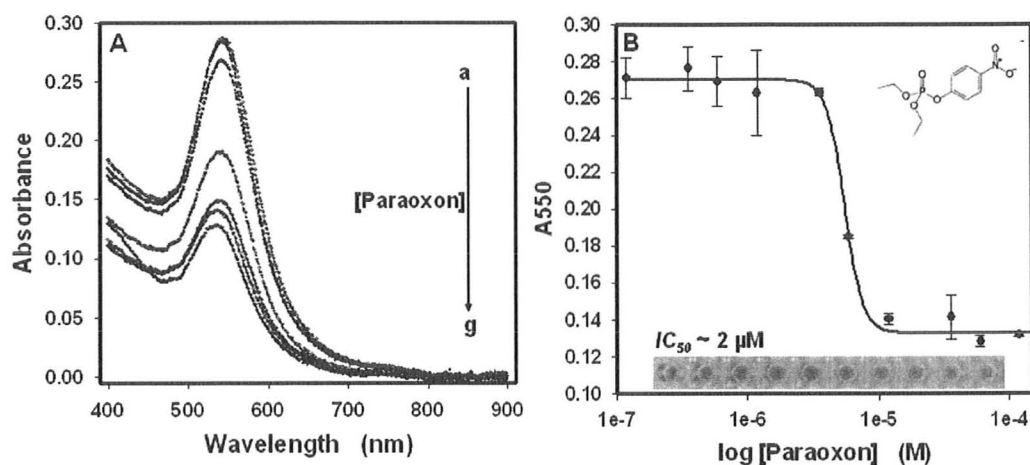
Figure 3.5. *Effect of paraoxon on activity of AChE. (A) Absorbance spectra showing the effect of Paraoxon on the growth of ATP-AuNPs. [Paraoxon]: (a) 0 M; (b) 4.0×10^{-8} M; (c) 4.0×10^{-7} M; (d) 1.0×10^{-6} M; (e) 2.0×10^{-6} M; (f) 4.0×10^{-6} M; (g) 4.0×10^{-5} M. Note: Overlapping spectrum were not included for sake of clarity. (B) Corresponding IC_{50} plot for Paraoxon as determined via solid phase enzyme assay. All assays include: AChE, 50.0 unit/mL; ATCh, 0.45 mM; Au(III), 0.83 mM; and ATP-AuNP; 28 nM*
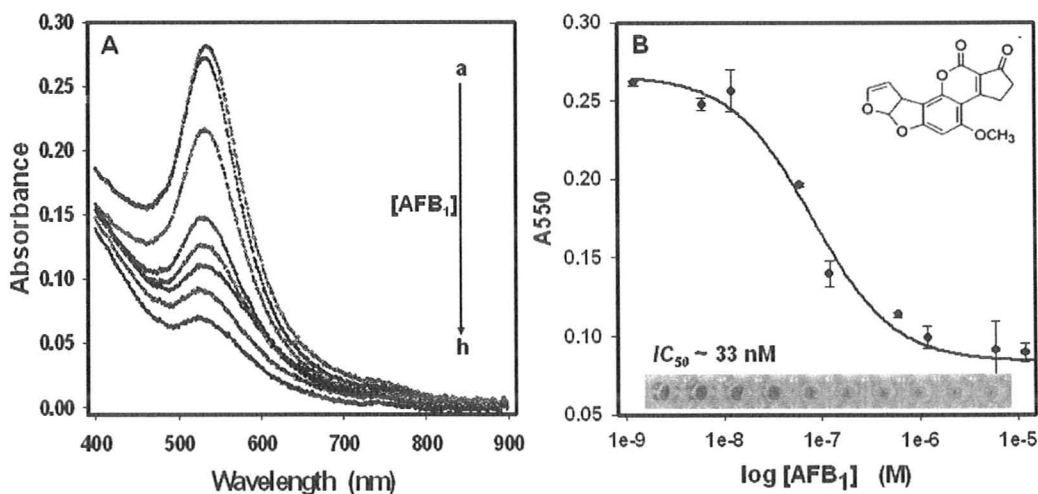

Figure 3.6. *Effect of [AFB₁] on AChE activity. (A) Absorbance spectra showing the effect of AFB₁ on the growth of ATP-AuNPs. [AFB₁]: (a) 0 M; (b) 4.0×10^{-10} M ; (c) 4.0×10^{-9} M; (d) 2.0×10^{-8} M ; (e) 4.0×10^{-8} M; (f) 2.0×10^{-7}M; (g) 4.0×10^{-7} M; (h) 2.0×10^{-5} M. Note: Overlapping spectrum were not included for sake of clarity. (B) Corresponding IC_{50} plot for Aflatoxin B₁ as determined via the solid phase enzyme assay. All assays include: AChE, 50.0 unit/mL; ATCh, 0.45 mM; Au(III), 0.83 mM; and ATP-AuNP, 28 nM.*

Long Term Stability: A potential benefit of immobilized enzymes is their resistance to denaturation.[21]   A number of enzymes, including AChE,[37] have been shown to possess excellent long term stability when entrapped within sol-gel derived silica materials. However, no studies exist relating to the stability of the primary AuNPs within the silica matrix, and thus was important to assess the stability of this sensing platform. For this purpose, the AChE/AuNP-doped silica materials were stored at 4 °C for 6 weeks, with assays performed on a weekly basis. These experiments indicated that AChE retained full activity and teh AuNPs retained their ability to grow and produce color changes over 8 weeks (study is ongoing, data not shown). Previous studies of entrapped enzymes have shown that some enzymes, such as Factor Xa, can remain active in sol-gel derived materials for several months.[34]   Hence, it is likely that the AChE/AuNP solid-phase assay platform should have a useful shelf life.

3.4 Conclusions

The data show that it is possible to enzymatically catalyze the growth of primary AuNPs from 3 nm to > 30 nm in diameter when a suitable enzyme is co-entrapped with the AuNPs within the pores of sol-gel derived silica materials, and that this process can be coupled to a large change in absorbance, which can be used to detect enzyme substrates or inhibitors. The bioassay demonstrated herein was based on acetylcholinesterase (AChE) catalyzed enlargement of gold nanoparticles, which resulted from reduction

of Au(III) by the product thiocholine. However, a wide range of different enzyme catalyzed reactions are amenable to this general assay format, including several redox enzymes, NAD^+-dependent biocatalytic transformations, and alkaline phosphatase catalyzed reactions. Thus, the soild-phase colorimetric assay platform should have good versatility.

Our results show that the assay is sufficiently sensitive to allow for detection of pesticides (Paraoxon) and toxins (Aflatoxin B_1) with detection limits that are in good agreement with the expected IC_{50} values. Observed detection limits are below the LD_{50} threshold for both compounds, suggesting that the solid phase assay should easily detect sub-lethal levels of these compounds. The ability to visually detect the color change, and the inability of the AuNPs to leach from the solid matrix make this assay format amenable to remote testing without the need for complex instrumentation.

Acknowledgements

3.5 Reference

1. Elghanian, R.; Storhoff, J.J.; Mucic, R.C.; Letsinger, R.L.; Mirkin, C.A. *Science,* **1997**, *277,* 1078-1080.

2. Willner, I.; Baron, R.; Willner, B. *Adv. Mater.,* **2006,** *18,* 1109-1120.

3. J. Wang, G. Liu, R. Polsky, A. Merkoci, *Electrochem. Commun.,* 2002, **4,** 722-726; J. Wang, G. Liu, A. Merkoci, *J. Am. Chem. Soc.,* 2003, **125,** 3214-3215; J. Wang, D.K. Xu, A.N. Kawde, R. Polsky, *Anal. Chem.,* 2001, **73,** 5576-5581.

4. Bruchez, M.; Moronne, M.; Gin, P.; Weiss, S.; Alivisatos, A.P. *Science,* **1998,** *281,* 2013-2016; Chan, W.C.W.; Nie, S. *Science,* **1998,** *281,* 2016-2018.

5. Willner, I.; Patolsky, F.; Wasserman, J. *Angew. Chem. Int. Ed.,* **2001,** *40,* 1861-1864.

6. Pavlov, V.; Xiao, Y.; Shlyahovsky, B.; Willner, I. *J. Am. Chem. Soc.,* **2004,** *126,* 11768 –11769.

7. Liu, J.; Mazumdar, D.; Lu, Y. *Angew. Chem. Int. Ed.,* **2006,** *45,* 7955-7959.

8. Velev, O.O.; Kaler, E.W. *Langmuir,* **1999,** *15,* 3693 –3698; Cao, Y.C.; Jin, R.; Nam, J.-M.; Thaxton, C.S.;. Mirkin, C.A. *J. Am. Chem.* Soc., **2003,** *125,* 14676-14677; Faulds, K.; Smith, W.E.; Graham, D. *Anal. Chem.,* **2004,** *76,* 412 –417.

9. Wang, J.; Rincon, O.; Polsky, R.; Dominguez, E. *Electrochem. Commun.,* **2003,** *5,* 83–86; Nam, J.M.; Thaxton, C.S.; Mirkin, C.A. *Science,* **2003,** *301,* 1884–1886.

10. Park, S.J.; Taton, T.A.; Mirkin, C.A. *Science,* **2002,** *295,* 1503–1506.

11. Xiao, Y.; Pavlov, V.; Levine, S.; Niazov, T.; Markovitch, G.; Willner, I. *Angew. Chem.,* **2004,** *116,* 4619–4622; *Angew. Chem. Int. Ed.,* **2004,** *43,* 4519–4522.

12. Shlyahovsky, B.; Katz, E.; Xiao, Y.; Pavlov, V.; Willner, I. *Small,* **2005,** *1,* 213-216.

13. Baron, R.; Zayats, M.; Willner, I. *Anal. Chem.,* **2005,** *77,* 1566-1571.

14. Zayats, M.; Baron, R.; Popov, I.; Willner, I. *Nano Lett.,* **2005,** *5,* 21-25.

15. Xiao, Y.; Pavlov, V.; Shlyahovsky, B.; Willner, I. *Chem. Eur. J.,* **2005,** *11,* 2698-2704.

16. Pavlov, V.; Xiao, Y.; Willner, I. *Nano Lett.,* **2005,** *5,* 649-653.

17. Basnar, B.; Weizmann, Y.; Cheglakov, Z.; Willner, I. *Adv. Mater.,* **2006,** *18,* 713-718.

18. Martinez, A.W.; Phillips, S.T.; Butte, M.J.; Whitesides, G.M. *Agnew. Chem. Int. Ed.,* **2007**, *46,* 1318-1320.

19. Camarero, J.A. *Biophys. Rev. Lett.,* **2 006,** *1,* 1-28.

20. Di Giusto, D.A.; King, G.C. *Top. Curr. Chem.,* **2006,** *261,* 131-168.

21. Jin, W.; Brennan, J.D. *Anal. Chim. Acta,* **2002,** *461,* 1-36.

22. Gill, I. *Chem. Mater.,* **2001,** *13,* 3404-3421.

23. Avnir, D.; Coradin, T.; Lev. O.; Livage, J. *J. Mater. Chem.,* **2006,** *16,* 1013–1030.

24. Pierre, A.C. *Biocat. Biotrans.,* **2004,** *22,* 145-170.

25. Coradin, T.;. Boissiere, M.; Livage, J. *Curr. Med. Chem.,* **2006,** *13,* 99-108.

26. Besanger, T.R.; Brennan, J.D. *J. Sol-gel Sci. Technol.,* **2006,** *40,* 209-225.

27. Anitha, K.; Mohan, S.V.; Reddy, S.J. *Biosens. Bioelectron.,* **2004**, *20,* 848-856; Doong, R.-A.; Tsai, H.-C. *Anal. Chim. Acta,* **2001,** *434,* 239-246; Du, D.; Chen, S.; Cai, J.; Zhang, A. *Biosens. Bioelectron.,* **2007,** *23,* 130-134.

28. Marrs, T.C. *Pharmacol. Ther.,* **1993,** *58,* 51-66.

29. Arduini, F.; Errico, I.; Amine, A.; Micheli, L.; Palleschi, G.; Moscone, D. *Anal. Chem.,* **2007,** *79,* 3409-3415.

30. Hussein, H.S.; Brasel, J.M. *Toxicology,* **2001,** *167,* 101-134.

31. Busbee, B.D; Obare, S; Murphy, C.J; *Adv. Mater.,* **2003**, 15, 414-416.

32. Zhao, W.; Gonzaga, F.; Li, Y.; Brook, M.A. *Adv. Mater.,* **2007,** *19,* 1766–1771.

33. Bhatia, R. B.; Brinker, C. J.; Gupta A. K.; Singh, A. K. *Chem. Mater.,* **2000,** *12,* 2434-2441.

34. Besanger, T.R.; Chen, Y.; Deisingh, A.K.; Hodgson, R.; Jin, W.; Mayer, S.; Brook, M.A.; Brennan, J.D. *Anal. Chem.,* **2003,** *75,* 2382-2391.

35. Skerritt, J.H.; Guihot, S.L.; Asha, M.B.; Rani, B.E.A.; Karanth, N.G.K.; *Food Agric. Immun.,* **2003,** *15,* 1-15.

36. Delmulle, B.S.; De Saeger, S.M.D.G.; Siba, L.; Barna-Vetro, I.; Van Peteghem, C.H. *J. Agric. Food Chem.,* **2005,** *53,* 3364-3368.

37. Pandey, P.C.; Upadhyay, S.; Pathak, H.C.; Pandey, C.M.D.; Tiwari, I. *Sens. Actuators B,* **2000,** *62,* 109–116.

Chapter 4: Colorimetric Detection of Enzyme Inhibitors using Sol-Gel/Enzyme/AuNP Composites. Part 2: Development of Bioactive Paper Sensors for Acetylcholinesterase Inhibitors

The following chapter was submitted to the scientific journal *Analyst,* for review, under the Title: **Colorimetric Detection of Enzyme Inhibitors using Sol-Gel/Enzyme/AuNP Composites. Part 2: Development of Bioactive Paper Sensors for Acetylcholinesterase Inhibitors** Roger E. Luckham and John D. Brennan.* Submitted on 7th May 2009 under the Manuscript ID: B909074F

I was responsible for all data collection and analysis. I wrote the first draft of the manuscript and Dr. Brennan provided editorial input to generate the final draft.

Abstract

A bioactive paper-based colorimetric "dipstick" bioassay is reported that is based on acetylcholinesterase (AChE) catalyzed enlargement of gold nanoparticles that are co-entrapped with the enzyme in a sol-gel based silica material that is coated on a functionalized paper substrate. Test solutions containing acetylthiocholine (ATCh) and a Au(III) salt are over spotted to the sensing area of the bioactive test strips containing small (3 nm diameter) primary gold nanoparticles (AuNP). Biocatalyzed hydrolysis of ATCh *via* AChE leads to formation of thiocholine, which in turn reduces the Au(III) onto the entrapped nanoparticles, producing particle growth and a concomitant increase in color intensity that can be correlated to the amount of substrate or inhibitor present in test solutions. The entrapped AuNP cannot leach from the silica material, leading to a bioactive paper assay that can utilize visual detection of a color change as a simple readout. Our results show that the dipstick based bioassay is sufficiently sensitive to allow for detection of Paraoxon with a detection limit of 1 μM. Detection can be made by eye or using a digital camera and image analysis, avoiding the need for sophisticated instrumentation.

Keywords: Dipstick; Bioactive paper, Colorimetric Biossay, Gold nanoparticle, Acetylcholinesterase, Sol-gel

4.1 Introduction

For more than a century, paper-based materials have been used extensively in areas such as food packaging and manufacturing of protective clothing. Recently, there has been widespread interest in the development and use of "bioactive paper," which uses a bio-recognition element, whether it be DNA aptamers,[1-3] enzymes[4] or antibodies,[5,6] that are deposited on the paper surface for the sensing of a wide range of chemical and biochemical species. These paper-based sensors reflect the fact that paper is inexpensive, disposable, and environmentally friendly and can transport liquids via capillary action with no need for external power.[7]

Paper-based sensors have been available since the mid twentieth century. The earliest reported paper-based colorimetric biosensor was developed in 1956,[8] and could monitor glucose levels in urine in the range of 0 – 2 wt% using physisorbed glucose oxidase, horseradish peroxidase and *o*-tolidine. Since then, a number of simple test-strip based sensors have been reported, the most successful of which are based on lateral flow devices[9,10] (*e.g.,* the home pregnancy test strip). These assays utilize sandwich or displacement immunoassays to detect a range of anlyates, from small molecules to whole cells.[10,11] While simple, sensitive and cost effective, these devices are difficult to adapt for some low molecular weight analytes and generally are not used for multi-analyte detection.

A recent resurgence in bioactive paper sensors has resulted in devices that produce rapid colorimetric detection of 2 to 3 analytes simultaneously. For example, Martinez *et al.*[4] were able to run multiple bioassays by creating hydrophobic channels on an absorbent paper surface that allow for analyte solutions to be directed into well-defined sensing areas. Where this work is novel and exciting, the fabrication of the device itself required several time consuming and expensive steps, which precludes large-scale manufacturing. Consequently, the same group reported on a low cost printing technique for creating the hydrophobic patterns[11] and on the use of paper based devices to create three-dimensional microfluidic systems.[12] Even though cost effective, these devices utilized bio-recognition elements that were physically adsorbed onto the paper surface, which can be of limited use in terms of retaining long term bio-activity of fragile enzymes and antibodies. Furthermore, as a consequence, devices such as these are not amenable to traditional dip-tests, as significant leaching of biomaterials can ensue - owing to the relative ease with which these molecules move along paper fibers[13].

The encapsulation of biomolecules in sol-gel derived materials (mostly silica based) has provided a simple and viable avenue in the development of portable, "solid phase" and easily recycled analytical devices and biocatalysts for the detection of various target molecules – ranging from clinical[14-16] to environmental analytes[17-19] Furthermore, sol-gel encapsulation has been shown to enhance the activity of various bio-molecules over prolonged periods[20-22]. Moreover, as noted

in the preceding paper, such materials support the growth of gold nanoparticles (AuNPs) as an indicator of bioactivity and a mechanism of signal generation. Furthermore, we have recently demonstrated that sol-gel materials can be deposited on paper substrates by ink-jet spraying, resulting in enzymatically active paper materials suitable for biosensing.[23] Herein, we present an approach that combines both an enzyme and a signalling element in a sol-gel coating that is deposited on a paper substrate. The colorimetric biosensing platform utilizes the biocatalytic growth of sol-gel entrapped gold nanoparticles (AuNPs) within a thin silica film coated onto a paper substrate. As a model system, we utilize the enzyme acetylcholinesterase (AChE) to stimulate growth of primary gold nanoparticles entrapped in a biocompatible sol-gel matrix, which was cast on paper. As part of the development of bioactive paper test strips, we examine the effects of paper type, surface coating/modification and sol-gel material composition on sensitivity, long term stability and overall assay performance.

4.2 Experimental Section

Materials: Diglycerylsilane (DGS) was prepared by methods described elsewhere[24] using tetramethylorthosilicate (Sigma-Aldrich, Oakville, ON) and anhydrous glycerol (Fisher Scientific, Toronto, ON). (N-(3-triethoxysilylpropyl) gluconamide) (GLS) was obtained from Gelest (Philidelphia, USA). Methyltrimethoxysilane (MTMS), sodium silicate solution (~ 14% NaOH, ~ 27% SiO$_2$), Dowex 50WX8-100 ion-exchange resin, polyethylene glycol (PEG) 600

and 1000, Acetylcholinesterase, (AChE, 10000 Units per mg solid, from *electrophorus electricus*, EC 3.1.1.7), acetylthiocholine iodide (ATCh), gold chloride trihydrate, adenosine 5′-triphosphate disodium salt (ATP), and diethyl 4-nitrophenyl phosphate (Paraoxon) were obtained from Sigma-Aldrich. Mead brand cardboard (Hillroy, Toronto), and Whatman # 1, 541 and 542 filter papers were obtained from Sigma-Aldrich (Oakville, ON). Bleached, coated and uncoated packing materials as well as calendar paper were obtained from Cascades Inc., Canada. Cascades Inc., Canada also provided: Board-Jouquieŕe, Board-Toronto, Board-East Angus and Board-Versailles. Timbec Inc., Canada provided the Timbec softwood pulp. Distilled deionized water was obtained from a Milli-Q Synthesis A10 water purification system. All reagents were used as received.

Safety Conditions: *The* stock solutions of paraoxon (highly toxic compound) were handled with caution at all times. To avoid skin contact, the material was handled in fume-hood using appropriate personal safety equipment, including gloves, masks and safety glasses. These were employed at all times when handling this substance.

Procedures

Preparation of ATP-Capped Gold Nanoparticles: ATP-capped gold nanoparticles (ATP-AuNPs) were prepared as described by Zhao et al.[25] Briefly, 60 μL of 10 mM gold chloride solution was added to 60 μL of 10 mM

ATP solution. To this, 2.75 mL of deionized water was added followed by shaking and incubation for 30 minutes at room temperature. 100 μL of freshly prepared 0.01 M $NaBH_4$ solution was then added and the resulting solution shaken for 10 seconds followed by incubation at room temperature for 3 hrs. The resulting solution of nanoparticles has a mean diameter of 2-3 nm, and can withstand up to 1 M NaCl without aggregation.

Preparation of Sol-Gel Materials: A range of silica precursors were used to prepare sols for enzyme and AuNP entrapment and dip-casting onto paper, including sodium silicate, DGS, TMOS and TMOS/MTMS mixtures, as well as each the first three precursors mixed with varying levels of PEG 600 and 1000 Da. Mixtures of 10% GLS/SS and 10% GLS/DGS were also assessed[26],[27]. Sodium silicate sols were prepared by mixing 10 mL of ddH_2O with 2.9 g of sodium silicate solution (pH ~13) followed by addition of 5 g of Dowex cation exchange resin to replace Na^+ with H^+. The mixture was stirred for 30 seconds to reach a final pH of ~4, and then vacuum filtered through a Büchner funnel. The filtrate was then further filtered through a 0.45 μM membrane syringe filter to remove any particulates in the solution. To make the DGS precursor sol, 0.5 g of solid DGS was dissolved in 1 mL of ddH_2O and the resulting mixture was sonicated for 15 minutes. To make MTMS and TMOS precursors, 1.4 mL of ddH_2O and 0.1 mL of 0.1 N HCl were added to a vial. Then, 4.5 mL of MTMS or TMOS was added and the resulting mixture was sonicated for 20 minutes in ice-

cold water. In order to make MTMS-TMOS mixtures, 4.5 mL of the silanes listed above was divided proportionally using volume percentages of 20 – 40% MTMS in TMOS and then mixed with water and acid and co-hydrolyzed by sonication. GLS and PEG-modified silica matrices were prepared by adding GLS (10 wt. %, final concentration), in buffer, to SS and DGS. Similarly, PEG (5-10 wt %, final concentrations), in buffer, was added to all silica precursors.

In all cases, the precursor sol solutions were mixed in a 1:1 volume ratio with a buffered solution (100 mM Tris-HCl buffer, pH 8.0) containing AChE with ATP-AuNP (28 nM) and additives, at room temperature (20 ± 1 °C), to provide a final volume of 1000 μL of material in a micro-centrifuge tube, with a final enzyme concentration of 50 Unit.mL^{-1} (1 Unit = 1 μmole of acetylcholine hydrolyzed per min at 37 °C). This mixture was then vortex mixed for 10 sec. at which point, it was deposited manually on thin strips of paper (~ 0.5 x 4.0 cm) *via* a simple dip-casting method forming the bioactive paper sensor. The withdrawal speed was ~ 0.5 cm/s.. The sensors were then allowed to cure for 24 hrs at room temperature prior to use, or longer for long-term stability studies.

Paper Based Assays: Bioactive paper sensors were formed (as described above) using different sol-gel formulations and paper types, with and without AChE present to assess the effect of the supporting materials on signal and

background levels. 30 μL of an assay solution consisting of the appropriate test reagent (ATCh and Au(III)) was added overtop the sensing area. Typical concentrations of reagents were $0 – 0.45$ mM ATCh, 0.83 mM of Au(III), 28 nM ATP-AuNP and 50 Unit.mL^{-1} AChE. Note: The concentrations of ATP-AuNP were calculated based on a molar extinction coefficient of 6.5 x 10^5 cm^{-1} for particles on the order of 2-3 nm.[28] After color development, an image was taken using a Canon Powershot A630 8.0 MP digital camera in automatic mode with the macrofocus setting (1 cm focal length, no flash). The resulting jpeg images were analyzed using ImageJ freeware obtained from the NIH website (http://rsb.info.nih.gov/ij/). Images were first inverted and then color intensity was determined using a 256 bit scale, where zero corresponds to white and 256 corresponds to black.

Biosensor Fabrication on Pre-treated Mead Cardboard: A 40% (v/v) MTMS/TMOS derived sol was used to pre-treat Mead brand cardboard strips (~ 0.5 x 4.0 cm). Pre-treatment was achieved by manual dipcasting using a withdrawal speed of ~ 0.5 cm/s. The paper strips were allowed to stand at room temperature for 6 h to facilitate drying. SS derived sols containing 50 Unit.mL^{-1} AChE and 28 nM ATP-AuNPs were then cast on the pre-treated strips to form the sensor.

Inhibition Assays: To the paper sensor, 10 μL of paraoxon solution was over spotted and incubated at room temperature for 20 min. 20 μL of a solution containing appropriate concentrations of Au(III) and ATCh was then added and left for 30 minutes to allow full color development. Image analysis was done as described above. The color intensity obtained was then plotted against inhibitor concentration to derive IC_{50} plots. Note: assays were also carried out *via* dip-testing, with similar results. However, given the number of experiments needed in the developmental stages, simple over spotting was used in order to reduce the volume of reagents used.

Long Term Stability Studies: Bioactive paper sensors were placed in air tight plastic bags and stored at 4 °C for up to 8 weeks. Assays and images were carried out as described above. Activity was referenced to that obtained from a sample that had been aged for 1 day.

Scanning Electron Microscopy: Bioactive paper samples imaged by SEM were sputter-coated with platinum (layer thickness 15 Å) to avoid charging effects prior to SEM imaging. Images were acquired using a JEOL JSM-7000F (JEOL Ltd. Tokyo, Japan) instrument operating at 10 kV.

Optical Profilometry: The topography of paper and thin films coatings on paper were investigated to assess the effect of 40% MTMS/TMOS fictionalization. Data

were obtained using a WYKO NT1100 Optical Profiling System. All paper sensors were examined using the 20x magnification objective.

Contact Angle Measurements: In all cases the contact angle was used as a measure of hydrophobicity. A Krűss DSA Contact Angle Apparatus was used to determine the contact angle of water to the different paper substrates.

4.3 Results and Discussion

Selection of Paper Substrate: A number of formats are possible for portable, solid-phase paper-based assay platforms. The two most common formats are lateral flow devices, which make use of the capillary action of paper, and the standard dipstick, where the sensor is immersed in the test solution. The former assay has a potential advantage in that analytes may be separated during analysis[4], which can reduce matrix interferences. However, this format requires highly hydrophilic paper substrates that support capillary flow and which will also allow for reproducible bio-reagent loading in the fabrication process. For our paper-based assay, we chose to use an assay format involving addition of small quantities of test solution over the sensing area of the paper biosensor. From preliminary studies, it was noted that heavier paper types, with relatively high wet strength, such as coated Mead brand cardboard, were optimal for assays such as these, as reagents interact with such paper types in a more controlled manner, relative to more absorbent substrates. Furthermore, these paper substrates were

excellent for dip-casting, as they allowed for easy immersion into silica sols without bending or curling, and thus could support dip-casting of thin film coatings.

The choice of paper type is of particular importance in this work. The paper support must possess certain characteristics to support the assay platform under study: (1) it must be able to support coating with biologically doped silica; (2) it must be relatively non-absorbent, enabling the formation of a more defined sensing area by preventing extensive spreading (across and into the substrate) of aqueous components; (3) it must not degrade the bio-recognition element(s) or other assay reagents in any way; and (4) the surface must be uniform to allow for reproducible enzyme loading and signal generation. As a starting point, the respective reagents were entrapped into a sodium silicate (SS) derived sol and deposited on various paper types to assess their applicability to such an assay platform. SS is a very simple, biocompatible sol-gel precursor that produces materials which maintain the activity of enzymes[29], and does not produce any byproducts (i.e. alcohols, glycerol, etc) that might interfere with the growth of AuNPs[21-30] For this reason, SS was used for evaluation of various paper substrates.

A series of different paper materials were examined, including calendar (high gloss) paper, Whatman #1, #541, 542 filter papers, uncoated bleached packing paper, and several coated cardboard materials as well as a soft wood pulp and a 40%MTMS/TMOS functionalized Mead cardboard surface as a
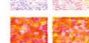
Paper type	Adhesion	Cracking	Signal: Background (S/B)	Consistency on paper	Positive Control- 50 U/mL AChE Present (Signal)	Negative Control- No AChE (Background)
Calendar paper	Poor	**	**	Does not coat paper	**	**
Unbleached coated packing paper	Good	Minimal	0.397 ± 0.829	Coats surface		
Coated bleached packing paper	Very Good	Moderate	0.909 ± 0.568	Coats surface		
Uncoated bleached packing paper	**	**	0.710 ± 1.01	Absorbs sol		
Coated Mead cardboard	Very Good	Minimal	0.377 ± 0.029	Coats surface		
Board-Jouquieře	Very Good	Minimal	1.27 ± 1.13	Coats surface		
Board-Toronto	Very Good	Minimal	0.678 ± 0.351	Coats surface		
Board-East Angus	Very Good	Minimal	1.00 ± 0.923	Coats surface		
Board-East Versailles	Very Good	Minimal	0.153 ± 0.237	Coats surface		
Whatman# 1	**	**	1.17 ± 0.168	Absorbs sol		
Whatman# 541	**	**	1.44 ± 1.06	Absorbs sol		
Whatman# 542	**	**	1.02 ± 0.897	Absorbs sol		
Timbec softwood pulp	**	**	0.722 ± 0.044	Absorbs sol		
40% MTMS/TMOS Functionalized Mead	Excellent	Minimal	4.15 ± 0.002	Coats Surface		
96 Well Plate Assay	–	–	25.2 ± 1.38	–		

Table 4.1. *The effect of paper type on reproducibility of assay. All images were processed using ImageJ, a background subtraction (50% pixel) followed by contrast adjustment (0.5%) better depicts color formation.*

highly hydrophobic support for dip-casting. Table 4.1 shows results obtained from assays performed on the various paper substrates using SS as the sol-gel precursor. It is clear from Table 4.1 that the highly absorbent paper types such as uncoated board and filter paper are not suitable for this assay platform. These paper substrates allowed for aqueous sensor components to spread over relatively large areas and absorb through the paper – leading to signal: background ratio approaching one (or less).

The optimal paper substrate, in terms of the interaction with the silca

Sol-gel Materials	Adhesion	Cracking	Contact Angle (°)	Signal: Background
SS	Inconsistent	Minimal	24.7 ± 1.00	1.83 ± 1.02
10% GLS/SS	Inconsistent	Moderate	15.8 ± 0.540	0.987 ± 0.761
5% PEG600/SS	No Adhesion	--	--	--
10% PEG600/SS	Inconsistent	Cracking	1.40 ± 0.180	0.990 ± 0.888
5% PEG1000/SS	Inconsistent	Cracking	6.40 ± 0.140	1.33 ± 0.991
10% PEG1000/SS	Inconsistent	Cracking	2.80 ± 0.070	0.992 ± 1.19
DGS	Inconsistent	Cracking	11.5 ± 0.170	1.14 ± 0.790
10% GLS/DGS	Inconsistent	Minimal	9.60 ± 0.080	0.634 ± 0.332
5% PEG600/DGS	No Adhesion	--	--	--
10% PEG600/DGS	Inconsistent	Minimal	6.50 ± 0.150	0.668 ± 1.10
5% PEG1000/DGS	Inconsistent	Moderate	5.50 ± 0.320	0.243 ± 0.310
10% PEG 1000/DGS	Inconsistent	Moderate	5.50 ± 0.310	1.02 ± 0.554
TMOS	Inconsistent	Minimal	7.00 ± 0.400	1.23 ± 0.117
20% MTMS/TMOS	Inconsistent	Minimal	31.4 ± 1.34	0.820 ± 0.901
30% MTMS/TMOS	Inconsistent	Minimal	57.6 ± 0.310	1.00 ± 0.448
40% MTMS/TMOS	Excellent	Minimal	115 ± 0.140	0.795 ± 0.999

Table 4.2. *The effect of Sol-gel layers on Mead Cardboard surface.*

coating, was a white-resin coated cardboard material from Mead (Hillroy, TO). This material was easy to coat with SS, provided very good adhesion with minimal cracking of the silica materials (after 24 hours storage), and did not interfere with the assay reaction. However, a signal to background ratio (S/B) of 1.83 ± 1.02 (Table 4.2) was quite low and showed poor reproducibility on this untreated surface. Possible explanations are: (1) the paper surface itself may be degrading the enzyme in some way; (2) given its porous and hydrophilic nature (see below), the bio-recognition element may penetrate too deeply into the paper surface, thus enabling AuNP growth within the resin coating and paper fibers rather than at the surface; or (3) not enough AChE

remained on the paper surface as a result of poor film adhesion. A similar trend was observed for all other white resin-coated materials (the exception being the lightly coated Board-East Versailles paper). However an appreciable signal could not be achieved with any untreated paper substrates, hence, we investigated coating of suitable paper substrates with a hydrophobic sol-gel derived film prior to casting of the SS/AChE coating. For this purpose a 40% (v/v) MTMS/TMOS precursor, containing co-hydrolyzed components, was used to coat the surface of the Mead paper and bioassays produced a S/B of 4.15 ± 0.002. MTMS is inherently hydrophobic and so treatment with 40%MTMS/TMOS resulted in a highly hydrophobic paper surface (Table 4.2). Moreover, the 40% MTMS/TMOS pretreatment allowed for uniform coating of the paper surface (see below), consequently resulting in more reproducible enzyme loading and less background signal.

Optimization of Silica Coatings: As previously discussed, SS derived films performed well when incorporated into this assay platform; however, SS showed inconsistent adhesion to untreated paper surfaces and severe cracking after only 3 days of storage. Therefore, an assessment was done on how different sol-gel derived silica materials performed when used for coating paper. The optimal material for the development of a bioactive coating should meet the following criteria: 1) it should be easy to deposit on the paper support; 2) it should show minimal shrinkage and cracking and have good adhesion to the material on which

it is deposited; 3) it must not interfere with the assay; 4) it must retain the entrapped enzyme in an active state; and 5) it should show good long-term stability after deposition.

A series of materials were evaluated against these criteria, including SS, DGS, TMOS and MTMS/TMOS mixtures, along with materials containing 10% (w/v) of a sugar- modified silane (GLS) and 5 or 10% (w/v) PEG 600 or 1000 Da. Table 4.2 shows the different materials studied and their respective performance on Mead cardboard. The general trend as illustrated in this table is that all of the thin films showed cracking and/or poor adhesion (after 24 hours) with the exception of SS (good adhesion) and 40% MTMS/TMOS, which showed excellent adhesion.

The 40% MTMS/TMOS material showed good adhesion and minimal cracking even after 3 months curing at room temperature. Unfortunately, such coatings showed no activity for AChE, while SS based coatings showed the best activity, but had poor reproducibility, and severe cracking and shrinkage after just a few days of aging. For this reason, we investigated further, 40% MTMS/TMOS as an intermediate layer to allow better adhesion of SS to the paper substrate.

Effect of 40% MTMS/TMOS coating as an adhesion layer: To fully understand the effect of the 40% MTMS/TMOS adhesion layer, SEM and optical profilometry experiments were carried out, along with contact angle
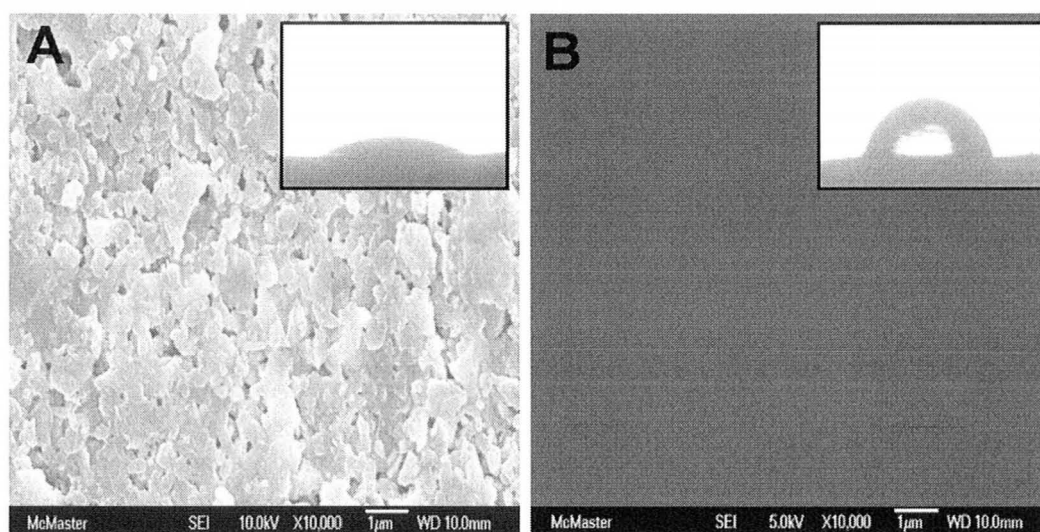
Figure 4.1. *SEM images showing the varying morphologies of Mead brand cardboard before (A) and after (B) functionalization with 40%MTMS/TMOS. Inset: Images of drops formed on respective surfaces.*

measurements. Figure 4.1 shows SEM images of untreated Mead (A) and Mead that was coated with 40% MTMS/TMOS (B). From these images it is quite clear that the coating reduces roughness while also increasing the contact angle. Figure 4.2 shows the corresponding x,y-profiles of the untreated (A) and 40% MTMS/TMOS treated Mead paper (B) obtained from profilometry. These data show a decreased average peak-to-valley roughness (Ra) for 40% MTMS/TMOS coated paper (Ra = 441.65 nm) compared to untreated Mead (Ra = 972.00 nm), indicating that the coating likely fills the pores within the paper and produces a relatively uniform surface for subsequent coating with enzyme-doped silica films.

The contact angle for 40% MTMS/TMOS treated paper was found to be 115 ± 2° (Table 4.2) while that of untreated Mead was found to be 29 ± 1°. The
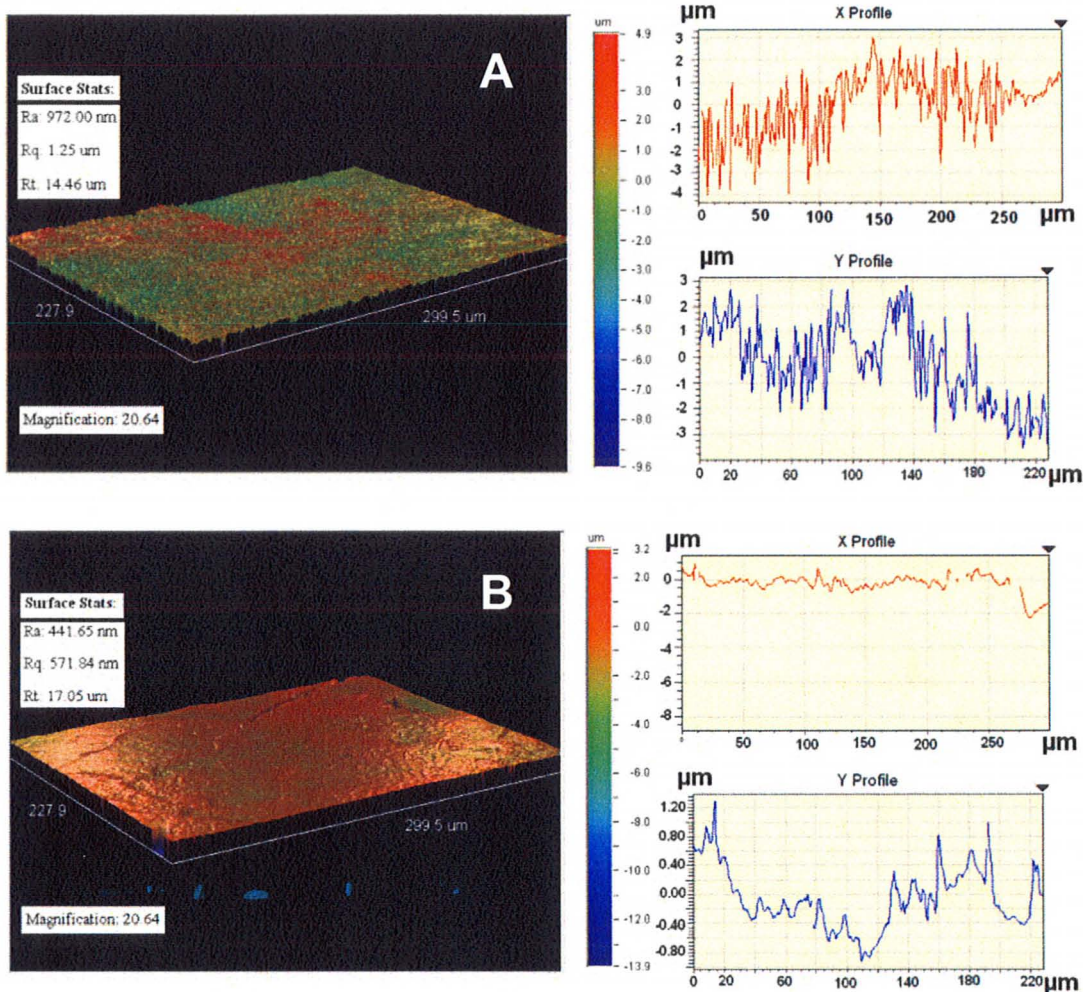
Figure 4.2. *Surface topography of pre-treated and 40%MTMS/TMOS functionilzed Mead brand cardboard. Three-dimensional Optical Profilometry images showing the varying morphologies of Mead brand cardboard before (A) and after (B) functionalization with 40%MTMS/TMOS.*

increased contact angle is indicative of increased hydrophobicity[31] which likely aids in more reproducible enzyme/test solution loading, as increased water blocking capabilities should allow enzyme and the test solution to remain at the surface of the sensing area as opposed to seeping into the paper substrate. Test solutions completely seeped into the untreated sensor strips in

only 5-10 min but showed no such behaviour on the pre-coated paper.

Optimization of Dipstick Assay Conditions: To optimize the conditions for the dipstick assay format, SS derived sols containing optimum levels of AChE and AuNPs were deposited on Mead cardboard, which was pre-functionalized with 40% MTMS/TMOS. A test solution containing the appropriate concentration of ATCh and Au(III) was then added. All assays were allowed to run for 30 min. after which time, an image was taken. The quantitative data was obtained using image analysis of the color intensity of the sensing area on the paper as described above. All assays were performed using the following conditions: [AuNP] = 28 nM, [AChE] = 50 unit/mL, [Au(III)] = 0.83 M and [ATCh] = 450 µM.

Figure 4.3 shows the effect of [ATCh] on signal and background levels. The data show that as the concentration of ATCh increases so too does the color intensity with saturation occurring at 450 µM and a signal change of ~ 5-fold in color intensity. On the other hand, increasing concentrations of ATCh had little effect on the background signal with no AChE present on sensor (<2 fold increase in signal). These data provide clear evidence that quantitative assays are possible using the colorimetric dipstick assay.

Quantitative Dipstick Assay for AChE Inhibitors: It is well known that AChE can be inhibited by a range of compounds, including organophosphates,
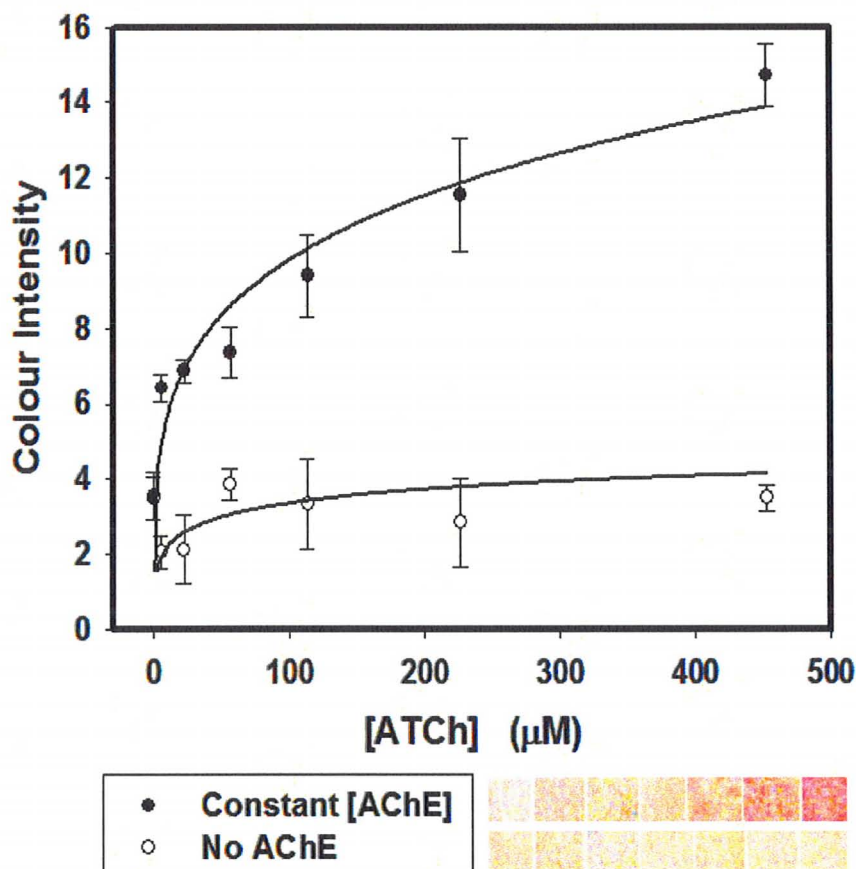
Figure 4.3. *The effect of [ATCh] on the growth of ATP-AuNPs in a SS SG matrix on a paper substrate. The effect of the SG/Paper matrix on background is also shown. All paper-based sensors include AChE, 50.0 unit/mL and ATP-AuNP, 28 nM Over-spotting solutions containing varying [ATCh], as shown, and Au(III), 0.83 mM*

carbamates, aflatoxins and compounds such as galanthamine and sanguinine, which are often used as therapeutics for treatment of Alzheimer's disease.[32] To assess the potential of the dipstick as a tool to detect AChE inhibitors, a preliminary assay was performed to determine the effect of paraoxon on the growth of AuNPs. As seem in Figure 4.4, increasing concentrations of Paraoxon lead to a decrease in the color intensity, indicating inhibition of
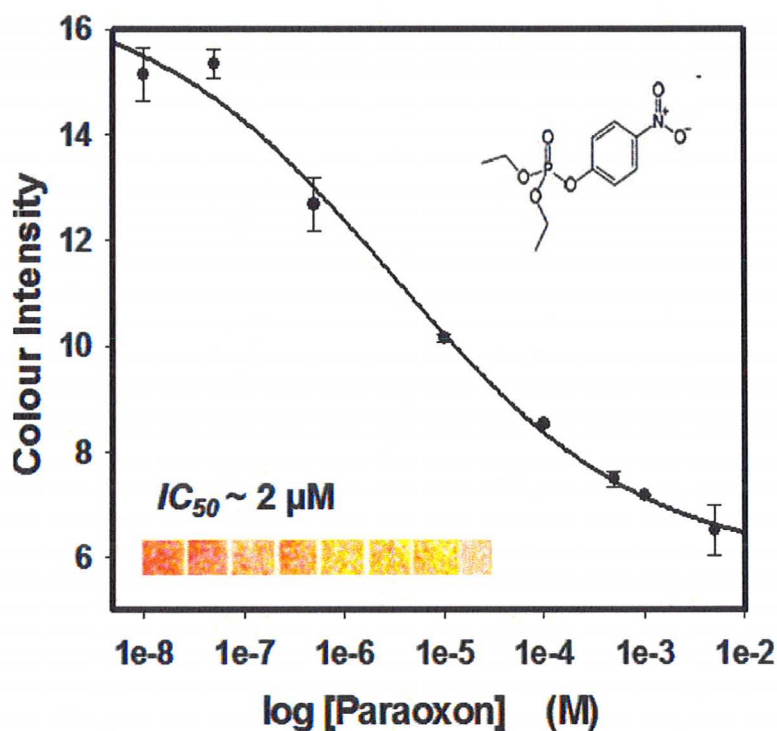
Figure 4.4. *IC_{50} plot for Paraoxon as determined via solid phase, paper based enzyme assay. All assays include AChE, 50.0 unit/mL, ATCh, 0.45 mM, Au(III), 0.83 mM and ATP-AuNP, 28 nM.*

AChE and decreased growth of AuNPs. The assay required 30 min. and produced close to a 3-fold reduction in color intensity. The concentration of 50% inhibition (IC_{50}) for Paraoxon was calculated to be 1.9 ± 0.1 µM (Figure 4.4), which is in good agreement with the literature value of between 0.73 and 3.1 µM[33]. The IC_{50} for pararoxon, as determined *via* 96 well plates assays (see preceding paper), with identical reagent concentrations, was also calculated to be 1.9 ± 0.1 µM, demonstrating that moving from 96-well plates to paper has no effect on assay sensitivity.

While IC_{50} values are useful for determining the potency of the inhibitor, a

more useful analytical parameter of merit is the limit of detection (LOD). In the case with this work, where the amount of available substrate and enzyme is not known, then comparison of LOD to toxicity (LD_{50}) of specific inhibitors is more applicable. The LD_{50} for Paraoxon in relation to rats (orally administered), as reported by manufacturers MSDS, is 6.5 µM (1.8mg/kg), while the LOD for Paraoxon (S/B < 3) as determined by our paper-based assay platform was calculated to be 1 µM. Hence, it is clear that the sol-gel based, bioactive paper sensor is able to detect sub-lethal concentrations of Paraoxon.

Long Term Stability: A potential benefit of immobilized enzymes is their resistance to denaturation[34-36]. A number of enzymes, including AChE[37] have been shown to possess excellent long term stability when entrapped within sol-gel derived silica materials. However, no studies exist that describe the stability of AChE in sol-gel derived coatings on paper substrates. For this purpose, the paper based biosensors were stored at 4 °C for 12 weeks, with assays performed after such time. Previous studies of entrapped enzymes have shown that some enzymes, such as Factor Xa, can remain active in sol-gel derived materials for several months.[38] Hence, it is likely that the AChE/AuNP paper-based assay platform should have a useful shelf life. Figure 5.5 shows the long term stability of the enzyme in monolithic siilca (A) and within sol-gel derived siilca films on paper (B). In each case, the enzyme retained >90% activity after 3 months storage. The slightly lower bioactivity after 3 months for the paper-based sensors
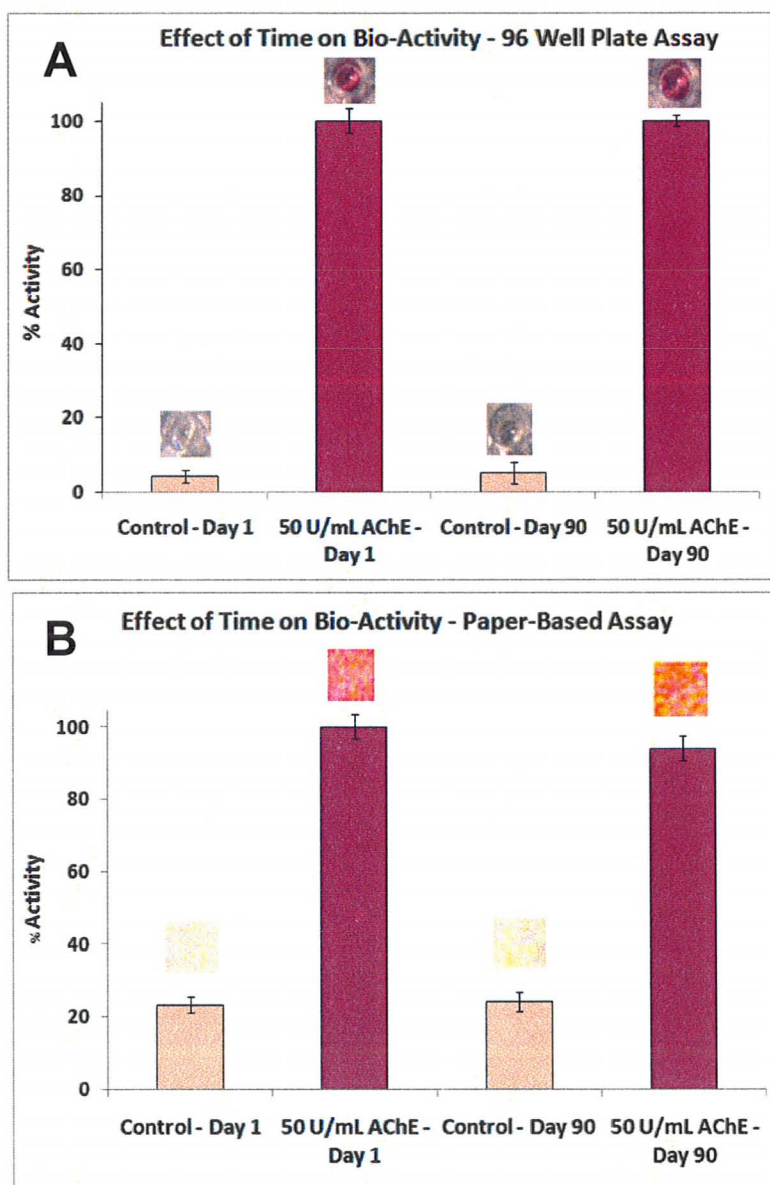
Figure 4.5. *Effect of time on Bioactivity of AChE entrapped in a SS matrix in 96 well plates (A) and that which was deposited on paper (B).*

could be as a result of higher susceptibiity to dehydration for thin films relative to monoliths present in sealed 96 well plates.

4.4 Conclusions

The data show that sol-gel derived silica materials are sufficiently versatile to be used not only as an entrapment media, but also a functionalization agent to make surfaces more uniform and hydrophobic. This is particularly important in the present sensing system, as it allows for more reproducible enzyme loading on rough and non-uniform paper surfaces.

Our results show that the assay is sufficiently sensitive to allow detection of ATCh or Paraoxon either by eye or with a digital camera and image analysis software, avoiding the need for expensive and sophisticated instrumentation. The test strips allow for detection of pesticides (Paraoxon) with detection limits that are well below the LD_{50} threshold for this compound, suggesting that the colorimetric sensor should easily detect sub-lethal levels of these types of toxins.

Acknowledgements

4.5 References

1. Navani, N.K.; Li, Y.F. *Curr. Opin. Chem. Biol.,* **2006,** *10,* 272–281.

2. Liu, J.; Mazumdar, D.; Lu, Y. *Angew. Chem. Int. Ed.,* **2006,** *45,* 1 – 5.

3. Su, S.; Nutiu, R.; Filipe, C.D.M.; Li, Y.; Pelton, R. *Langmuir,* **2007,** *23,* 1300 1302.

4. Martinez, A.W.; Phillips, S.T.; Butte, M.J.; Whitesides, G.M. *Agnew. Chem. Int. Ed.,* **2007,** *46,* 1318-1320.

5. Klewitz, T.; Gessler, F.; Beer, H.; Pflanz, K.; Scheper, T. *Sens. Actuators B.,* **2006,** *113,* 582–589.

6. Xu, C.; Wang, H.; Peng, C.; Jin, Z.; Liu, L. *Biomed. Chromatogr.,* **2006,** *20,* 1390–1394.

7. Martinez, A.W.; Phillips, S.T.; Whitesides, G.M. *Proc. Natl. Acad. Sci. USA,* **2008,** *105,* 19606-19611.

8. Comer, J.P. *Anal. Chem.,* **1956,** *28,* 1748-1750.

9. von Lode, P. *Clin. Biochem.,* **2005,** *38,* 591-599.

10. Mabey, D.; Peeling, R.W.; Ustianowski, A.; Perkins, D.M. *Nat. Rev.,* **2004,** *2,* 231-240.

11. Bruzewicz, D.A.; Reches, M.; Whitesides, G.M. *Anal. Chem.,* **2008,** *80(9),* 3387–3392.

12. Martinez, A.W.; Phillips, S.T.; Whitesides, G.M. *Proc. Natl. Acad. Sci. USA,* **2008,** *105,* 19606-19611.

13. Liu, J.; Mazumdar, D.; Lu, Y. *Angew. Chem. Int. Ed.,* **2006,** *45,* 7955 –7959.

14. Sampath, S.; Lev, O. *J. Electroanalysis,* **1996,** *8,* 1112.

15. Pankratov, I. Lev, O. *J. Electroanal. Chem.,* **1995,** *393,* 35-41.

16. Park, T.; Iwouoha, E. Smyth, M.; Freaney, R.; McShane, A. *Talanta,* **1997,** *44,* 973.

17. Doong, R.; Tsai, H. *Anal. Chim. Acta,* **2001,** *434,* 239–246.

18. Yu, D.; Volponi, J.; Chhabra, S.; Brinker, C.J.; Mulchandani, A.; Singh, A.K. *Biosens. Bioelectron..* **2005,** *20,* 1433–1437.

19. Du, D.; Chen, S.; Cai, J.; Zhang, A. *Talanta,* **2008,** *74,* 766-772.

20. Reetz, M. T.; Zonta, A.; Simpelkamp, J. *Biotechnol. Bioeng.,* **1996,** *49,* 527-534.

21. Jin, W.; Brennan, J.D. *Anal. Chim. Acta,* **2002,** *461,* 1-36.

22. Pandey, P.C.; Upadhyay, S.; Pathak, H.C.; Pandey, C.M.D.; Tiwari, I. *Sens. Act. B,* **2000,** *62,* 109–116.

23. Hossain, S.M.Z.; Luckham, R.E.; Smith, A.M.; Lebert, J.M.; Davies, L.M.; Pelton, R.H.; Filipe, C.D.M.; Brennan, J.D. *Anal. Chem.,* 2009, in press.

24. Brook, M.A.; Chen, Y.; Guo, K.; Zhang, Z.; Brennan, J.D. *J. Mater. Chem.,* **2004,** *14,* 1469-1479.

25. Zhao, W.; Gonzaga, F.; Li, Y.; Brook, M.A. *Adv. Mater.,* **2007,** *19,* 1766–1771.

26. Lin, T.; Wu, C.; Brennan, J.D. *Biosens. Bioelectron.,* **2007,** *22,* 1861–1867.

27. Chen, Y.; Zhang, Z.; Sui, W.; Brennan, J.D.; Brook, M.A. *J. Mater. Chem.,* **2005,** *15,* 3132–3141.

28. Pavlov, V.; Xiao, Y.; Shlyahovsky, B.; Willner, I. *J. Am. Chem. Soc.,* **2004,** *126,* 11768 –11769.

29. Gupta, A.K.;. Singh, A.K.; Bhatia, R.B.; Brinker. C.J. *Chem. Mater.,* **2000,** *12,* 2434-2441.

30. Di Risio, R.; Yan, N. *Macromol. Rapid Commun.,* **2007,** *28,* 1934-1940.

31. Shen, W.; Filonanko, Y.; Truong, Y.; Parker, I.H.; Brack, N.; Pigram, P.; Liesegang, J. *J. Colloids Surf. A,* **2000,** *173,* 117-126.

32. Wilkinson, D.; Murray, J. *Int. J. Geriatric Psych.*, **2001**, *16*, 852-857.

33. Skerritt, J.H.; Guihot, S.L.; Asha, M.B.; Rani, B.E.A.; Karanth, N.G.K.; *Food Agric. Immunol.*, **2003**, *15*, 1-15.

34. Klibanov, A.M. *Anal. Biochem.*, **1979**, *93*, 1-25.

35. Kulshrestha, Y.; Husain, Q. *Enz. Microb. Technol.*, **2006**, *38*, 470–477.

36. Rauf, S.; Ihsan, A.; Akhtar, K.; Ghauri, M.A.; Rahman, M.; Anwar, M.A.; Khalid, A.M.; *J. Biotechnol.*, **2006**, *121*, 351–360.

37. Pandey, P.C.; Upadhyay, S.; Pathak, H.C.; Pandey, C.M.D.; Tiwari, I. *Sens. Act. B*, **2000**, *62*, 109–116.

38. Besanger, T.R.; Chen, Y.; Deisingh, A.K.; Hodgson, R.; Jin, W.; Mayer, S.; Brook, M.A.; Brennan, J.D. *Anal. Chem.*, 2003, **75**, 2382-2391.

Chapter 5: Development of a Bioactive Paper Sensor for Detection of Neurotoxins Using Piezoelectric Inkjet Printing of Sol-Gel Derived Bioinks

The following chapter was publication in the scientific journal *Analytical Chemistry,* under the citation: S.M. Zakir Hossain, Roger E. Luckham, Anne Marie Smith, Julie M. Lebert, Lauren M. Davies, Robert H. Pelton, Carlos D.M. Filipe and John D. Brennan, **Development of a Bioactive Paper Sensor for Detection of Neurotoxins Using Piezoelectric Inkjet Printing of Sol-Gel Derived Bioinks.** *Analytical Chemistry,* **2009**, *81,* 5474–5483.

The data collection was a collaborative effort between Dr. Hossain, two summer students and me. I was responsible for the collection and analysis of all SEM and Optical Profilometry data. Preliminary work with ink-jet printing of bio-doped *sol-gel* inks was done in conjunction with Lauren Davies. Lauren was also responsible for the preliminary work with PVAm. Dr. Hossain was responsible for all other PVAm data generation and analysis. The biosensor design was done by me. Some inhibition experiments and biosensor fabrication was done by Dr. Hossain and me, while Dr. Hossain was responsible for the analysis of all such data. The bio-ink optimization was done by Dr. Hossain, Anne Marie Smith and me.

The writing of the manuscript was also a collaborative effort between Dr. Hossain and me. The version presented here was produced after editorial input from Dr. Brennan.

Abstract

There is an increasing interest in new strategies to rapidly detect analytes of clinical and environmental interest without the need for sophisticated instrumentation. As an example, the detection of acetylcholinesterase (AChE) inhibitors such as neurotoxins and organophosphates has implications for neuroscience, drug assessment, pharmaceutical development, and environmental monitoring. Functionalization of surfaces with multiple reagents, including enzymes and chromogenic reagents, is a critical component for effective development of "dipstick" or lateral flow biosensors. Herein, we describe a novel paper-based solid-phase biosensor that utilizes piezoelectric inkjet printing of biocompatible, enzyme doped sol-gel based inks to create colorimetric sensor strips. For this purpose, polyvinylamine (PVAm, which captures anionic agents) was first printed and then AChE was overprinted by sandwiching the enzyme within two layers of biocompatible *sol-gel* derived silica on paper. AChE inhibitors, including paraoxon and aflatoxin B_1, were detected successfully using this sensor by measuring the residual activity of AChE on paper as followed by Ellman's colorimetric assay with capture of the 5-thio-2-nitrobenzoate (TNB^-) product on the PVAm layer. The assay provided good detection limits (paraoxon ~100 nM; aflatoxin B1~ 1 nM) and rapid response times (< 5 min). Detection could be achieved either by eye or using a digital camera and image analysis software, avoiding the need for expensive and sophisticated instrumentation. We demonstrate that the bioactive paper strip can be used either as a dipstick or a

lateral flow-based biosensor. The use of sol-gel based entrapment produced a sensor that retained enzyme activity and gave reproducible results after storage at 4 °C for at least 60 days, making the system suitable for storage and use in the field.

Keywords : bioactive paper, sol-gel, inkjet printing, biosensor, neurotoxins

5.1 Introduction

Recently, paper-based patterned solid-phase sensors (which are simple, portable, disposable and inexpensive) have been developed to run multiple bioassays and controls simultaneously.[1-7] These portable biosensing papers are extremely useful in remote settings as well as less industrialized countries where simple bioassays are essential in the first stages of detecting disease, and for monitoring environmental and food based toxins. However while these bioactive paper sensors show promise, all paper-based sensors reported to date have utilized bio-recognition elements that are physically adsorbed onto the paper surface – no permanent immobilization method such as covalent or affinity attachment or entrapment techniques have been employed. As a result, paper-based sensors have been utilized only as lateral flow sensors and have not been amenable to dipstick sensing formats.

The automated deposition and permanent immobilization of biorecognition molecules on solid surfaces is a critical step in the development of bioactive paper-based sensors. To achieve this goal it is necessary to develop protein immobilization methods that are compatible with automated coating and/or printing methods and which retain the biomolecule at the surface of the paper substrate. In this work, we explore the use of biocompatible sol-gel derived materials for this purpose. It has been shown that entrapment of biomolecules within sol-gel derived materials allows proteins to retain their bioactivity for prolonged periods of time.[8,9] Furthermore, sol-gel based materials have previously

been shown to be amenable to ink-jet deposition (although not with proteins)[10] or screen printing with entrapped enzymes.[11]   However, biocompatible sol-gel materials with entrapped proteins have not yet been deposited via ink-jet printing and have not been incorporated within bioactive paper sensors.

Several conventional deposition techniques such as dip coating,[12] spin coating,[13] aerosol spraying,[14] and electrophoretic deposition[15] have previously been used to deposit bioactive sol-gel derived materials. Among these, dip and spin coating are not practical for large-scale production. In addition, they are time consuming and are wasteful when dealing with expensive bioreagents. Aerosol spraying can be used for deposition of biomaterials, but is not easily adaptable to formation of millimeter scale patterns. Electrophoretic deposition is normally used for fabrication of electrodes and the process requires an electrically conductive surface.[16]

On the other hand, the inkjet printing technique for deposition of materials on paper has attracted attention because the system is simple, rapid, scalable, compatible with paper substrates and amenable to pattern formation.[9, 17-20] As a result, a variety of biomaterials can be deposited on a solid support in a single or multiple layers at ambient temperature with relatively low shear rates with bio-activity retained for extended periods.[21, 22] Using this technology, cells/ tissue,[23, 24] DNA,[25] antibodies,[14] and enzymes,[2,10,24] have been dispensed, deposited or patterned in either 2D or 3D arrangements. However, the most critical part of inkjet printing is probably the formulation of the bioink and its rheological

properties, in particular the viscosity and surface tension.[19,21] Several additives are introduced in the ink formulations to optimize the physical properties and to make them stable and ejectable. The specific challenge associated with the formulation of enzyme containing bioinks for reliable piezoelectric inkjet printing has been reported.[10] Printing of biocompatible sol-gel derived inks is an even larger challenge since short gelation times of silica sols can cause gelation and clogging of the inkjet nozzles, especially when specific proteins (in buffer) are added to the sol-gel material. At physiological pH, where most enzymes thrive, gelation of most biocompatible sol-gel precursors occurs within a minute to a few hours depending on buffer strength and type or additives being used.[26] For this reason, we have explored a multi-stage ink-jet deposition method wherein the silica sol and the buffered protein are deposited from separate ink-jet cartridges and thus do not interact prior to deposition on the paper surface, avoiding gelation in the ink-jet nozzle.

To evaluate the potential of ink-jet deposition for fabrication of bioactive paper sensors, we have used the detection of organophosphates via inhibition of immobilized acetylcholinesterase (AChE) as a model system. Organophosphates (e.g., paraoxon) and mycotoxins (e.g., aflatoxin B1) are classified as extremely hazardous compounds due to their potent toxicity to the human nervous system.[27,28] Organophosphate compounds are widely used as agricultural pesticides, insecticides and chemical warfare agents. These compounds are very stable and can rapidly diffuse into ground water reservoirs and thus exhibit a

threat of contamination. Mycotoxins, particularly aflatoxin B1 (AfB1), are carcinogenic contaminants of food and animal feeds and as such are used as biochemical markers for food spoilage. The currently available methods for the determination of these compounds are liquid/gas chromatography,[29,30] optical and electrochemical biosensors,[31-34] surface plasmon resonance,[35] semiconductor quantum dots,[36] ion-selective field-effect transistors (ISFET),[37] carbon nanotube[38] and nanoparticle based sensors,[39,40] as well as several immunoassays.[35,41] Though these systems have high selectivity and adequate sensitivity, almost all of them either require sophisticated instrumentation, skilled operators, significant sample pretreatment, and/or long analysis times. Moreover, most of these detection systems are not amenable to rapid screening in emergency situations, in remote settings or in developing countries, where simple and portable bioassays are essential for monitoring toxic compounds in the environment or foodstuffs. Therefore, it is critical to develop robust, highly sensitive, simple, stable, portable and user-friendly methods to test for the presence of toxic compounds.

As a signal generation method, we have utilized the well known Ellman colorimetric assay (Scheme 5.1).[42] However, to allow permanent capture of the highly colored 5-thio-2-nitrobenzoate (TNB$^-$) anion, we have incorporated a cationic capture region onto the paper via ink-jet printing of polyvinylamine (PVAm). The binding of toxins (*e.g.,* paraoxon, AfB1) to AChE reduces AChE activity, and the residual activity is monitored based on the yellow color intensity that was produced.
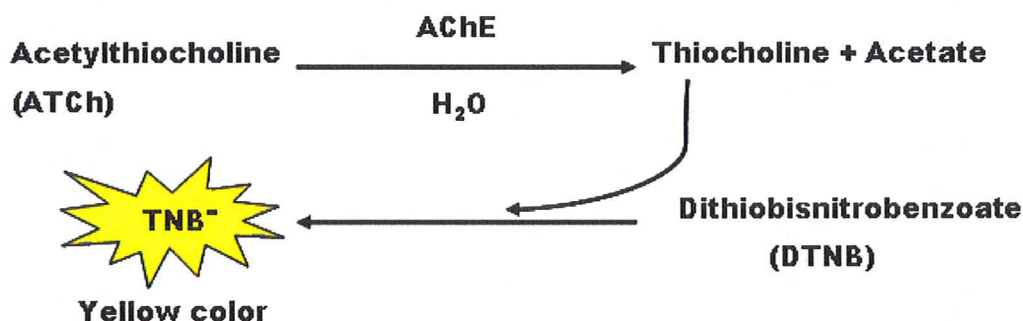
Scheme 5.1. *Schematic representation of the detection principle of the Ellman assay. Acetylcholinesterase (AChE) hydrolyzes the acetylethiocholine (ATCh) and forms thiocholine (TCh), which then reacts with dithiobisnitrobenzoate (DTNB) to generate 5-thio-2-nitrobenzoate (TNB, an anion), which is yellow in color.*

Following this simple and reliable assay mechanism, we show that it is possible to detect the AChE inhibitors in a rapid and cost effective manner using either a dipstick or lateral flow biosensing format.[31,43,44] This is the first report on the utilization of piezoelectric inkjet printing in the development of sol-gel based paper biosensors, and thus provides a new platform for fabrication of bioactive paper strips for detection of drugs or environmental pollutants that affect both animals and humans.

5.2 Experimental Section

Chemicals: Sodium silicate solution (~14% NaOH, ~27% SiO_2), tetraethylorthosilicate (TEOS, 98%), Dowex 50WX8-100 ion-exchange resin, acetylcholinesterase (AChE, from *electrophorus electricus*, EC 3.1.1.7), paraoxon, aflatoxin B1 (AfB1, from *aspergillus flavus*), 5,5'-dithiobis-(2-

nitrobenzoic acid) (DTNB), carboxymethylcellulose sodium salt (CMC), and Triton X-100 were obtained from Sigma-Aldrich. Anhydrous glycerol and acetylthiocholine iodide (ATCh) were purchased from Fluka BioChemika Ultra (UK). Diglyceryl silane (DGS) was synthesized in our lab using by transesterification of TEOS with anhydrous glycerol as described in detail elsewhere.[45] Polyvinylamine (PVAm; 1.5 MDa) was obtained from BASF (Mississauga, Canada), as a gift. Mead brand cardboard paper substrate with a white hydrophobic clay coating (Manufactured by Hilroy, Toronto, Canada) was purchased from McMaster University Bookstore. Distilled deionized water (ddH$_2$O) was obtained from a Milli-Q Synthesis A10 water purification system. All other reagents were of analytical grade.

Procedures

Preparation of Solutions: Stock solutions of the ATCh, paraoxon and AfB1 were made up daily and were not used for more than 3 h after preparation to minimize the potential for hydrolysis. Tris buffer (100 mM, pH 8) was used for dilution of ATCh. A mixture of Tris buffer (50mM, pH 6.8) and 5% cyclohexane (Sigma) was used for dilution of paraoxon, while a mixture of Tris buffer (50mM, pH 6.8) and 5% methanol (Sigma) was used for dilution of AfB1. These solvents not only aid in dissolution of the AChE inhibitors, but also enhance the affinity of paraoxon [46] and aflatoxin[31] for binding to AChE. Furthermore, this level of organic solvent has been shown not to affect the stability of AChE in any way.

Note that experiments conducted without organic solvent present produced significantly lower detection limits for paraoxon or AfB1 (data not shown). Therefore, for practical applications, it is recommended that low levels of organic solvents be used not only for dissolution purposes but also to enhance sensitivity. Distilled deionized water (ddH$_2$O) was used to dissolve PVAm. All other solutions were prepared using Tris buffer (100 mM, pH 8) if not otherwise stated. CAUTION: Both AfB1 and paraoxon are extremely toxic. These materials should be handled with gloves and used in a fumehood.

Preparation of Sol-gel Materials: Two biocompatible sol-gel precursors, diglyceryl silane (DGS) and sodium silicate (SS) were used to prepare sols for enzyme entrapment and printing onto paper. DGS sols were made by mixing 10 mL of ddH$_2$O with 1 g of finely ground DGS. The mixture was sonicated on ice bath for 20 min to dissolve the DGS and then filtered through a 0.22 μm membrane syringe filter to remove any particulates in the solution.

SS sols were prepared by mixing 10 mL of ddH$_2$O with 2.9 g of sodium silicate solution (pH ~13) followed by addition of 5 g of Dowex cation exchange resin to replace Na$^+$ with H$^+$. The mixture was stirred for 30 seconds to reach a final pH of ~ 4, and then vacuum filtered through a Büchner funnel. The filtrate was then further filtered through a 0.45 μm membrane syringe filter. These sols were used to formulate silica-containing inks as described below.
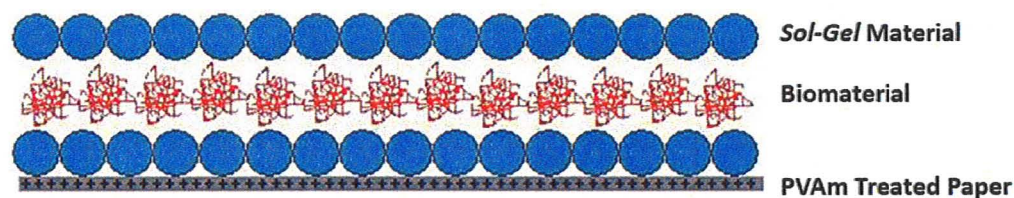
Scheme 5.2. *Ink-jet printing strategies for sol-gel derived silica materials. Schematic illustration of inkjet printing sequence of PVAm, sodium silicate (SS) based sol-gel derived silica matrix, and the tris buffer (100 mM, pH 8.0) containing enzyme acetylcholinesterase (AChE) and dithiobisnitrobenzoate (DTNB) layers on paper for development of a portable solid-phase biosensor.*

Construction of Bioactive Paper-Based Solid-Phase Sensor: The papers were coated with a total of three different materials in a specific sequence. In general, this involved: 1) printing of a PVAm underlayer directly onto the paper surface; 2) printing of a silica sol intermediate layer; 3) printing of a buffered enzyme solution containing AChE (final conc. 50 U/mL) and DTNB (final conc. 500 µM); and 4) printing of a silica sol overlayer, as shown in Scheme 5.2. Between printing of the different silica and bio inks, 15-20 min was allowed for air drying. The different printing solutions (PVAm, sol or enzyme) were modified by addition of glycerol to control viscosity and Triton X-100 to control surface tension so as to optimize the printing performance (ability to jet the inks) as well as the enzyme activity, as described below. As noted in Table 1, addition of glycerol to PVAm inks was not necessary as the viscosity of an aqueous solution of this polymer was on the order of 3 cP. This high viscosity of the 0.5 wt% solution is likely due to the high molecular weight (ca. 1.5 MDa) of the polymer. The solutions were deposited using a piezoelectric inkjet printer (DMP-2800) from Fujifilm Dimatix, Inc (Japan) using Drop Manager software (version

Bioink Formulation (with 0.1 wt.% Triton X-100)	AChE Activity	Viscosity (cp)	Surface Tension (mN/m)	Jetting Conditions	Bioink Jettability	Movies of Drop Formation
Bioinks for AChE						
Tris buffer (100mM, pH 8)	+	1.01 ± 0.02			None	
1 % (v/v) Glycerol + Tris buffer	+	1.06 ± 0.03			None	
10 % (v/v) Glycerol + Tris buffer	+	1.35 ± 0.08			Sporadic	
20 % (v/v) Glycerol + Tris buffer	+	1.91 ± 0.11		Firing voltage: 40 v	Good	
30 % (v/v) Glycerol + Tris buffer	+	2.80 ± 0.13			Excellent	
40 % (v/v) Glycerol + Tris buffer	+	4.21 ± 0.09		Wave form: Single	Excellent	
50 % (v/v) Glycerol + Tris buffer	+	6.85 ± 0.21	30~38	pulse. Fall in two steps	Excellent	See supplementary movies
Bioinks for SS *sol-gel* material				Pulse width: 70 µs		
Sodium silicate (SS)	+	1.33 ± 0.04			None	
1 % (v/v) Glycerol + SS	+	1.44 ± 0.07		Meniscus vacuum:	Poor	
10 % (v/v) Glycerol + SS	+	1.67 ± 0.10		4.0-4.5 inches H₂O	Sporadic	
20 % (v/v) Glycerol + SS	+	2.00 ± 0.13			Good	
30 % (v/v) Glycerol + SS	+	2.67 ± 0.16		Firing frequency: 5 kHz	Excellent	
40 % (v/v) Glycerol + SS	+	3.67 ± 0.19			Excellent	
50 % (v/v) Glycerol + SS	+	6.00 ± 0.23			Excellent	
Bioink for PVAm						
PVAm (0.5 wt. %)	**	3.08 ± 0.14			Excellent	

Note: +, the AChE retains activity (> 95%) ; **, not applicable

Table 5.1. *Bioink formulations and ink-jet deposition parameters.*

1.3.0.7). This system has a microelectromechanical system (MEMS)-based cartridge-style printhead that allows filling with desired bioinks (ca. 0.5-2 mL). Each cartridge has 16 nozzles linearly spaced at 254 microns with typical drop sizes of 1-10 pL. The instrument is equipped with a drop imaging system (Drop Watcher) that allows observation and capture of the events during drop formation on the printhead nozzles and the trajectory of the drops after ejection. Jetting conditions are described in Table 5.1. In all cases the bioactive inks were printed by applying 16 piezo firings with one printing cycle per ink in a stepwise fashion as a 0.25 x 0.25 cm square pattern onto Mead brand cardboard (paper substrate, 10 x 8 cm) using a separate cartridge for each of the PVAm, silica and enzyme

"inks". For control experiments, a buffer that did not contain AChE was printed between the silica layers. Other controls involved printing of AChE + DTNB directly onto the PVAm underlayer without a silica coating, and printing of AChE + DTNB onto PVAm/silica without printing a silica overlayer.

Ink Viscosity and Surface Tension Measurements: The dynamic viscosity of the bioink components was measured using a capillary viscometer (Cannon-Fenske viscometer, size 75, Vineland, NJ) at room temperature. The viscometer was calibrated with MilliQ water (viscosity ~1cP) before measuring the viscosity of the bioinks. Surface tension values were measured using a Krüss pendant drop apparatus. The shape of the pendant drop was analyzed using DSA10 shape analysis software by applying the Laplace equation. Pendant drops were formed by a Krüss needle with an outer diameter of 1.5 mm, connected to a 1 mL Perfektum glass syringe from Popper & Sons Inc. MilliQ water with surface tension of 72.8 mN/m was used to calibrate the needle's inner diameter. All surface tension values of pendant drops were measured at 22 °C with temperature controlled by a NESLAB thermostat system.

Surface Topography: Paper substrates were subjected to optical profilometry and SEM imaging prior to deposition of any materials, after inkjet deposition of PVAm and after deposition of both PVAm and the silica/enzyme/silica layers. Optical profilometry images were obtained using WYKO NT 1100 Optical

Profiling System using the VSI measurement mode and a magnification of 20X. For SEM, samples were sputter-coated with platinum (layer thickness 15 Å) to avoid charging effects and were imaged using a JEOL Ltd. (Tokyo, Japan) JSM - 7000F instrument operating at 5 kV and a probe distance of 5.8 mm.   The hydrophilic or hydrophobic nature of surface was also estimated by measuring the contact angle of ddH$_2$O drop on paper using a Krűss pendant drop apparatus.

Monitoring AChE Activity on Paper: Prior to monitoring AChE activity on paper, the activity of AChE as a function of enzyme concentration was optimized. Different concentrations of AChE (0~200 U/mL) were entrapped in SS+30% glycerol in a 96 well plate (total volume of 80 μL). A mixture (20 μL) of DTNB (500 μM) and ATCh (300 μM) was then added into each well and incubated for 5 min to allow color development.   The absorbance at 412 nm was then measured using a TECAN Safire microwell plate reader.

The AChE activity on the bioactive paper strip was evaluated by measuring the color intensity produced by the enzymatic reaction using Ellman's method. The performance can be assessed in two ways: a) by direct addition of substrate solution to sensing area, and b) by immersion into the substrate solution. The performance of our sensor was essentially the same for both these cases. However, in the case of direct analyte addition, only small amounts of reagent are needed (5 μL) relative to dipstick sensors (~2 mL), reducing cost per assay.   For optimization of AChE activity, small amounts (5 μL) of different concentrations

of the substrate ATCh (0 – 500 μM) was added directly onto the sensing area of the paper strip and incubated for 5 min at room temperature to allow the yellow color to develop. The color intensity of the sensing areas was quantified by obtaining a digital image (Canon A630, 8.0 MegaPixel operated in automatic mode with no flash and with the macroimaging setting on) and using ImageJ software to analyze the jpeg images. ImageJ software uses a 256 bit color scale and for our image processing the images were inverted so that areas that were originally white became black and corresponded to a color intensity of zero and while areas that were originally black became white and corresponded to 256. Based on this scale, increases in the amount of yellow color cause an increase in color intensity of our sensor strips. To account for variations in color intensity owing to differences in environmental illumination, a background subtraction (color intensity of the paper surface closest to the sensing area) was done for each data point.

The long-term stability of the enzyme printed on the paper strip was evaluated over a period of 60 days with the paper strip stored at 4 °C. The assay conditions were the same as those described above.

Monitoring the Effect of PVAm: In order to investigate the effect of the PVAm underlayer on the sensor performance, a lateral flow-based paper chromatographic system was developed. In this case, strips of Whatman No. 1 filter paper (Sigma-Aldrich) were used in place of the Mead cardboard as the Whatman paper is more

hydrophilic and thus supports capillary flow of aqueous solutions. The Whatman paper strips (1x10 cm) were printed with aqueous inks containing various levels of PVAm (0-1 wt. %) and were allowed to air dry for 15 min. The PVAm treated strips were then immersed into a solution of 5-thio-2-nitrobenzoate (TNB⁻, the colored product of the AChE catalyzed reaction), which was produced enzymatically from ATCh (final conc. 300 μM), DTNB (final conc. 500 μM), and AChE (final conc. 50 U/mL) with the sensing area above the liquid level. The retardation factor (Rf) was calculated based on the ratio of migration distance of the product (TNB⁻) relative to the migration distance of solvent (Milli-Q water) from this lateral flow based platform.

Lateral flow and dipstick assay formats were also developed to monitor the capability of PVAm to capture and preserve the color produced from the AChE catalyzed reaction when performed on paper. In this case, Whatman (for lateral flow) or Mead cardboard dipsticks (1 x 10 cm) were prepared using ink-jet deposited PVAm (0 or 0.5 wt%), silica (SS + 30% glycerol) and AChE+DTNB (50 U/mL+500 μM in 30% glycerol, with 1 wt% Triton X-100 present in all solutions) as described above, followed by placing the sensor strip into a solution of substrate (300 μM ATCh) with the sensing area located above the liquid level (lateral flow) or within the solution (dipstick) and allowing the color to develop for 5 min. Following the assay the resulting color intensity remaining on the paper strip was monitored once a day for up to three weeks.

Measurement of AChE Inhibitors using Bioactive Paper: The inhibitory effects of paraoxon and AfB1 on the solid-phase biosensor were evaluated by measuring the decrease in the color intensity produced by the Ellman reaction. The PVAm/silica/AChE+DTNB/silica bioactive paper strip was first incubated with various concentrations of paraoxon solution (5 μL, 0-100 μM) or AfB1 solution (5 μL, 0-100 μM) [CAUTION: these assays should be performed in a fumehood using appropriate protective apparel], for 10 min after which 10 μL of a solution of 300 μM ATCh was deposited onto the paper strip and incubated for 5 min. The intensity was determined by analyzing a digital image with the ImageJ software as described above.

5.3 Results and Discussion

Bioink Formulation and Jetting: Initial attempts at ink-jet deposition of sol-gel based bioinks utilized silica sols to which buffered proteins had been added. While it was possible to produce protein-doped sols with relatively long gelation times, it was not possible to deposit such materials without gelation occurring in the nozzles of the ink-jet cartridge. For this reason all further studies on sol-gel based inks utilized a multi-layer deposition method wherein the silica sol and buffered aqueous protein solutions were deposited from separate cartridges so as to avoid mixing prior to deposition on the paper substrate.

Both the silica and aqueous protein "inks" were optimized to allow reproducible jetting onto paper substrates. Physico-chemical properties such as

surface tension and viscosity are critical parameters to make the ink stable and ejectable. Several additives (e.g., surfactants, viscosity modifiers) are generally incorporated in the ink formulations to optimize these rheological properties. However, inappropriate additives may often negatively affect enzyme activity. Therefore, it is essential to produce a suitable ink formulation in which the enzyme is active and at the same time produces stable and reproducible drops during jetting. To adjust the ink surface tension (initially in the range of 60-78 mN.m^{-1} without surfactant) to the printable range (30-40 mN.m^{-1}), Triton X-100, a mild detergent, was used as a surfactant. To determine the effect of Triton X-100 on AChE activity, a solution of AChE (50 U/mL) in Tris buffer containing 0.1 wt. % of Triton X-100 was prepared, and then the enzyme activity in solution was measured using the Ellman assay. No significant loss of AChE activity was observed in the presence of this low level of Triton X-100. Therefore, 0.1 wt. % Triton X-100 was included in all bioink formulations (e.g., AChE, sol-gel derived silica, PVAm) to get the optimum surface tension for printing (Table 5.1).

In order to adjust the ink viscosity (initially in the range of 1.01-1.33 cP without viscosity modifiers) to the desired value (2-10 cP), two well-known viscosity modifiers, carboxymethylcellulose sodium salt (CMC) and anhydrous glycerol, were investigated. PEG and PVA, though biocompatible, were not examined as these species have a tendency to promote macroscopic phase separation in sol-gel derived silica,[47,48] which could result in significant protein leaching.[49] CMC, a charged polymer, was chosen as it has previously been
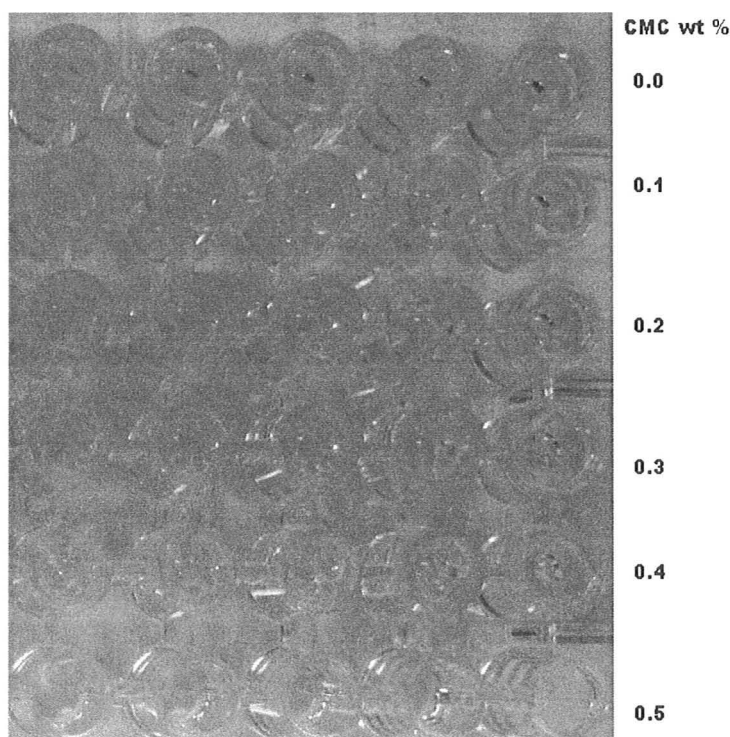
Supplementary Fig. 5.1 *Effects of CMC dosages on AChE activity in Ellman Assay. Different dosages of CMC (0~0.5 wt. %) and AChE (50 U/mL) were mixed (total 80 µL) in a 96 well-plate, and then a mixture (20 µL) of ATCh (300 µM) and DTNB (500 µM) were pipetted into each well.*

demonstrated to be an effective viscosity modifier for inkjet deposition of horseradish peroxidase.[10] Glycerol was chosen owing to its compatibility with both proteins [50] and with the sol-gel process.[45]

Initial studies on the effects of CMC (0~0.5 wt. %) on AChE activity in solution showed that this additive led to a significant decrease in AChE activity at concentrations above 0.2 wt% (Supplementary Fig. 5.1). Therefore, CMC was not investigated further as a viscosity modifier. On the other hand, glycerol did not produce a decrease in AChE activity, even at levels of 30% v/v. Addition of this

level of glycerol to either the SS derived silica sol or AChE-based inks also resulted in excellent drop formation and jettability, as shown in Table 5.1. However, all inks prepared from DGS derived silica sols, while jettable, resulted in poor adhesion and cracking after drying on the paper substrate, and thus were not investigated further. The origin of the cracking for DGS materials is not fully understood, however, the hydrolysis and condensation kinetics of DGS and sodium silicate are quite different, as has been noted in our previous papers.[51,52] This is likely to lead to a difference in the degree of cross linking and significant differences in pore sizes. DGS has a larger proportion of small micropores, which are significantly affected by hydration stress during drying and rehydration.[45] This could explain the higher degree of cracking for DGS based materials.

The drop formation and jettability of a series of silica based inks are shown in Supplementary Movies that are available online. Based on the excellent ink-jetting properties and the high quality of the resulting deposited materials, all inks were formulated with 30 % (v/v) glycerol and 0.1 wt% Triton-X100 using sodium silicate as the silica precursor.

Coating Properties: To characterize the coatings on paper substrates, optical profilometry, contact angles and SEM images were obtained for both unmodified and modified paper substrates. Figure 5.1A shows optical profilometry images of paper that is coated with PVAm only (Figure 5.1A(a)), and with both PVAm and the silica/AChE+DTNB/silica layers (Figure 5.1A(b)).
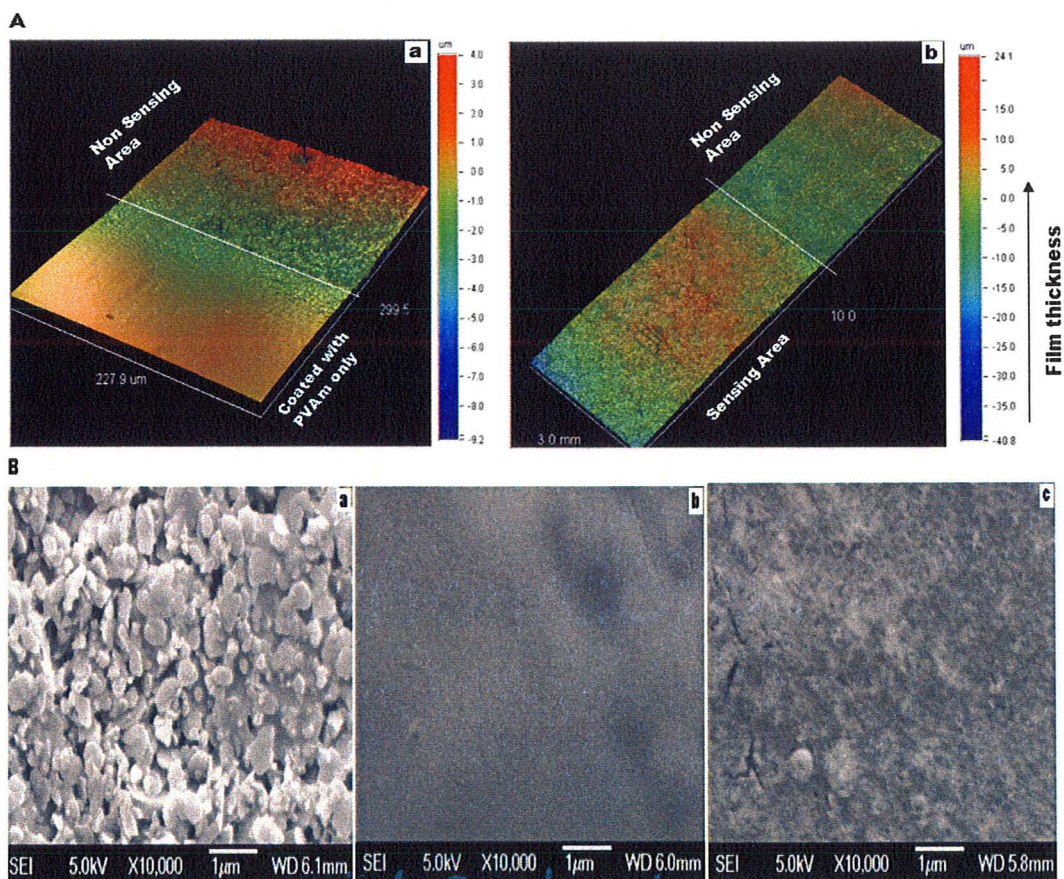
Figure 5.1. *Plane characterization of pre-treated paper, PVAm treated paper and biosensor surfaces. Topography of ink-jet sprayed PVAm, and AChE (50 U/mL) and DTNB (500 μM) doped sodium silicate (SS) thin films on paper. (A) Profilometry images of paper that is coated with or without PVAm only (a), and both PVAm and the silica/AChE+DTNB/silica layers (b). (B) SEM images of unmodified (a), modified with PVAm only (b), and modified with PVAm, and AChE and DTNB doped silica matrix on paper (c). Unmodified paper surface was rough, while the modified surfaces were relatively smooth.*

No bioinks were printed on the non sensing region. The profilometry results show that the PVAm layer is approximately 4 μm thick, while the sol-gel based coating had an average thickness of about 24 μm. Similar results were obtained for layers printed on glass slides (data not shown), suggesting that the majority of the

sensing layer was present on top of the paper rather than within the paper. This is further supported by the contact angles for PVAm coated and PVAm free Mead cardboard and Whatman paper substrates, which were approximately 112.2 ± 1.1°, 50.1 ± 0.3° and zero, respectively. The results indicate that the PVAm layer imparts high hydrophobicity to an already coated paper surface, and thus liquid penetration into the surface is improbable.

Figure 5.1B shows SEM images of the unmodified paper (Figure 5.1B(a)), PVAm coated paper (Figure 5.1B(b)) and paper that was coated with both the PVAm and silica/AChE+DTNB/silica layers (Figure 5.1B(c)). The unmodified paper surface is very rough (average roughness of ± 972 nm) and heterogeneous, and clearly shows the presence of significant amounts of fillers (i.e., clay particles) at the surface of the paper and no evidence for paper fibers at the surface. This is consistent with the fact that the Mead paper used in this study had a protective coating. The deposition of PVAm resulted in a much smoother surface (± 554 nm), and suggests that the cationic polymer likely provides a barrier coating above the filler layer onto which the silica layer is deposited, consistent with the data described above. Thus, in addition to acting as an anion capture agent, PVAm also produces a more uniform surface which may prevent enzyme leaching into the paper. Deposition of the silica/AChE+DTNB/silica layer resulted in a relatively homogeneous, crack-free layer (roughness of ± 668 nm) which showed no evidence of large scale macropores (diameter > 0.5 μm), consistent with the inability of glycerol to act as a porogen. Taken together, the

profilometry and SEM images show that the sol-gel based ink layer is present on top of the paper, rather than penetrating through the paper. This is important as it should help to retain the colorimetric signal within a thin layer rather than having it diffuse throughout the thickness of the paper, making visualization easier.

Monitoring AChE Activity and Its Storage Stability: Prior to developing the dipstick sensor the activity of AChE was evaluated as a function of enzyme concentration (0-200 U/mL) via the Ellman assay when entrapped in sol-gel derived monolithic silica prepared from SS with 30% glycerol. The signal, measured 5 min after addition of 300 μM ATCh and 500 μM DTNB, increased linearly over the concentration range from $0 - 50$ U.mL^{-1} after which the signal showed negative deviation and reached a plateau at $\sim$100 U.mL^{-1} (data not shown). A value of 50 U/mL was chosen the best compromise between a low enzyme loading, a sufficiently high signal (> 4-fold increase over background) and good long-term stability. The high activity of entrapped AChE is in agreement with previous reports showing that the enzyme is active and stable in sol-gel derived silica materials.[53]

Based on the AChE activity data, a solid-phase bioactive paper based sensor was constructed by multilayer inkjet printing of several bioinks in the order: PVAm, silica, 50 U/mL AChE + 500 μM DTNB, silica using the compositions listed in Table 5.1 with 30% glycerol added to all inks except PVAm. This resulted in a layered system as shown in Scheme 5.2. The effects of adding
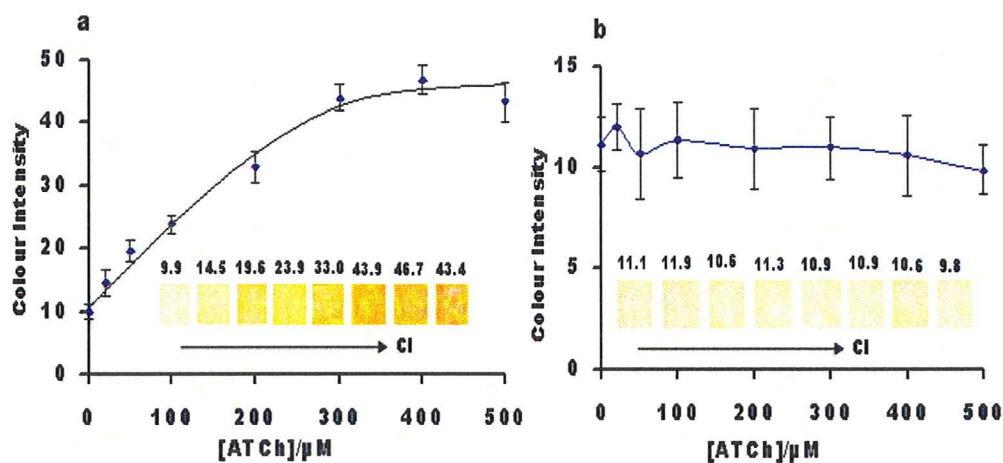
Figure 5.2. *Assessment of signal levels and external reagents on background signal. Dose-dependent effects of acetylthiocholine (ATCh) in the presence (a) and absence (b) of AChE (50 U/mL) doped silica matrix on paper, in which PVAm (0.5 wt. %) was printed prior to printing of the silica and AChE layers. Inset is the color intensity (CI) generated at each ATCh concentration. All points are means ± s.d. of five independent experiments for each concentration.*

varying levels of ATCh over the bioactive paper sensor are shown in Figure 5.2a (a separate paper sensor is used for each ATCh concentration). Here it is seen that as the concentration of ATCh increases so too does the color intensity, recorded 5 min after addition of the substrate over the sensing area. The color intensity saturated at a level of ~300 µM ATCh and suggested a K_M of ca. 150 µM, which is in good agreement with previous literature reports.[40] The color intensity was about four-fold higher than that of a negative control (absence of ATCh but with AChE present).

To ascertain whether or not the supporting silica or PVAm materials degraded DTNB or ATCh, a similar experiment was conducted using the same inks as above but with AChE absent from the aqueous ink layer. As shown in Figure
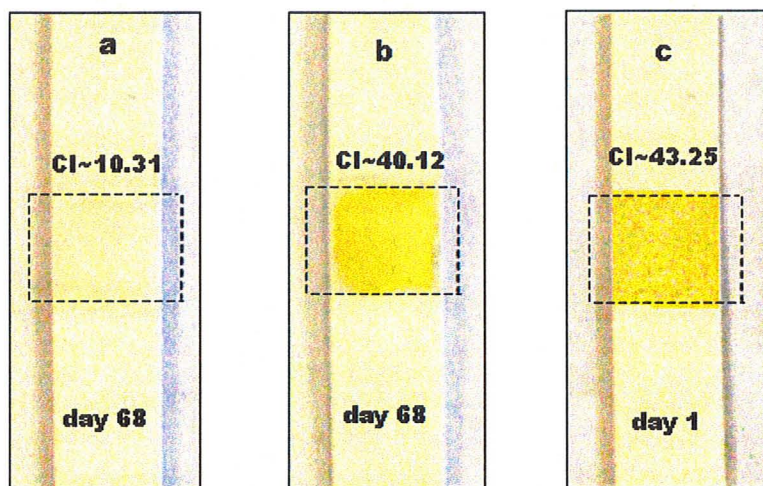
Supplementary Fig 5.2. *Long-term stability of AChE and DNTB within the layered coating (e.g., PVAm, silica, AChE+DTNB, silica) of the paper-based sensor. The sensor was stored at 4°C for 68 days and overspotted with 10 μL ATCh (300 μM). (a) When AChE was absent (control), and (b) when AChE was present. (c) Color formation when all bioinks were present and overspotted with 10 μL ATCh (300 μM) at day 1.*

5.2b, the responses remained at the baseline signal upon addition of varying levels of ATCh and were similar to signals obtained from control experiments performed in the absence of substrate. Thus, our results confirm that the change in the color intensity is due to the AChE catalyzed hydrolysis of ATCh to TCh which then reduces DTNB to TNB⁻. Furthermore, this result shows that the AChE is able to withstand the shear forces associated with ink-jet deposition and remains active when deposited between silica layers on a paper substrate.

The long-term stability AChE within the layered coating on the paper substrate was also investigated.   Our results (Supplementary Figure 5.2) demonstrated that the enzyme retained >95% of its initial activity over a period of

at least two months when stored at 4 °C, indicating that both the enzyme and the DTNB reagent remained viable during storage. The observed stability of the enzyme when entrapped in silica is in agreement with previous reports[53] and shows that the bioactive paper sensor should have a sufficient shelf-life to allow storage and shipping.

To further assess the "sandwich architecture", two controls were done to assess the effects of both the PVAm and the silica layers on AChE activity and stability. In the first case, the enzyme was printed directly onto PVAm without silica. In this case, the enzyme showed activity on day 1, but no activity by day 2, likely owing to dehydration and/or strong electrostatic interactions between the enzyme and the cationic polymer which caused denaturation. In the second case, the enzyme+DTNB solution was printed onto the silica material that covered the PVAm layer, but the silica overlayer was not added. Such sensors showed activity that was comparable to the "sandwich architecture" device after 2 days, however, after prolonged storage the "non-sandwich" device produced significantly lower signal as a result of enzyme inactivation. Additionally, using this approach, it was not possible to employ the sensor for dip-stick assays as the enzyme readily desorbed from the paper/silica surface.

Effects of PVAm on Biosensor Performance: Two problems that were initially encountered when carrying out the Ellman assay using sol-gel entrapped AChE on the paper-based sensor were dispersion of the colored product over a large

area, leading to lower color intensity, and loss of color intensity with time. The former issue is expected based on the ability of the small molecular weight colored product to readily move through the pores of the silica matrix and thus leach out of the sensing area. The latter issue appears to be related to a secondary chemical reaction of the TNB⁻ with either the silica or some component in the paper, causing complete loss of color intensity over a period of a few days (see below). This makes storage of used sensors for future reference impossible. Therefore, trapping and preserving the color within a finite region is required to obtain the highest output signals and keep the signal stable over long periods of time. We reasoned that the best method for capturing the anionic colored product was to introduce a cationic polymer, PVAm, onto the surface of the paper. This polymer has recently been shown to be useful for enhancing the wet strength of paper,[54] and thus should be compatible with the substrate, and binds strongly to silica,[55] which should promote adhesion of the silica overlayer and not interfere with this coating layer. However, introduction of PVAm directly to a silica sol causes very rapid gelation owing to base catalyzed condensation, and hence this polymer was printed on paper prior to printing of the silica sol to avoid this problem.

To examine the effect of PVAm on sensor performance, a series of experiments were performed. Initial studies utilized a paper chromatographic set-up (lateral flow-based) to assess the ability of PVAm coatings containing varying levels of the polymer to retain the anionic product. For this purpose, hydrophilic
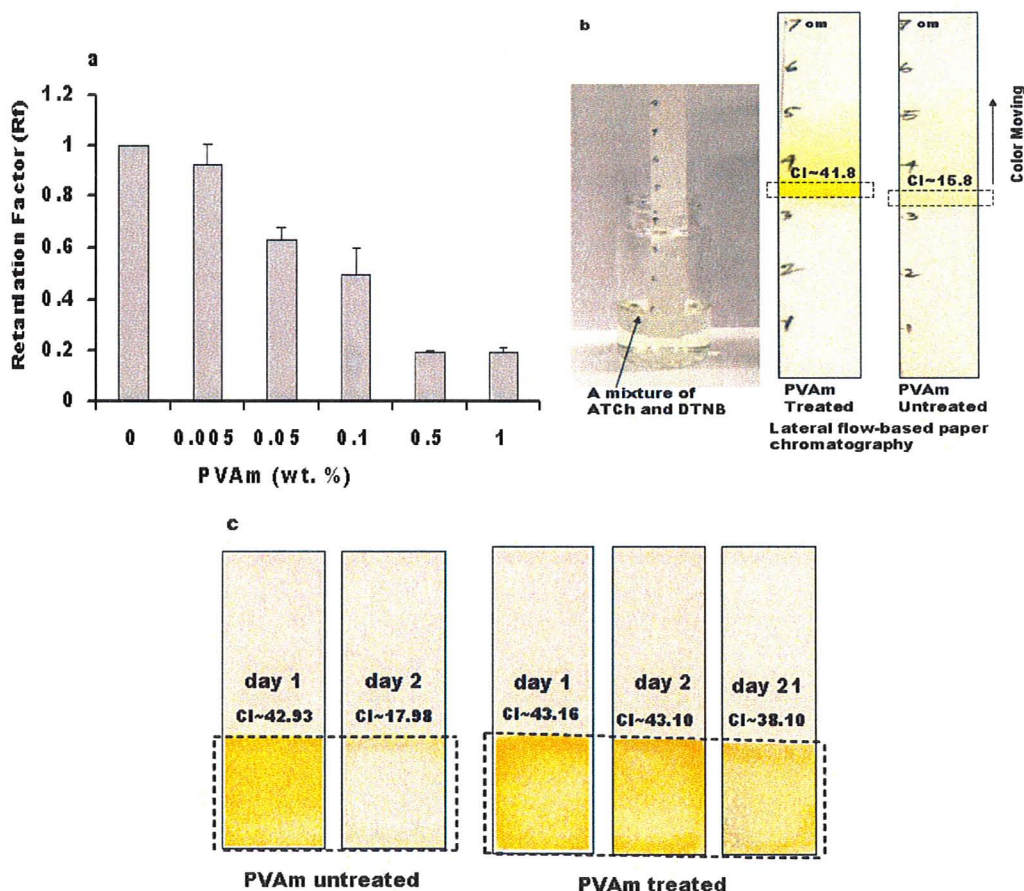
Figure 5.3. *Effects of cationic PVAm on entrapment as well as preservation the anionic TNB in lateral flow-based paper chromatographic system. (a) The values of retardation factor (Rf) for anionic TNB in Milli-Q water in the presence of indicated PVAm levels. (b) Colour intensity (CI) due to elution of ATCh (300 µM, final conc.) in the lateral flow based platform. The areas within the dashed boxes were printed without (control) and with PVAm (0.5 wt. %) followed by printing of AChE (50 U/mL). PVAm concentrates the reaction product, the yellow TNB anion, while in the control experiment, the yellow TNB anion is dispersed over a large area. (c) Cardboard dipstick with inkjet printed PVAm or control (no PVam) and silica/AChE/DTNB/Silica layers after being immersed in ATCh solution. Both materials show an initial color response, but only the PVAm (0.5 wt%)-treated paper retains the reaction product (a yellow TNB⁻) for a period of 3 weeks, while the PVAm untreated paper failed to retain the color.*

whatman 1 paper strips were printed with solutions containing 0 - 1 wt% of

PVAm and a solution of TNB⁻ (produced by mixing 300 µM ATCh, 500 µM

DTNB and 50 U/mL of AChE in Milli-Q water) was allowed to travel up the paper *via* capillary action. Figure 3a shows the values of retardation factor (Rf), a measure of the relative mobility of TNB⁻, as a function of PVAm concentration and demonstrates that the Rf values decreased with increasing levels of PVAm up to a level of 0.5 wt% of PVAm. Thus, 0.5 wt % PVAm was utilized in further studies to trap the negatively charged analyte.

Figure 5.3b shows the colour intensity due to elution of Ellman's solution using the lateral-flow based paper chromatographic system. The areas within the dashed boxes were either treated or not treated (control) with 0.5 wt% PVAm, deposited via ink-jet spraying onto Whatman 1 paper, followed by printing of the silica/AChE+DTNB/silica layers over the same area. We found that PVAm was able to trap and concentrate the TNB⁻ reaction product without diminishing the color intensity, while the unmodified paper (control) failed to trap the yellow color. As a result, the intensity of the yellow color was much higher when PVAm was present (0.25 x 1 cm), which should produce a better detection limit when using the paper to sense AChE substrate or inhibitors.

The capability of PVAm to preserve the TNB⁻ product for an extended period of time was also investigated. For this, Mead cardboard dipsticks were coated with the PVAm ink followed by silica/AChE+DTNB/silica ink layers and the dipsticks were immersed into a solution of 300 μM ATCh for 1 min. Images were obtained 30 min or 24 h after exposure to ATCh. A control sample was also tested in which the PVAm underlayer was not present. Figure 3c shows images of

the dipsticks under the different testing conditions, and clearly demonstrates that the PVAm is able to retain the yellow product while untreated paper causes the yellow color to disappear almost completely after only 24 h.   Further testing revealed that the PVAm layer was capable of retaining the color for at least three weeks. Thus, the bioactive paper strips can be stored for future reference.

Neurotoxin Measurement Based on AChE Inactivation: Neurotoxins such as paraoxon and aflatoxin B1 are well known inactivators of acetylcholinesterase.[27,28,31,46] The ability to detect these compound using the ink-jet printed AChE-based paper sensor was investigated by using an overspotting method wherein small volumes of reagents were added to the sensing area directly.   In this case, as little as 10 μL of solutions containing various concentration of paraoxon or AfB1 could be tested by applying them onto the sensing area of the strip, incubating for 10 min at room temperature, adding 10 μL of a solution containing 300 μM ATCh and finally measuring the color intensity after 5 min using a digital camera and image processing software. Figure 5.4a shows the dose-dependent inhibition effects of paraoxon, while Figure 5.4b shows the semi-logarithmic plot of color intensity, corresponding to the same experiments, demonstrating an IC_{50} in the range of 1 μM and a detection limit (S/N = 3) of ca. 100 nM. Figure 5.5a and Figure 5.5b show the dose-dependent inhibition responses and a semi-logarithmic plot of color intensity, respectively, shows the dose-dependent inhibition effects of paraoxon, while Figure 5.4b shows
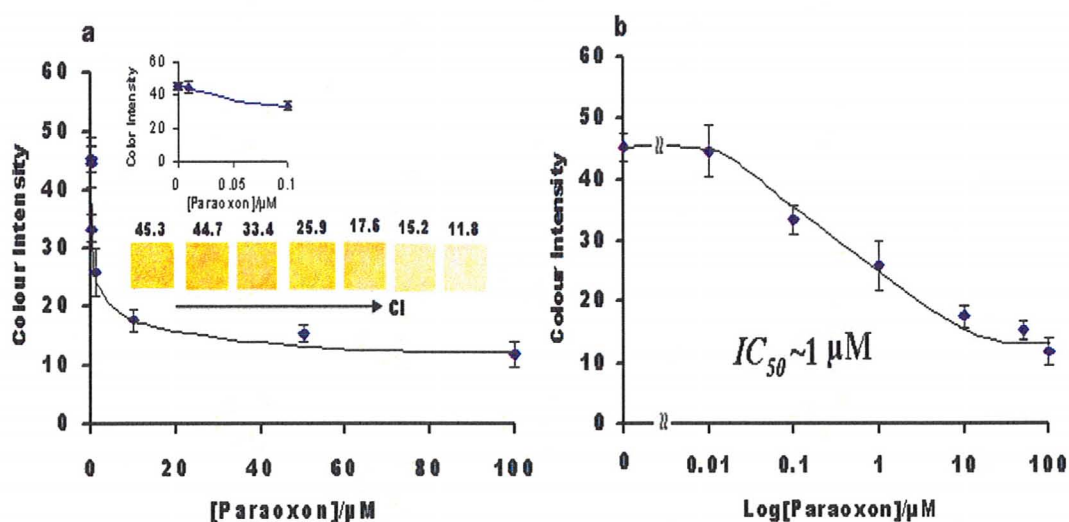
Figure 5.4. *Effect of paraoxon on AChE activity. Dose-dependent inhibition of acetylcholinesterase (AChE) by various concentrations of paraoxon (a). Insets are the color intensity (CI) at each paraoxon concentration and dose-dependent inhibition responses with the lower levels of paraoxon. (b) Semi log plot of data in panel (a). PVAm and AChE (50 U/mL) and DTNB doped silica layers were printed on paper before conducting experiments. All points are means ± s.d. of five measurements for each concentration.*

the semi-logarithmic plot of color intensity, corresponding to the same experiments, demonstrating an IC_{50} in the range of 1 μM and a detection limit (S/N = 3) of ca. 100 nM. Figure 5.5a and Figure 5.5b show the dose-dependent inhibition responses and a semi-logarithmic plot of color intensity, respectively, for AfB1, and show that the IC_{50} in this case is ca 100 nM, with a LOD of ~30 nM. A comparison of the responses obtained at 100 nM of either paraoxon or AfB1 show that AfB1 is a more potent inhibitor (~45% inhibition vs. ~25% inhibition for paraoxon), in agreement with previous studies.[31,35,40]

The insets for Figures 5.4 and 5.5 show the images of the paper strips at each inhibitor concentration, and clearly demonstrate that detection of the inhibitors is
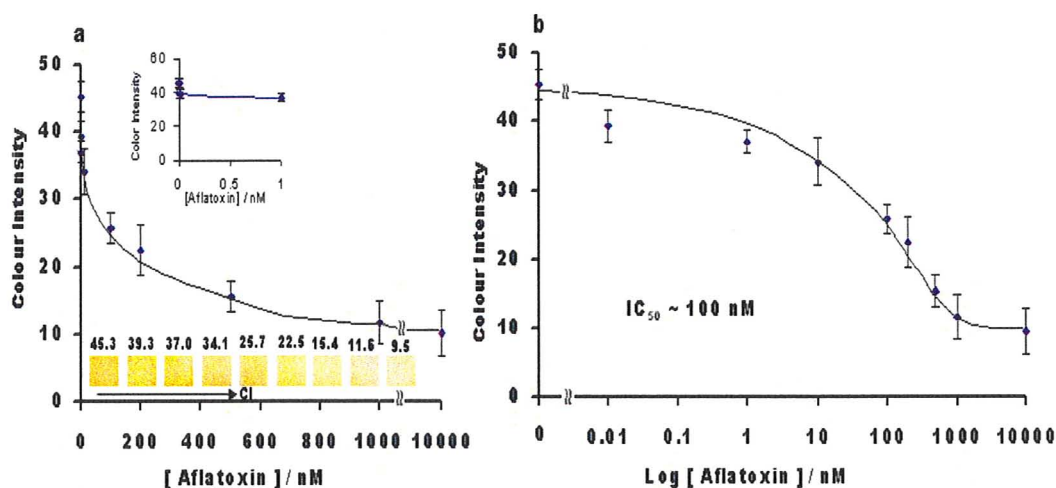
Figure 5.5 *Effect of Aflatoxin B₁ on AChE activity. (a) Dose-dependent inhibition effects of aflatoxin B1 on AChE activity. Insets are the color intensity (CI) at each aflatoxin B₁ concentration and dose-dependent inhibition responses with the lower levels of aflatoxin B1. (b) Semi log plot of the data shown in Panel (a). Data are means ± s.d. of five independent measurements for each concentration.*

possible using the naked eye. This is an important aspect of the bioactive paper strips, as this permits the use of the test strips directly in the field and eliminates the need for sophisticated instrumentation. The presence of a simple colorimetric readout also enables rapid imaging and transmission to a central lab for further quantitative analysis using a simple cell phone camera combined with e-mail or MMS messaging.[3,5,7] Hence, rapid, on-site qualitative or quantitative analysis of organophosphates or aflatoxins should be possible using this bioactive paper platform.

5.4 Conclusion

In this study, we introduced a novel sol-gel based method for coating enzymes onto paper substrates using ink-jet printing of various "ink" layers to produce a bioactive paper sensor for detection of AChE substrates and inhibitors based on Ellman's colorimetric assay. Our data show that AChE can be printed between two biocompatible silica layers on paper and that the enzyme retains full activity for at least 2 months when stored at 4 °C. Use of PVAm as a cationic capture agent on the paper significantly enhances the signal intensity owing to the ability to concentrate the anionic TNB⁻ product in a finite region, and also retains the signal over several months. When used in combination with digital imaging and image processing, the bioactive paper sensor can be used for quantitative assessment of AChE inhibitors, including paraoxon and AfB1, by monitoring the residual activity of the entrapped enzyme. Our experimental data are consistent with those previously reported using conventional instrumental methods. The ability to utilize ink-jet printing for deposition of biological reagents opens the door to automated fabrication of bioactive paper sensors, and should enable elaborate patterns of enzymes to be printed to produce multi-analyte sensor strips. The entrapment of the enzyme at the paper surface allows the sensor to be used for either lateral flow or dipstick sensing applications, and eliminates the potential for enzyme leaching. A drawback of the current sensor is the need to have the substrate, ATCh, present in the test solution, making it necessary to perform a sample pretreatment step prior to analysis. Further efforts are needed to modify

this bioactive solid-phase paper sensor into a fully reagentless, multiplexed and low sample volume biosensor. Our efforts in these areas will be reported in due course.

Acknowledgements

5.5 Reference

1. Li, X.; Tian, J.; Nguyen, T.; Shen, W. *Anal. Chem.* **2008**, *80 (23)*, 9131-9134.

2. Abe, K.; Suzuki, K.; Citterio, D. *Anal. Chem.* **2008**, *80 (18)*, 6928-6934.

3. Martinez, A.W.; Phillips, S.T.; Butte, M.J.; Whitesides, G.M. *Angew. Chem., Int. Ed.* **2007**, *46*, 1318-1320.

4. Zhao, W.; Ali, M.M.; Aguirre, S.D.; Brook, M.A.; Li, Y. *Anal. Chem.* **2008**, *80(22)*, 8431-8437.

5. Bruzewicz, D.A.; Reches, M.; Whitesides, G.M. *Anal. Chem.* **2008**, *80(9)*, 3387-3392.

6. Su, S.; Ali, M.M.; Filipe, C.D.M.; Li, Y.; Pelton, R. *Biomacromolecules* **2008**, *9(3)*, 935-941.

7. Martinez, A.W.; Phillips, S.T.; Whitesides, G.M. *Proc. Natl. Acad. Sci. USA* **2008**, *105(50)*, 19606-19611.

8. Goring, G.L.G.; Brennan, J.D. *J. Mater. Chem.* **2002**, 12, 3400-3406.

9. Harrell, T.M.; Hosticka, B.; Power, M.E.; Cemke, L.; Hull, R.; Norris, P.M. *J. Sol-gel Sci. Technol.* **2004**, 31, 349-352.

10. Sabina Di Risio and Ning Yan. *Macromol. Rapid Comm.* **2007**, *28 (18-19)*, 1934-1940.

11. Wang, J.; Pamidi, P.V.A.; Park, D.S. *Anal.Chem.* **1996**, *68*, 2705-2708.

12. Liu, J.; Mazumdar, D.; Lu, Y. *Angew. Chem. Int. Ed.* **2006**, *45*, 7955-7959.

13. No, H.-Y.; Kim, Y.A.; Lee, Y.T.; Lee, H.-S. *Anal. Chim. Acta* **2007**, *594*, 37-43.

14. Jordan, J.D.; Dunbar, R.A.; Bright, F.V. *Anal. Chem. Acta* **1996**, *332*, 83-91.

15. Katagiri, K.; Hasegawa, K.; Matsuda, A.; Tatsumisago, M.; Minami, T. *J. Am. Ceram. Soc.* **1998,** 81(9), 2501-2503.

16. Van der Biest, O.O.; Vandeperre, L.T. *Annu. Rev. Mater. Sci.* **1999**, *29*, 327-352.

17. Percin, G.; Khuri-Yakub, B.T. *Rev. Sci. Instrum.* **2003**, *74(2)*, 1120-1127.

18. Tsai, M.H.; Hwang, W.S. Chou, H.H.; Hsieh, P.H. *Nanotechnology* **2008**, *19*, 335304-335313.

19. Calvert, P. *Chem. Mater.* **2001**, *13(10)*, 3299-3305.

20. Allain, L.R.; Stratis-Cullum, D.N.; Vo-Dinh, T. *Anal. Chim. Acta* **2004**, *518*, 77-85.

21. De Gans, B.-J.; Duineveld, P.C.; Schubert, U.S. *Adv. Mater.* **2004**, *16(3)*, 203-213.

22. Hasenbank, M.S.; Edwards, T.; Fu, E.; Garzon, R. Kosar, T.F.; Look, M.; Mashadi-Hossein, A.; Yager, Y. *Anal. Chim. Acta* **2008**, *611*, 80-88.

23. Xu, T.; Jin, J.; Gregory, C.; Hickman, J.J. *Biomaterials* **2005**, *26*, 93-99.

24. Ilkhanizadeh, S.; Teixeira, A.I.; Hermanson, O. *Biomaterials* **2007**, *28*, 3936-3943.

25. Bietsch, A.; Hegner, M.; Lang, H.P.; Gerber, C. *Langmuir* **2004**, *20*, 5119-5122.

26. Besanger, T.R.; Hodgson, R.J.; Green, J.R.A.; Brennan. J.D. *Anal. Chim. Acta* **2006**, *564*, 106-115.

27. Marrs, T.C. *Pharmacol. Ther.* **1993**, *58(1)*, 51-66.

28. Rosenfeld C.A.; Sultatos, L.G. *Toxicol. Sci.* **2006,** *90(2)*, 460-469.

29. Blesa, J.; Seriano, J.M.; Molto, J.C.; Marin, R.; Manes, J. *J. Chromatogr. A* **2003**, *11*, 49-54.

30. Ventura, M.; Gomez, A.; Anaya, I.; Diaz, J.; Broto, F.; Montserrat, A; Luis, C. *J. Chromatogr.* **1990**, *1084*, 25-29.

31. Arduini, F.; Errico, I.; Amine, A.; Micheli, L.; Palleschi, G.; Moscone, D. *Anal. chem.* **2007**, *79*, 3409-3415.

32. Harmon, H.J. *Biosens. Bioelectron.* **2001**, *16*, 1035-1041.

33. Arduini, F.; Amine, A.; Moscone, D.; Ricci, F.; Palleschi, G. *Anal. Bioanal. Chem.* **2007**, *388*, 1049-1057.

34. Goryacheva, Y.; De Saeger, S.; Eremin, S.A.; Petehhem, C.V. *Food Add. Cont.* **2007**, *24(10)*, 1169-1183.

35. Lin, T.-J.; Huang, K.-T.; Liu, C.-Y. *Biosens. Bioelectron.* **2006**, *22*, 513-518.

36. Gill, R.; Bahsahi, L.; Freeman, R.; Willner, I. *Angew. Chem.* **2008**, *120*, 1700-1703.

37. Hai, A.; Ben-Haim, D.; Korbakov, N.; Cohen, A.; Shappir, J.; Oren, R.; Spira, M.E.; Yitzchaik, S. *Biosens. Bioelcetron.* **2006**, *22*, 605-612.

38. Liu, N.; Cai, X.; Lei, Y.; Zhang, Q.; Chan-Park, M.B.; Li, C.; Chen, W.; Mulchandani, A. *Electroanalysis* **2007**, *19 (5)*, 616-619.

39. Pardo-Yissar, V.; Katz, E.; Wasserman, J.; Willner, I. *J. Am. Chem. Soc.* **2003**, *125*, 622-623.

40. Pavlov, V.; Xiao, Y.; Willner, I. *Nano Lett.* **2005**, *5(4)*, 649-653.

41. Micheli, L.; Greco, R.; Badea, M.; Moscone, D.; Palleschi, G. *Biosens. Bioelectron.* **2005**, *21*, 588-596.

42. Ellman, G. L.; Courtney, K. D.; Andres, V.; Featherstone, R. M. *Biochem. Pharmacol.* **1961,** *7*, 88-95.

43. Marx, S.; Zaltsman, A. *Intern. J. Environ. Anal. Chem.* **2003**, *83(7-8)*, 671-680.

44. Virel, A.; Laura, S.; Pavlov, V. *Anal. Chem.* **2009,** *81(1)*, 268-272.

45. Brook, M.A.; Chen, Y.; Guo, K.; Zhang, Z.; Brennan, J.D. *J. Mat. Chem.* **2004**, *14*, 1469-1479.

46. Zhang, C.; Malhotra, S.V. *Talanta* **2005**, *67*, 560-563.

47.   Goring, G.L.G.; Brennan, J.D. *Chem. Mat.* **2007**, *19*, 5336-5346.

48.   Hodgson, R.; Chen, Y.; Zhang, Z.; Tleugabulova, D.; Long, H.; Zhao, X.; Organ, M. G.; Brook, M. A.; Brennan, J.D. *Anal. Chem.* **2004**, *76*, 2780-2790.

49.   Besanger, T.R.; Brennan, J.D. *J. Sol-gel Sci. Technol.* **2006**, *40*, 209-225.

50.   Voss, R.; Brook, M.A.; Thompson, J.; Chen, Y.; Pelton, R.H.; Brennan, J.D. *J. Mater. Chem.* **2007**, *17*, 4854-4863.

51.   Tleugabulova, T.; Zhang, Z.; Brennan, J.D. *J. Phys. Chem. B* **2003**, 107, 10127-10133.

52.   Tleugabulova, D.; Duft, A.M.; Zhang, Z.; Chen, Y.; Brook, M.A.; Brennan, J.D. *Langmuir*, **2004**, *20*, 5924-5932.

53.   Pandey, P.C.; Upadhyay, S.; Pathak, H.C.; Panday, C.M.D.; Tiwari, I. *Sens. Act. B* **2000**, *62*, 109-116.

54.   Koruso, K; Pelton, R. *J. Pulp Paper Sci.* **2004**, *30*, 228-232.

55.   Sharma, J.; Tleugabulova, D.; Czardybon, W.; Brennan, J.D. *J. Am. Chem. Soc.* **2006**, *128*, 5496-5505.

Chapter 6: Conclusions and Future Outlook

6.1 Summary of Thesis Project

The ultimate goal of this thesis project was to investigate the coupling of sol-gel entrapped enzyme to paper substrates toward the development of a portable and inexpensive solid-phase biosensing platform to screen for small molecule analytes.

In Chapter 3, AChE activity is monitored *via* the enzyme stimulated growth of small AuNP within the confines of the SS matrix, in the presence of Au(III), which results in a concomitant color change. We demonstrated that as the AuNP grow they are entrapped within the sol-gel matrix and cannot leach. Thus, the signal obtained is large and permanent, allowing for sensors to be kept for future reference. In optimizing the assay, it was discovered that the choice of AuNP was of particular importance. The AuNPs provide the physical platform upon which growth takes place and so it is imperative that they remain evenly dispersed throughout the glass, else the signal achieved will not be reproducible. For this purpose, it was discovered that ATP capped AuNP colloidal solutions was sufficiently stable as it can tolerate more than 200 mM salt without aggregating out of solution.

The solid phase biosensor was used to assess varying levels of Paraoxon (analogue for bio-terror agent) and Aflatoxin B$_1$ (biomarker for food spoilage). It was discovered that this assay platform was sufficiently sensitive to detect

Paraoxon to 3 μM and Aflatoxin B$_1$ to as low as 15 nM. These values are well below the lethal dosage of these compounds.

To make the solid-phase biosensor platform more portable and versatile, AChE-AuNP doped SS was deposited on a paper support by a simple dip-casting method to form a dip-stick type platform (Chapter 4). Of several sol-gel materials tested a 40%MTMS/TMOS (methlytrimethoxy silane, tetramethlyorthosilicate) solution showed the best adhesion to the paper surface and resistance to cracking over a period of 2 months.

The hydrophobic 40%MTMS/TMOS sol was used to pre-treat the paper substrate followed by the coating of a SS-AChE-AuNP composite. This worked well, with S/B = 4.15 ± 0.002. To assess the applicability of the sensor, a series of Paraoxon concentrations were tested and a detection limit of 1 μM was established.

The deposition technique used in the aforementioned work was dip-casting and even though conceptually solid, it is time consuming, tedious and leads to wastage of expensive bio-reagents. Hence, in Chapter 6, ink-jet printing of enzyme doped sols was investigated. A unique sandwich type fabrication technique was devised whereby sol-gel materials (at more stable pH) and the bio-materials were printed separately and in layers so that AChE was sandwiched between layers of SS to form the sensor. In an attempt to lower assay time, the Ellman assay was used to monitor AChE activity for this ink-jet printed sensor, with a cationic polymer; PVAm (polyvinylamine, 1.5 MDa), used to trap the

anionic product molecules over a designated region. PVAm did not only effectively trap the yellow color, it also preserved it for significantly longer periods of time.

With this novel approach, a series of Paraoxon and AFB_1 levels were assessed and it was determined that these compounds can be detected to 100 and 1 nM respectively, in ca. 5 min.

Overall, the work in this thesis shows that the paper-based biosensing platform has significant potential for rapid, small-molecule sensing in a mode that should be useful in the developing world, as not only is this sensing platform inexpensive, portable and highly sensitive, it requires no sophisticated instruments. Detection can be made by eye or with digital camera and ImageJ freeware.

6.2 Future Outlook

Notwithstanding the success of this thesis project, there are a number of fundamental questions that remains to be answered. A major object of this project was to develop a generic solid-phase platform to monitor and detect inhibitors of a wide range of 'redox' enzymes. However, all work was done with only AChE. It has been shown that other metal salts, such as Ag(I), have been utilized to allow detection of enzymatic reactions such as the hydrolysis of p-aminophenol phosphate by alkaline phosphatase to yield p-aminophenol, which catalyzes the reduction of Ag^+ onto Au NPs.[1] Therefore, it should be possible to incorporate

other such enzyme into our solid-phase assaying platform. Key issues to be looked at would be: (1) whether or not these enzymes remain active in sol-gel derived material; (2) the effect of the sol-gel matrix on other regent components, (3) to investigate strategies that would reduce assaying time.

With regard to the bioactive paper sensors, this platform could be modified to accommodate a single reagent rather than two as is the case with the assays described here. The reagent indophenyl acetate (IPA) can act directly as an AChE substrate, which after enzyme catalyzed hydrolysis changes color from yellow to blue. With such as distinct change in color, this type of assay could be quite useful as a litmus paper type, qualitative test for inhibitors of AChE. Furthermore, if this substrate is stable on the paper surface it could lead to the development of a reagentless sensor where all sensor components are pre-deposited on the paper test strip. Presently, a lateral flow device such as this is being developed in our laboratory.

Another future goal is to alter this system so that it is more robust and efficient – allowing for multiplexed, low sample volume assays to be run simultaneously.[2,3,4] This can be achieved by creating hydrophobic and hydrophilic channels on an absorbent paper substrate *via* patterned ink-jet deposition of hydrophobic materials (*e.g.,* MTMS or polystyrene). With this system, different assay components as well as control components can be printed in well-defined compartments on the paper surface. Other reagent components as well as analytes can be introduced simultaneously by utilizing the capillary flow capabilities of the

paper. Such sensors could be extremely useful in remote settings as well as less industrialized countries where simple bioassays are essential in the first stages of detecting disease, and for monitoring environmental and food based toxins. Such a simple, inexpensive, low-volume, portable, solid-phase biosensing platform is currently under investigation in our laboratory.

6.3 References

1. Basnar, B.; Weizmann, Y.; Cheglakov, Z.; Willner, I. *Adv. Mater.* **2006**, *18*, 713-718.

2. Li, X.; Tian, J.; Nguyen, T.; Shen, W. *Anal. Chem.* **2008**, *80 (23)*, 9131-9134.

3. Abe, K.; Suzuki, K.; Citterio, D. *Anal. Chem.* **2008**, *80 (18)*, 6928-6934.

4. Martinez, A.W.; Phillips, S.T.; Butte, M.J.; Whitesides, G.M. *Angew. Chem., Int. Ed.* **2007**, 46, 1318-1320.